UNCLASSIFIED

CF-55-8-188

PHYSICS

UNITED STATES ATOMIC ENERGY COMMISSION

IMMISCIBLE-LIQUID-COOLED, FLUID-FUEL REACTOR

By
W. D. Burch
C. H. Cater
D. L. Hathway
B. S. Maxon
N. R. Williamsen
O. O. Yarbro

August 1955

Oak Ridge School of Reactor Technology
Oak Ridge, Tennessee

Technical Information Service Extension, Oak Ridge, Tenn.

UNCLASSIFIED

DISCLAIMER

This report was prepared as an account of work sponsored by an agency of the United States Government. Neither the United States Government nor any agency Thereof, nor any of their employees, makes any warranty, express or implied, or assumes any legal liability or responsibility for the accuracy, completeness, or usefulness of any information, apparatus, product, or process disclosed, or represents that its use would not infringe privately owned rights. Reference herein to any specific commercial product, process, or service by trade name, trademark, manufacturer, or otherwise does not necessarily constitute or imply its endorsement, recommendation, or favoring by the United States Government or any agency thereof. The views and opinions of authors expressed herein do not necessarily state or reflect those of the United States Government or any agency thereof.

DISCLAIMER

Portions of this document may be illegible in electronic image products. Images are produced from the best available original document.

2

Date Declassified: March 19, 1956.

LEGAL NOTICE

This report was prepared as an account of Government sponsored work. Neither the United States, nor the Commission, nor any person acting on behalf of the Commission:

A. Makes any warranty or representation, express or implied, with respect to the accuracy, completeness, or usefulness of the information contained in this report, or that the use of any information, apparatus, method, or process disclosed in this report may not infringe privately owned rights; or

B. Assumes any liabilities with respect to the use of, or for damages resulting from the use of any information, apparatus, method, or process disclosed in this report.

As used in the above, "person acting on behalf of the Commission" includes any employee or contractor of the Commission to the extent that such employee or contractor prepares, handles or distributes, or provides access to, any information pursuant to his employment or contract with the Commission.

This report has been reproduced directly from the best available copy.

Issuance of this document does not constitute authority for declassification of classified material of the same or similar content and title by the same authors.

Since nontechnical and nonessential prefatory material has been deleted, the first page of the report is page 5.

Printed in USA. Price 70 cents. Available from the Office of Technical Services, Department of Commerce, Washington 25, D. C.

AEC, Oak Ridge, Tenn.

PAGES 3 to 4

WERE INTENTIONALLY

LEFT BLANK

CF-55-8-188

OAK RIDGE SCHOOL OF REACTOR TECHNOLOGY

F. C. VonderLage, Director

"IMMISCIBLE-LIQUID-COOLED, FLUID-FUEL REACTOR"

Prepared by:

W. D. Burch, Group Leader
C. H. Cater
D. L. Hathway
B. S. Maxon
N. R. Williamsen
O. Q. Yarbro

THIS PAGE

WAS INTENTIONALLY

LEFT BLANK

PREFACE

In September, 1954, a group of men representing various scientific and engineering fields embarked on the twelve months of study which culminated in this report. For nine of these months, formal classroom and student laboratory work occupied their time. At the end of that period, these six students were presented with a problem in reactor design.

This is a summary report of the study, the research, the problems and the solutions which developed during the final ten-weeks period of the school term. It must be realized that, in so short a time, a study of this scope cannot be guaranteed complete or free of error. This "thesis" is not offered as a polished engineering report but rather as a record of the work done by the group under the leadership of the group leader. It is reproduced for use by those persons competent to assess the uncertainties inherent in the results obtained in terms of the preciseness of the technical data and analytical methods employed in the study. In the opinion of the students and faculty of ORSORT, the problem has served the pedagogical purpose for which it was intended.

As a matter of historical fact and pride we point out that similar investigations by student groups of previous ORSORT classes have led to sufficiently encouraging results to warrant more exhausive studies; in at least one instance, a reactor first investigated by a student group is soon to become a physical reality. There is also recorded an instance in which calculations contained in a similar report were uncritically abstracted and applied to a study for which they were never intended. It is to avoid the recurrence of the latter experience that we have taken some pains to acquaint the reader with the character of this report.

The faculty wishes to join the authors in an expression of appreciation for the assistance which various members of the Oak Ridge National Laboratory have so generously contributed. In particular, the guidance of the group consultant, Lloyd G. Alexander, is gratefully acknowledged.

F. C. VonderLage

for

The Faculty of ORSORT

ACKNOWLEDGEMENT

The helpful suggestions of O. E. Dwyer and F. T. Miles, of Brookhaven National Laboratory, are gratefully acknowledged.

Assistance by the group advisors was appreciated.

ABSTRACT

A central station power fluid fuel reactor has been designed in which heat is removed by direct contact of the fuel with an immiscible coolant. Object of this design is to minimize fuel holdup outside the reactor core by utilizing the excellent heat transfer characteristics of direct contact cooling.

TABLE OF CONTENTS

1.0 Introduction - Choice of System 15

1.1 Objectives of Proposed Reactor System 15

1.2 Systems Considered 15

1.21 Bismuth Fueled Reactor, Internally Cooled by Water and Sodium 16

1.22 Direct Liquid Contact Cooling 17

1.221 Powered Pump - Centrifugal Separator 17

1.222 Jet Pump - Heat Exchanger 18

1.223 Jet Exchanger - Centrifugal Separator 19

1.3 Choice of Physical Systems 20

1.4 Choice of Chemical Systems 21

2.0 Reference Design Data 23

2.1 Overall Design 24

2.2 Core Design 24

2.3 Blanket Design 24

2.4 Heat Exchanger 25

2.41 Circular Disc Jet Pump Exchanger 25

2.42 Jet Exchanger - Centrifugal Separator 26

2.5 Chemical Processing 26

2.6 Steam Cycle 27

2.7 Estimated Costs 28

	Page
3.0 Design of Core	30
3.1 Parametric Study of Effect of Core Parameters on Breeding Ratio	30
3.2 Effect of Heat Exchanger on Core Design	33
3.3 Flow Arrangement - Pressure Drop	37
3.4 Fission Product Poison Fraction	40
3.5 Poison Effect of Entrained Coolant	40
4.0 Breeding Blanket	42
4.1 General Considerations - Blanket Configuration	42
4.2 Two-Group Study of Blanket Variables	43
4.3 Neutron Losses in Proactinium and Fission Products	50
4.4 Higher Uranium Isotope Build-Up	50
4.5 Over-All Neutron Balance	51
5.0 Direct Liquid Contact Heat Exchange	52
5.1 Proposed Objectives of Direct Contact Exchanger	52
5.2 Disc Type Jet Pump Exchanger	53
5.21 Disc Type Jet Pump - Pumping Performance	56
5.22 Disc Type Jet Pump - Heat Exchange Performance	62
5.23 Disc Type Jet Pump - Separation Characteristics	65
5.3 Fluid Contacting Centrifugal Pump Exchanger	68
5.31 Centrifugal Pump Exchanger - Pumping Performance	70
5.32 Centrifugal Pump Exchanger - Heat Exchange	74
5.33 Centrifugal Pump Exchanger - Separation	75
5.4 Summary - Evaluation of Two Exchangers	78
6.0 Chemical Processing	78
6.1 Core Processing	78

		Page
	6.11 Volatile Fission Product Removal	71
	6.12 Salt Soluble Fission Products	71
	6.13 Salt Insoluble Fission Products	71
	6.14 Processing Cycles and Poison Level	82
	6.2 Blanket Processing - U^{233} Removal	83
7.0	Steam Cycle	86
8.0	Control of the Reactor and Power Output	90
9.0	Materials of Construction	92
10.0	Economics of the Proposed Reactor	94
	Appendix	96
	Bibliography	141

SUMMARY

A new concept of heat removal from a fluid fuel reactor was investigated to determine what economic advantages might be attained by minimizing fuel holdup in the primary heat exchanger. A central station power reactor of 300 Mw electrical capacity has been designed in which a liquid fuel is cooled by direct contact with an immiscible liquid in a jet pump. Fuel liquid is a solution of U^{233} at a concentration of 305 ppm in molten bismuth. Coolant is the KCl-LICl entectic which melts at 684°F. Breeding is accomplished in an external blanket using a 10% by weight dispersion of thorium in bismuth as the fertile material.

The reactor cores is a 6' by 6' right circular cylider of graphite with 1 1/2 inch fuel tubes. Moderator to fuel solution volume ratio is one. Moderator to fertile slurry ratio in the 3 foot blanket is two. To minimize fuel holdup in external piping flow in the core is through a two-pass arrangement with a cross-over header at the bottom of the core.

Heat exchange takes place in a circular disc jet pump located 3 feet above the top of the core. Transfer of momentum from the coolant to the fuel supplies the driving force to overcome friction losses in the core. To reduce entrainment of coolant with the fuel, an annular settling ring limits velocity of the fuel stream to 1 foot per second as it returns to the core. Heat from the blanket is removed in a conventional shell and tube exchanger.

The bulk of the heat from the core is utilized in the steam boilers. The remaining fraction superheats the saturated steam from the boiler to 759 °F. In the main superheater, heat from the blanket raised the steam temperature to the throttle conditions of 1000°F at 1450 psia. Efficiency

in the straight expansion cycle without reheat to a condenser back pressure of 1 1/2 inches of Hg is 39 percent. Moisture content is 12%.

A small but insignificant savings in power cost is realized by reduction of the U^{233} inventory through use of the high performance jet pump heat exchanger. Total fuel inventory charges amount to only .03 mills/kwh and 70% of this inventory is in components outside the core and primary heat exchanger system (blanket and processing plant holdup for Pa decay). From this it can be seen that inventory charges for fissionable material within the reactor core and heat exchanger are such a small fraction of the total power cost that no significant cost reduction is possible through improved heat exchanger performance. This point was particularly true for this reactor system because of the low critical fuel concentration.

Other costs closely parallel those of the Liquid Metal Fuel Reactor designed at Brookhaven National Laboratory which employs the same type reactor fuel with a conventional primary heat exchanger. Some saving might accrue from a reduction in the primary heat exchanger costs, but this is offset by the added cost of the fused salt system. Chemical processing costs are nearly identical for both systems.

In the present direct liquid contact cooling design, several problems arose which could not be treated by analytical means.

1. Exact heat exchange performance in the jet pump is unknown because of the uncertainty of drop size and heat transfer coefficient within the jet. It was shown that if the fuel were dispersed in drops no larger than 1/8 inch in diameter, heat exchange was adequate in the 0.2 second contact time in the jet pump.

2. Entrainment of the high neutron cross section salt with the fuel would constitute a serious poison in the core. Dimensions of an adequate settling ring for phase separation can only be determined experimentally. One alternative is the development of a salt coolant with lower cross section. A possibility is the $NaF-BeF_2$ eutectic.

3. Suitable material of construction for the jet pump which would stand up under the high jet velocities required and the mixture of molten bismuth and fused salt at temperatures up to 1400°F is not known. Two possible materials exist. Graphite is corrosion resistant but probably is subject to erosion at the high jet velocities. Molybdenum should be satisfactory but at the present time suitable fabrication techniques are not known.

An alternate heat exchanger was investigated in which partial counter-current heat exchange is effected by admitting coolant in tangentical jets. Phase separation is also enhanced through centrifugal action. However, flow patterns were so complex that an adequate analytical treatment of pump performance and possible flow rates was not developed.

1.0 INTRODUCTION - CHOICE OF SYSTEM

1.1 Objectives of Proposed Reactor Design

Fluid fuel reactors have been shown to have several advantages over heterogeneous reactors for power production. However, the fluid fuel reactors in general introduce new and different problems to the field of reactor technology. One distinct disadvantage of this type reactor is the large inventory of fissionable material contained outside the core in piping, heat exchanger, and pumps. In some cases, such as in the homogeneous reactors with D_2O solutions and the Liquid Metal Fuel Reactor, which employs molten bismuth, the fuel bearing liquid is also quite valuable. This holdup of valuable material outside the reactor core, if excessive, not only inflicts an economic penalty, but also creates a potential safety hazard in that several critical masses of fissionable material are contained within close proximity.

The object of this study was to design a fluid fueled central station power reactor with an absolute minimum of fuel solution contained in reactor externals.

Of course, economics must be an underlying objective of any power reactor design. Advantages achieved in reducing fuel inventory, if brought about through expensive and complex designs, may have little significance. Thus, a secondary objective was the investigation of the feasibility of the proposed reactor for economic power production in comparison with reactors of similar design.

1.2 Systems Considered

While the original proposal did not define the exact method to achieve the above objectives, one means of doing this was suggested. This

consisted of employing a secondary coolant stream immiscible with the fuel solution, to remove heat by direct liquid contact of the fuel and coolant streams in a liquid jet near the core-reflector interface. In this scheme, fuel holdup in external piping is virtually non-existent; this, coupled with the excellent heat transfer characteristics of direct liquid contact which keeps heat exchanger holdup low, reduces external fuel solution holdup to a minimum.

Since the problem was not restricted to the above scheme, several other designs were proposed in the initial phases of the work to achieve in some measure the stated objectives. Those designs which appeared most promising were investigated further. From preliminary calculations the performance of each system was estimated and on this basis, a system was chosen from a reference design study.

1.21 Bismuth Fueled Reactor, Internally Cooled by Water and Sodium

In many respects, bismuth is an excellent carrier for fissionable material in a fluid fuel power reactor. It has a low capture cross section, is suitable for high temperature operation, has good heat transfer properties, and is relatively non-corrosive.

In this design (Section 5.1 in Appendix) it was proposed to contain a molten bismuth-uranium fuel solution in double-walled tubes within the core. No fuel would be circulated outside the core. Cooling would be affected by circulating another non-fuel bearing liquid or liquids within the core. Liquids proposed were sodium and water. This design obvicusly eliminated external fuel holdup while introducing several other real disadvantages. These are:

1. Poisoning effects of the coolant, water and sodium, and the steel tube walls. From the preliminary calculations maximum breeding ratio attainable was estimated only in the order of 0.3. This would introduce a serious economic handicap.

2. Increased critical mass due to poisons in the core. While external fuel holdup was eliminated, the total fuel requirements would not be materially changed.

3. Complex physical system. Construction of a system to contain three incompatible liquids within the core would be extremely difficult if possible at all.

1.22 Direct Liquid Contact Cooling

Several methods were proposed for cooling the fuel solution by direct liquid contact with an immiscible coolant. In general, these methods differed in physical design and theoretically could be applied to any of two or three different fuel-coolant systems.

1.221 Powered Pump - Centrifugal Separator

One unique design proposed for direct liquid contact cooling consisted of a powered centifugal separator located directly above the core (Appendix 5.2). Hot fuel is admitted in the form of small drops near the center of the turning bowl and coolant near the periphery. The centrifugal action induces counter-current flow of the liquids, and heat exchange takes place as the fluids move from one edge to the other of the whirling bowl. The big advantage of this design is that true counter-current heat exchange is achieved. The centrifugal force also aids in rapid separation of the phases. Although the idea appears sound and the turning bowl could be designed with only one atmospheric seal, the device would be quite monstrous sitting on

top of the core. Estimated size was 8 feet in diameter and 6 feet high. It would have to turn at only 50-100 rpm. It was proposed to pump the coolant with an impeller located above the separator, attached to and driven by the same shaft to which the separator was attached.

1.222 Jet Pump - Heat Exchanger

In defining the original proposal for a Reactor School summer project, the basic new idea presented was the removal of heat from a power reactor by contacting the fuel with an immiscible coolant in a jet pump located at the core-reflector interface. In the jet pump, heat transfer would be very rapid due to the high degree of turbulence in the jet mixing tube. Momentum transfer from the coolant to the fuel solution would provide the necessary head to overcome pressure losses in the core. Centrifugal separation of the phases also seemed advisable and was to be effected in a series of cyclones located on the core periphery. Three advantages were apparent for the system.

1. Mechanically, it is simple; there are no moving parts.

2. Heat transfer would be very rapid. Preliminary calculations showed that heat transfer would not be a problem, but were found later to be optimistic due to numerical error.

3. External hold-up would be very small.

Offsetting these advantages are three distinct drawbacks:

1. Co-current heat exchange in the jet necessitates a much higher overall temperature range within the system.

2. Very high jet nozzle velocities, in the order of 50 to 75 feet per second, are required to impart sufficient momentum to the fuel solution. It is possible no material of construction would withstand such velocities at

the high temperatures involved.

3. Transfer of kinetic energy in a jet pump is extremely inefficient.

1.223 Jet Exchanger - Centrifugal Separator

In an effort to achieve the advantages of both of the above schemes, a design was proposed in which heat exchange takes place in a large cylindrical vessel located, as in the other designs, on top of the core. The group making this design study cannot claim originality in this idea since a similar scheme for a heat exchanger had been proposed at Brookhaven National Laboratory[13]. The fuel stream would be admitted generally in the center of the vessel and the coolant in tangential jets at the periphery. The high velocity coolant imparts sufficient kinetic energy to the fuel to set up rapid swirling flow. Recovery of part of the velocity head and pressure head due to centrifugal force would supply driving force to pump the fuel stream. The centrifugal force would aid in phase separation.

Three main advantages were seen for this system over the ordinary jet pump.

1. Heat transfer would approach that obtained in true counter-current flow.

2. The coolant jets would not be subject to the high thermal stresses which appeared to be unavoidable in the noraml jet pump.

3. Phase separation should be rapid due to centrifugal force in the whirling fluid.

From the beginning the question arose as to whether the counter-current flow as was visualized was actually possible. Estimating performance of this system was extremely difficult.

1.3 Choice of Physical System

Approximately two weeks of study were spent in evaluating the above four systems before a choice was made for reference design.

From elementary nuclear calculations on the sodium-water internally cooled reactor, it was evident that breeding ratio was too low to achieve economic power, and this scheme was abandoned.

Preliminary calculations on the powered pump-separator indicated that the design could be made to operate, and while the turning bowl would be quite large, it would move relatively slowly compared to similarly sized equipment such as turbines, compressors, etc., however, it still was an extremely complicated system located in a high radiation field. While there were some advantages to the system not attainable in the others, the complexity of the machine was felt sufficient reason to discontinue work on this design.

This narrowed the choice to one of the two jet systems. It was evident from preliminary calculations that high jet velocities would be necessary to impart the required head to the fuel solution. While no data could be found on jet pumping of one fluid by another with greatly different densities, performance could be estimated from theoretical calculations.

In the initial investigation of heat transfer characteristics, it appeared that there would be no difficulties with either system. Heat transfer would be very rapid as long as drops of the dispersed phase were no larger than about an eighth to a quarter inch in diameter.

If all the advantages of the centrifugal exchanger-separator could be realized, it seemed quite superior to the jet pump. But, at that stage, operating characteristics of the former could hardly be visualized, let alone

be accurately calculated. Consequently, it was decided to continue work in parallel on both designs until a clear-cut choice could be made. Eventually both were carried through as far as time and analytical means permitted.

1.4 Choice of Chemical System

In the proposed reactor design, many rather stringent requirements are placed upon the choice of fuel and coolant. The most important of these are:

1. The fuel carrier and coolant must be mutually insoluble, or exhibit only a slight solubility.

2. Uranium must be soluble in the carrier and insoluble in the coolant.

3. The liquids must be stable chemically to each other.

4. Radiation damage products of one liquid must not adversely affect the other.

5. Densities of the liquids must be sufficiently different to afford rapid phase separation.

6. Interfacial tension must be such that there is no tendency for the liquids to emulsify.

7. Some material of construction must be stable in contact with a mixture of the liquids at operating temperatures.

8. The coolant should have low nuclear cross section to prevent poisoning by entrainment in the fuel.

Three fuel-coolant combinations were considered which might fulfill some or all of the above requirements. These were:

1. Aqueous fuel with an organic liquid coolant.

2. Fused fluoride fuel solution with liquid metal coolant.

3. Molten bismuth-uranium fuel with fused salt coolant.

While the aqueous fuel-organic coolant combination satisfies many of the requirements listed, it falls far short on some of the others, notably points 4 and 5. The use of organics in the core of a reactor, to many people acquainted with the radiation damage problem, is completely infeasible. However, a heterogeneous power reactor has been designed[2] to be cooled and moderated with bi-phenyl. In the present design two additional problems arise. First, radiation damage to the organic would be more severe than in a heterogeneous reactor because of the intimate contact between the fuel and coolant. In the heterogeneous system, damage is due to neutrons, beta and gamma rays, while in the fluid fuel reactor, in addition to these, fission fragments contribute greatly to the radiation damage. The second and more severe problem would arise due to the value of D_2O, which all aqueous power breeders employ as fuel carrying liquid. Radiation damage to the organic would produce H_2 which would be mixed with D_2 from D_2O decomposition. Thus, recombination would produce heavy water less enriched in deuterium. The suggested use of an organic with H_2 replaced by D_2 would not solve the problem because of the large losses of organic in the form of tars due to radiation damage.

The fused fluoride fuel-liquid metal coolant appears to satisfy most of the requirements. At least it is thought some combination could be found which would satisfy the mutual stability and solubility requirements. Radiation damage would not be a problem and on the surface no other serious difficulties appeared.

However, much more was known about the third system (uranium-bismuth fuel-fused salt coolant) from the work done during the past four years at Brookhaven National Laboratory on the Liquid Metal Fuel Reactor[3]. In the

development of chemical processing of the molten fuel by fused salt extraction of fission products, it has been shown that, under the proper oxidizing conditions, uranium will remain dissolved in bismuth while in contact with a eutectic mixture of LiCl-KCl. It was also found that the liquids are easily separated after mixing, due in part to the great density difference and also to the fact they show no tendency to emulsify. The liquids can be contained in the 400 series stainless steels. Obviously, from a nuclear standpoint, the LiCl-KCl eutectic would be a serious poison if carried with the fuel into the core.

After careful consideration of the above systems, the combination chosen for reference design was:

Fuel - Uranium dissolved in molten bismuth.

Coolant - LiCl-KCl eutectic (55% KCl by weight).

Certainly, ways should be investigated to minimize the potential poison effect of the coolant if this design is ever to be made practical. Several possibilities exist. Work is underway at BNL to replace the very high cross section LiCl with $MgCl_2$ or some other chloride. Conceivably, some fluoride eutectic could be used, though in general the melting points of most of the fluorides are too high to be considered. However, NaF_2-BeF_2 eutectic melts at 325°C, and thus could be postulated as a possible coolant. Only experimental work in the laboratory would show whether another proposed fused salt coolant would satisfy the stability requirements.

2.0 REFERENCE DESIGN DATA

In this section is presented significant data for the reference design. The reasoning behind the choices of these parameters is shown in

subsequent sections. All detailed calculations are illustrated by derivations and numerical examples in the appendix.

2.1 Overall Design

Type Reactor - Central Station Power

Electrical Power - 300 Mw

Heat Power - 770 Mw

Reactor Nuclear Type - Two region with breeding in external blanket.

2.2 Core Design

Fuel - Uranium dissolved in molten bismuth, at a concentration of 285 ppm by weight.

Moderator - Graphite

Fuel/Moderator Volume Ratio = 1

General Configuration - Two pass flow through right cylinder with entry and exit at top, and crossover header at bottom.

Dimensions:

Core: 6 feet by 6 feet right cylinder

Fuel Tubes: 1 1/2 inch diameter of 2.02 inch triangular centers

Average thermal flux - 2.95×10^{15} nv

Average fast flux - 3.95×10^{15} nv

Peak thermal flux - 7.3×10^{15}

Power generated - 650 Mw heat = 84.4% of total power.

2.3 Blanket Design

Fertile Material: Thorium as a 10% by weight dispersion in molten bismuth.

U^{233} concentration - 300 ppm

Graphite/bismuth and thorium volume ratio = 2

Blanket thickness = 3ft

Average thermal flux = 1.29×10^{14} nv

Average fast flux = 3.48×10^{14} nv

Power generated = 120 Mw heat, equal 15.6% of total power

Breeding ratio = 0.987

2.4 Heat Exchanger

Two different types of direct liquid contact heat exchangers were investigated, one in which heat exchange takes place within a circular disc jet pump and the other in which the fused salt coolant is admitted through peripheral jets and flows semi-counter currently to the uranium-bismuth fuel solution. While the latter appears to have several advantages over the circular disc jet pump scheme, its performance has not been estimated with any accuracy because of the complex flow arrangement.

2.41 Circular disc jet pump-exchanger

Jet radius = 1.9 ft

Coolant/fuel volume flow ratio = 2

Salt velocity in jet throat = 75 ft/sec

Head developed in fuel stream in jet pump = 14.0 psi

Pressure loss is ccolant stream across jet pump = 46.7 psi

Fuel drop size = 0.125 in D

Contact time = 0.2 sec

Temperatures:

Fuel inlet = 1407 °F

Fuel exit = 974°F

Coolant inlet = 700°F

Coolant exit = 917°F

2.42 Jet Exchanger - Centrifugal Separator

Coolant/fuel volume flow ratio = 2

Salt velocity in jet = 65 ft/sec

Number of jets = 4

Head developed in fuel stream = 14.0 psi (assuming 50% recovery of kinetic energy head).

Pressure low in coolant stream = 44 psi

Temperatures:

Fuel inlet = 1200°F

Fuel exit = 767°F

Coolant inlet = 700°F

$\Delta T = 433°F$

Coolant exit = 917°F

2.5 Chemical Processing

The core fuel solution will be processed for fission product removal and the blanket solution for uranium recovery by a scheme proposed at Brookhaven National Laboratory for the Liquid Metal Fuel Reactor and briefly outlined in Sections 6.1 and 6.2 of this report.

Processing Cycles:

Core coolant salt = 20 days

Core fuel steam = 173 days

Blanket = 34.7 days

These processing cycles will maintain fission product poison level at the arbitrarily assumed 0.05 fraction.

The blanket cycle is determined by the desired U^{233} concentration in the blanket which is in turn fixed by power generateion permitted in the blanket and the effect of concentration on breeding.

2.6 Steam Cycle

Turbine Type -

Pressure - 1450 psia

Temperature - 1000°F

Condenser back pressure - 1 1/2"

Moisture content of steam to condenser - 12 1/3%

Number feed water heaters - 5

Overall thermodynamic efficiency - 39%

Water Heaters

Heat transfer area = 1,810 ft^2

Number of tubes = 282

I.D. (tube) = 0.700"

Length = 35 ft

Over-all heat transfer coefficients = 938 BTU/hr.ft°F

Boiler

Heat transfer area = 13,100 ft^2

Number of tubes = 1,376

I.D. (tube) = 0.700"

Length = 52 ft

Over-all heat transfer coefficients = U_1 = 938 BTU/hr.ft^2 °F
U_2 = 382 BTU/hr.ft^2 °F

First Super Heater (Heat from fused salt)

Heat transfer area = 5,420 ft^2

Number of tubes = 1,376

I.D. (tube) = 0.700"

Length = 21.5 ft

Over-all heat transfer coefficient (U) = 383 BTU/hr.ft^2 °F

Second Superheater (heat from blanket)

Overall (U) = 383

$\Delta T = 150^{o}F$

Heat transfer area required - 7,130 ft

Number of exchangers

Tubes per exchanger - 1376

Inside diameter (tube) - 0.700"

Length - 28.3 ft

Feed Water Heaters

Number - 5

Temperature rise of feed water - 416

Percent of throttle steam bled off to feed water heaters - 42%

2.7 Estimated Costs

Using the best available figures from the cost analysis of the Liquid Metal Fuel Reactor[3], the cost of electric power from the LMFR is 7 mils/Kwh. Using the same costs where applicable, the cost of power from the direct liquid contact cooled reactor proposed in this report is 6 mills/kwh. This saving is due entirely to the lower unit construction and operating costs of a larger plant. Bismuth, thorium, and U^{233} holdups throughout the system are shown in Table I and the power cost breakdown is presented in Table II. It can be seen that inventory charges are insignificant compared with the major power costs.

TABLE I

HOLD-UPS IN REACTOR SYSTEM

	Gal Bi	Tons Th	Kg. U
Core	685	--	7.2
Blanket	2450	12	28.3
Core Heat Exchanger, and Piping	2105	--	22.3
Blanket Heat Exchanger	368	2	4.1
Blanket Chemical Process	614	.5	40.8
Core Chemical Process	49	--	.7
Total	6271	14.5	103.4

TABLE II

POWER COST BREAKDOWN

Item	Mills/KWH
Capital Costs (not including boiler equipment)	2.13
Capital Costs (reactor and heat exchanger)	1.37
Chemical Processing	1.85
U^{233} Makeup (breeding ratio 0.98)	0.03
U^{233} Inventory at 4%	0.03
Bi Inventory at 12%	0.06
Station Operation and Maintenance	0.52
Total	5.99

3.0 DESIGN OF CORE

The only requirement specified when design of the core was undertaken was the power output -- 300 Mw of electricity. The thorium U^{233} breeding cycle was chosen since the reactor is basically thermal.

3.1 Parametric Study of Effect of Core Parameters on Breeding Ratio

While the primary purpose of this design was not to maximize breeding ratio, numerous previous studies have shown the necessity for a high breeding ratio if a reactor is to produce economic power. For this reason, a parametric study was undertaken to determine the effects of core size and moderator to fuel volume ratio (V_m/V_f) on breeding. After the parameter values which gave high breeding ratios were determined, the core was designed considering the flow arrangement (pressure drop calculations) in conjunction with nuclear calculations.

For the parametric study, a one-velocity, two-region nuclear model modified with a fast leakage correction was used. It was arbitrarily decided to breed in an external blanket, though subsequent studies have shown that the core of the two-region reactor to produce 300 Mw of electricity is too large to permit sufficient leakage to the blanket for high breeding ratios. Spherical geometry was assumed and the resulting core sizes converted to a right cylinder by equating the one region bucklings.

The only important effect of moderator to fuel ratio is the increase in thermal utilization with smaller V_m/V_f ratios. Figure 1 shows this effect. From this and Figure 2, which shows breeding ratio as a function of moderator to fuel ratio at various U^{233} core concentrations, it can be seen that breeding ratio is higher for low V_m/V_f ratios. From other considerations (see 3.3) a ratio of 1:1 was chosen as the smallest feasible.

ORNL-LR-Dwg.-10181
UNCLASSIFIED

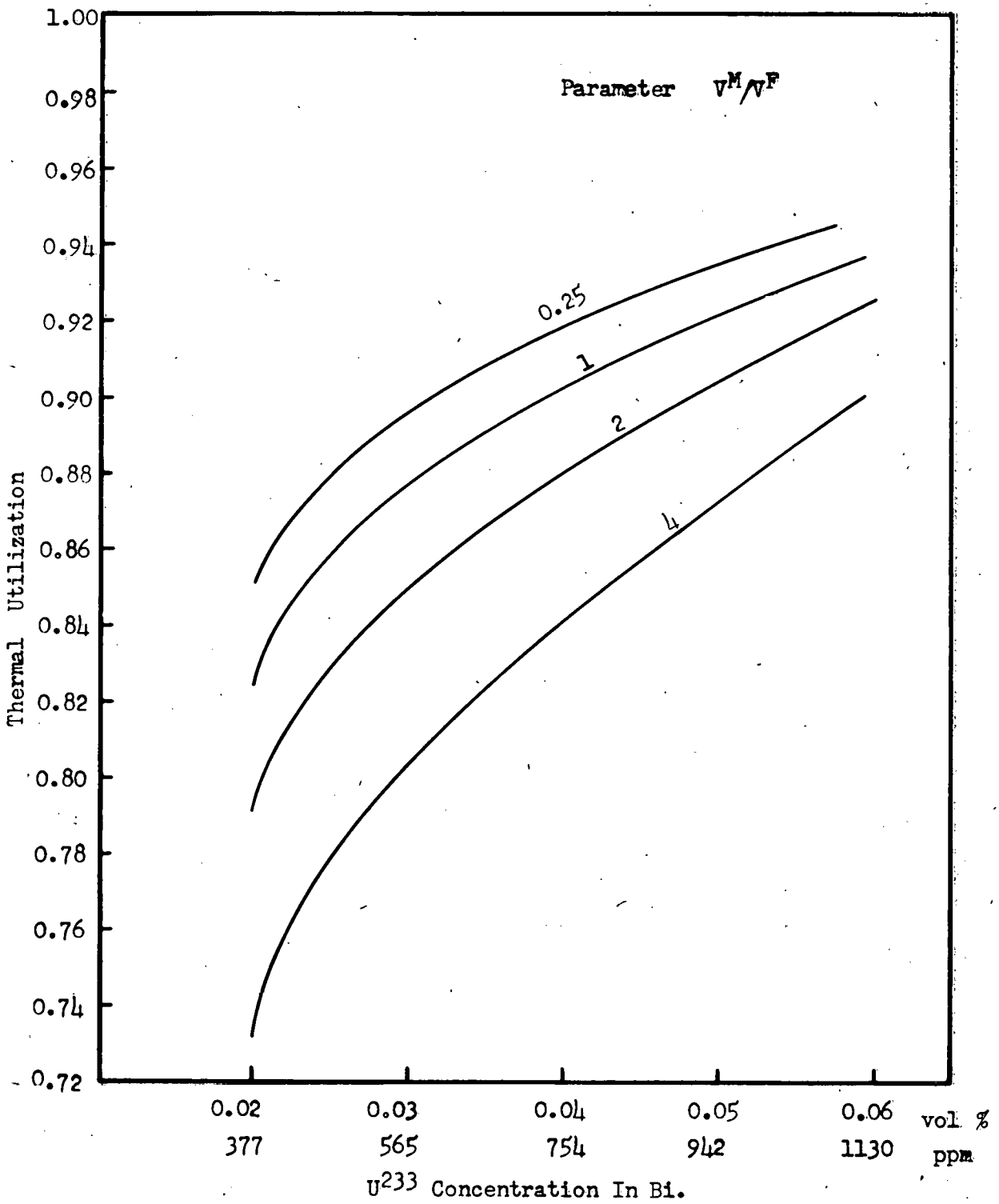

Figure 1

Thermal Utilization as a Function of U^{233} Concentration for Various Moderator to Fuel Ratios

Figure 2 32

Breeding Ratio Versus Fuel Concentration for Various V_c/V_{Bi}

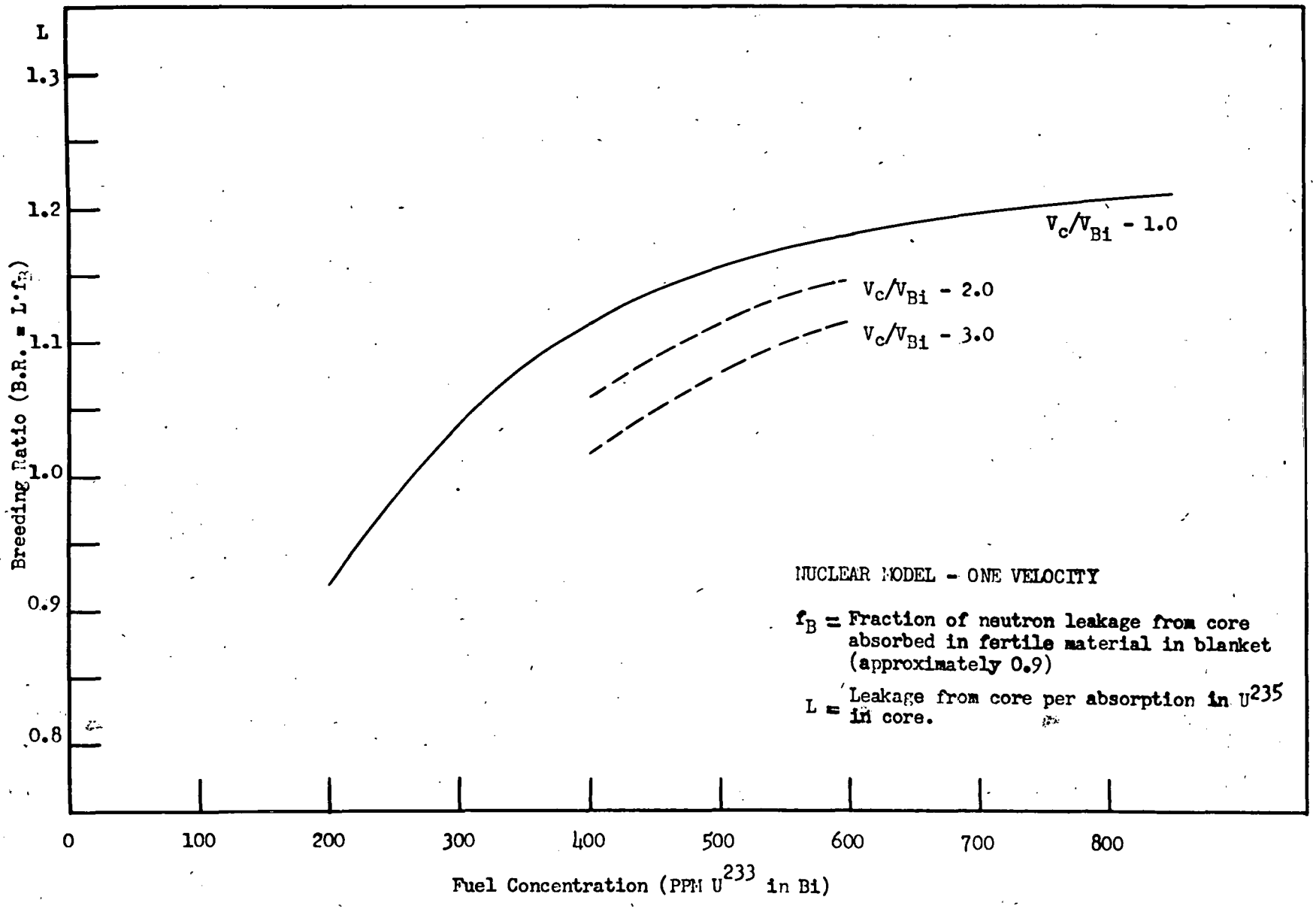

Using this ratio the critical size of the reactor is shown in Figure 3 and the critical mass in Figure 4 as a function of U^{233} concentration in the bismuth stream. For the 6 foot by 6 foot right cylindrical core configuration chosen, the critical concentration can be seen to be 390 ppm. Later more accurate two-group calculations made in determining blanket parameters showed the required core concentration to be 285 ppm.

3.2 Effect of Heat Exchanger on Core Design

In a circulating fuel reactor, one of the major holdups outside the core is in the piping from the top of the core out to the heat exchanger and then from the heat exchanger back to the core. For the flow rates required, if the fuel velocity in piping is limited to 10 ft/sec, flow area is about 6 1/2 square feet and holdup nearly 50 gallons per linear foot of pipe.

To minimize this external piping holdup, a two-pass flow pattern in the core is proposed. Fuel flows up the central region of the core, through the heat exchanger and settling annular ring, down the outside area of the core, across a header at the bottom and then back up the core center. With this arrangement the only external piping is that from the top of the core up through the moderator to the heat exchanger and that back to the outer edge of the core. Figure 5 shows this flow pattern and the heat exchanger in relation to the core and blanket.

In the initial design, the direct liquid contact heat exchanger was located in the blanket, just above the core. It became obvious, when the size of the heat exchanger was calculated, that in this position the salt was a serious poison. Therefore, the heat exchanger was moved up and three feet of reflector inserted between it and the core.

Figure 3 34

Core Radius Versus Fuel Concentration

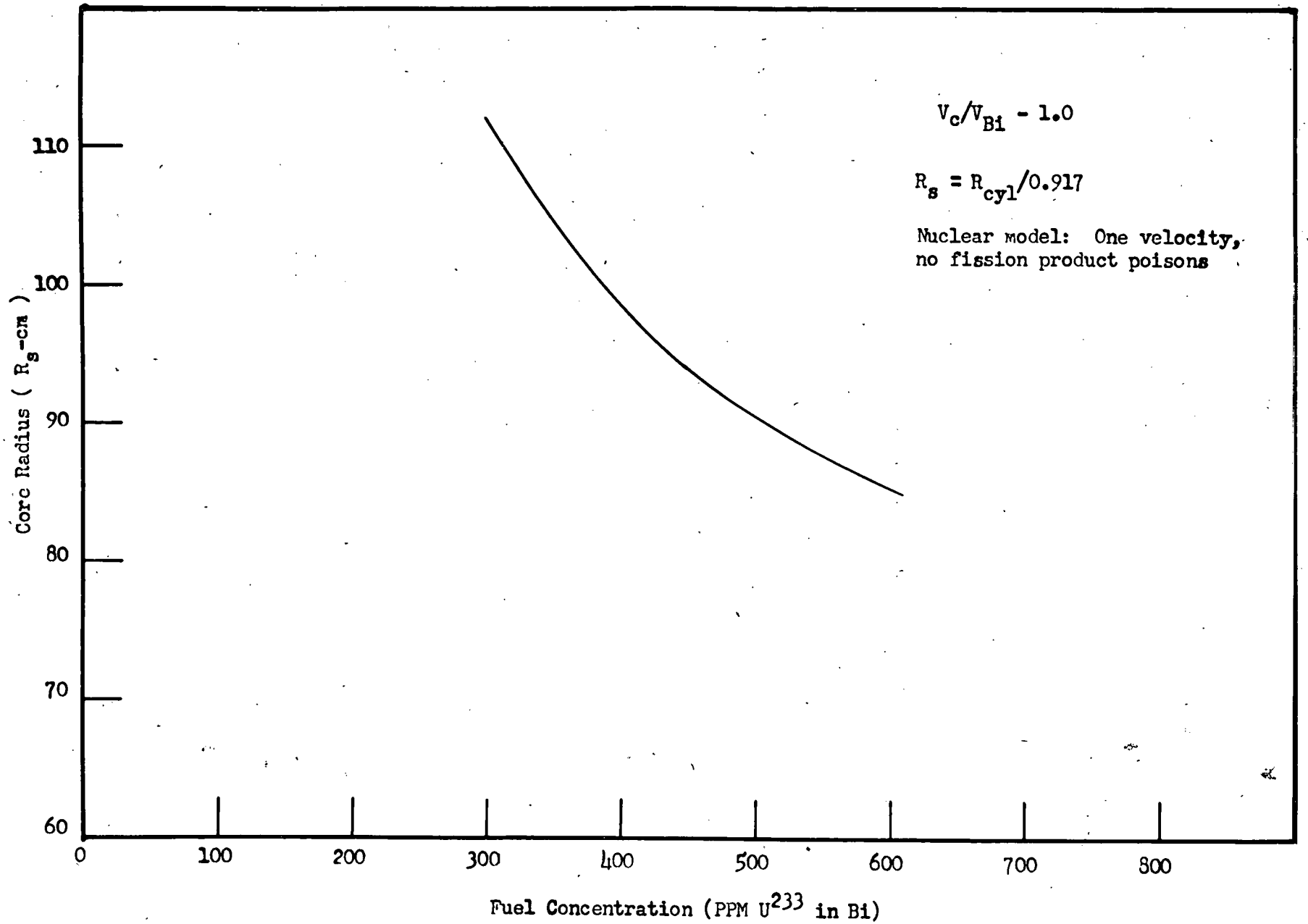

Figure 4 35
Critical Mass Versus Carbon to Bismuth Ratio
At Constant Breeding Ratio

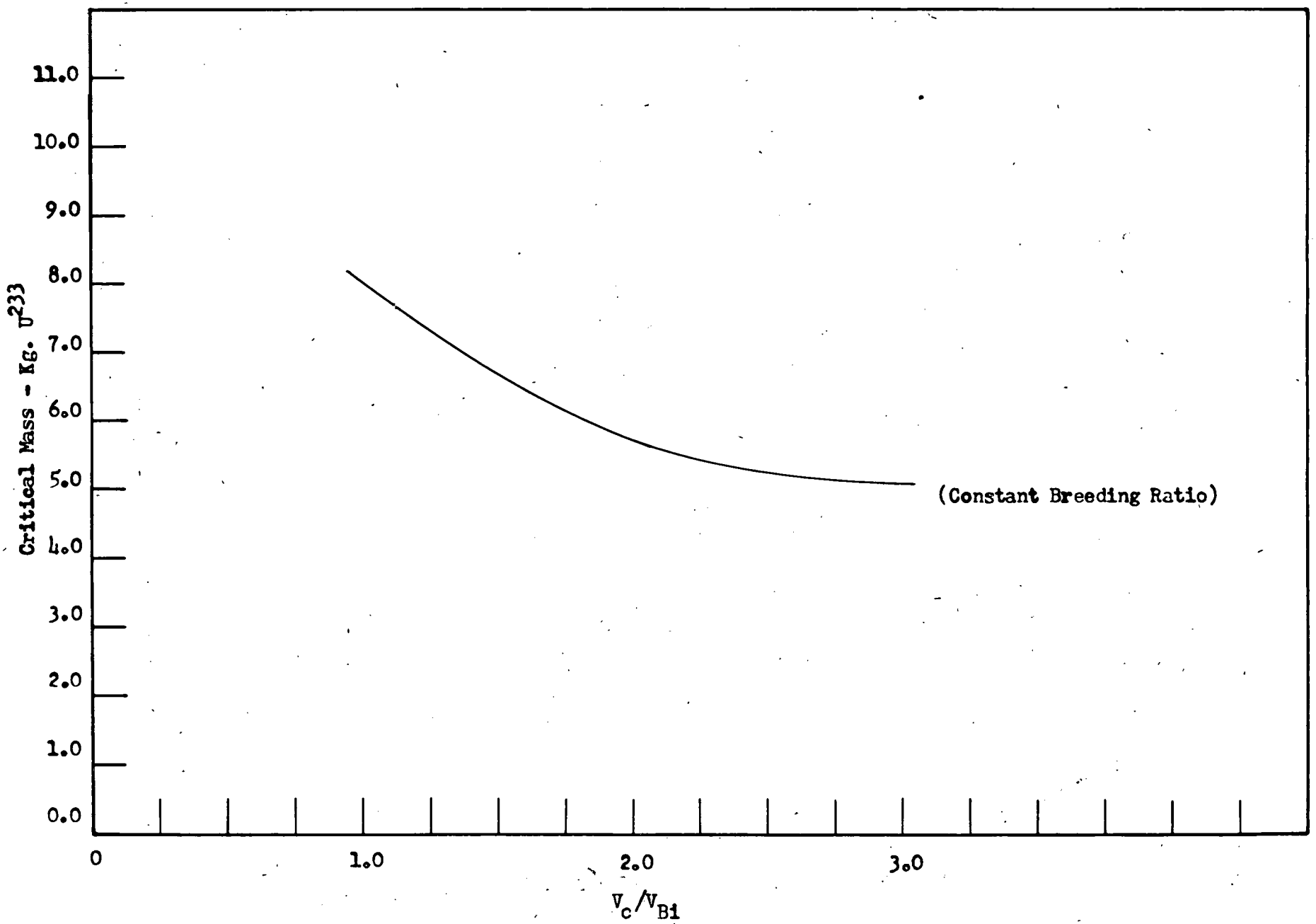

UNCLASSIFIED
ORNL-LR-DWG. 8280

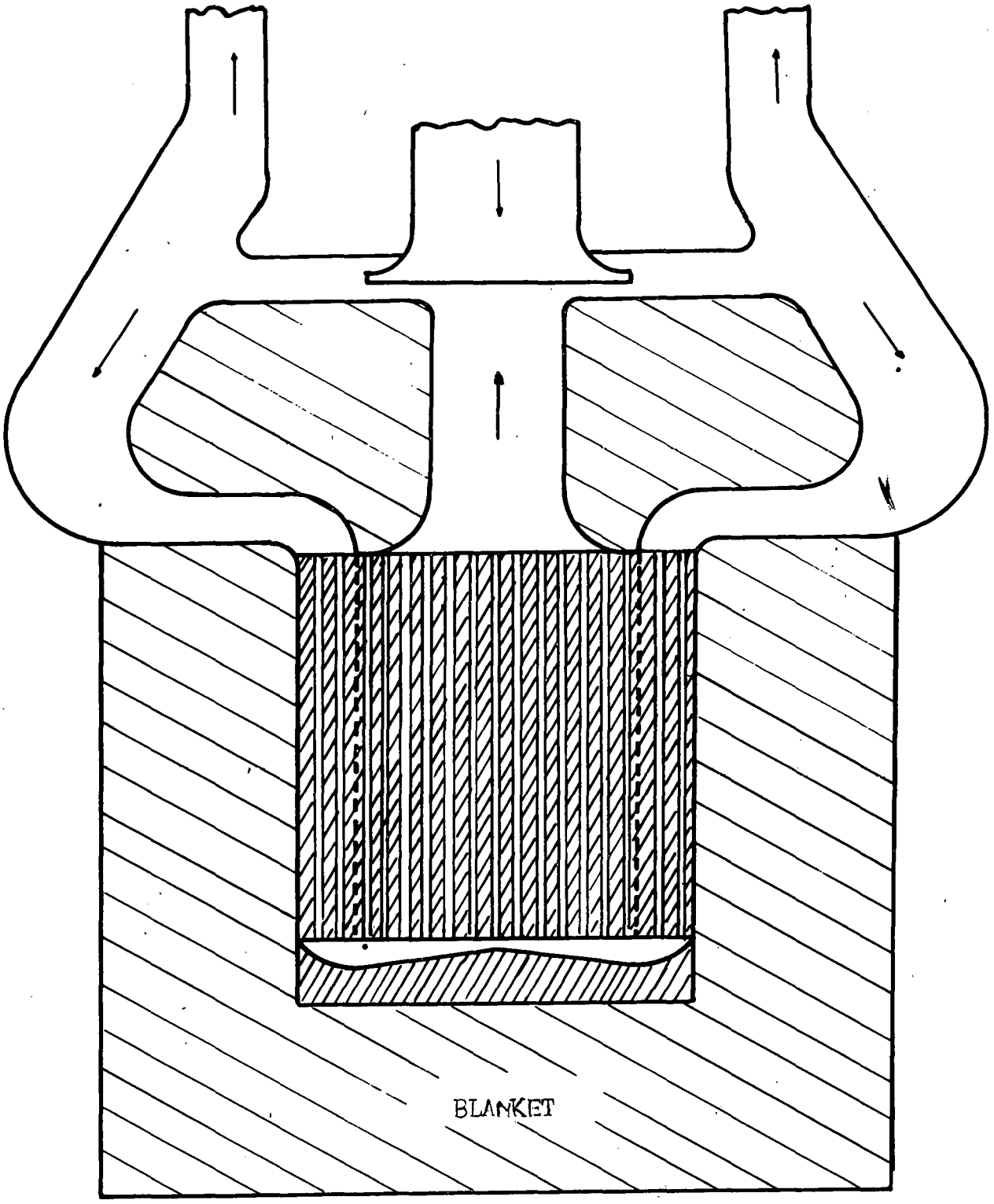

Figure 5

Reactor Core, Blanket, and Jet Pump Heat Exchanger

If it were not for the fuel entrance and exit lines from the core, the heat exchanger would capture very few neutrons. However, fuel in the lines effectively raises the concentration of U^{233} in the blanket segment on top of the core to a much higher level than in the rest of the reflector, thus increasing flux and fast leakage. An adequate mathematical analysis of the effect was not developed, so the exact effect of the heat exchanger is unknown. In essence, the heat exchanger should not be considered a neutron poison at its location above the reflector, since the problem of entrance and exit lines is present in any design.

3.3 Flow Arrangement - Pressure Drop

When the nuclear calculations pointed out the advantage in going to low moderator to fuel ratios, several core configurations were investigated to determine how low this ratio might conveniently be made. It was agreed that the fuel passages should be circular holes in solid moderator blocks to simplify fabrication.

The effect of the tube size on nuclear homogeneity was investigated. For a 1 1/2 inch tube, flux depression in the center of the tube was considerably less than one per cent, so there was no disadvantage is using large size tubes from a nuclear standpoint.

The pressure drop through the core was then calculated for various tube sizes and core diameters assuming a fixed temperature rise across the core. The curves are shown in Figure 6. It can be seen that for tubes larger than about one inch in diameter, pressure drop through the core decreases very little with increasing tube size. In this range, most of the pressure drop is in contraction and expansion losses which are essentially independent of tube size. A 1 1/2 inch fuel tube diameter was chosen for reference

UNCLASSIFIED
ORNL-LR-DWG. 8281

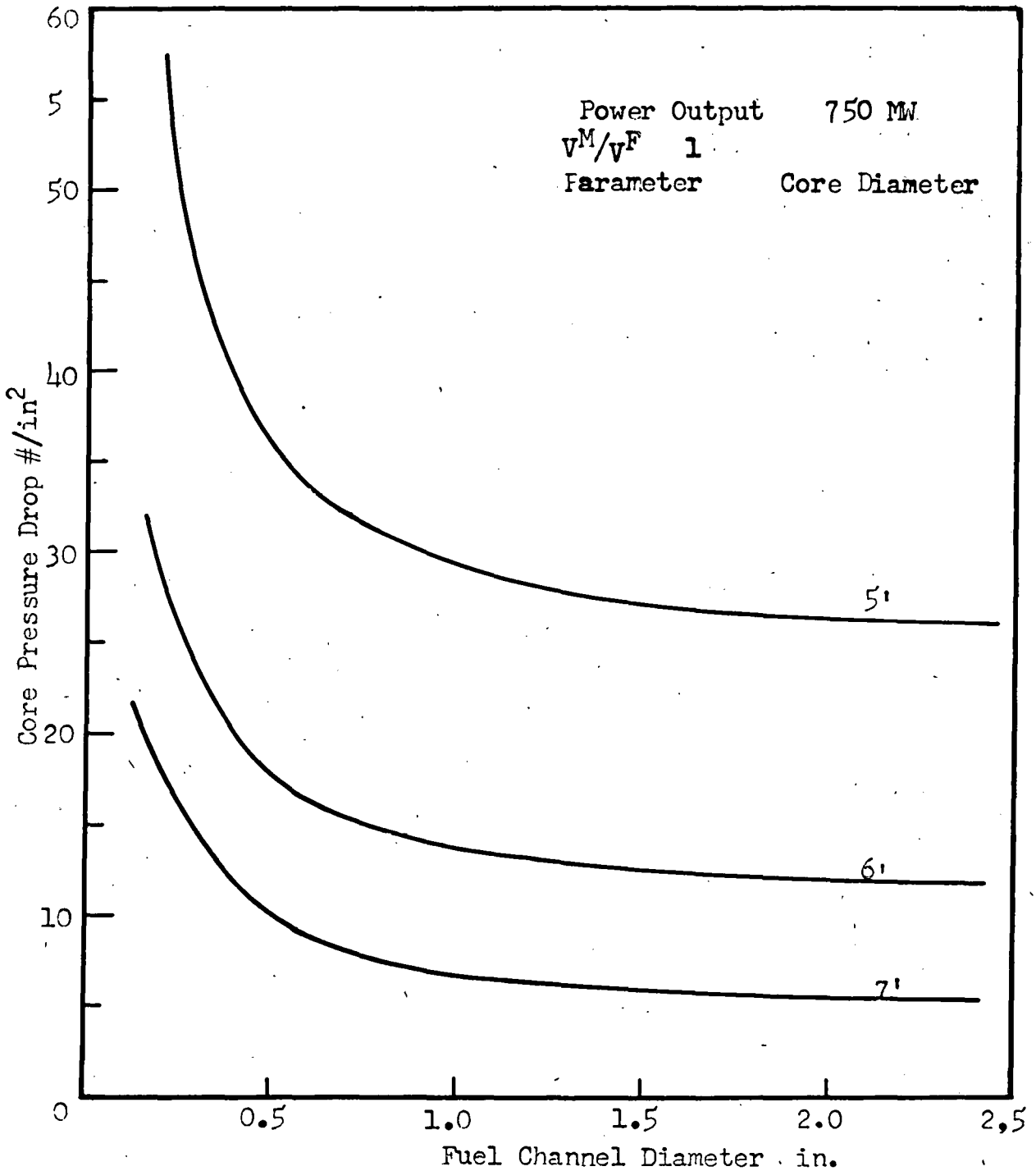

Figure 6

Pressure Drop Versus Fuel Channel Diameter for Various Core Diameters

design, though there would be definite advantages in going to even larger size tubes for ease of fabrication. The core contains 1152 1 1/2 inch diameter tubes. For a diameter of 2 1/2 inches, this number would be reduced to 415.

The lower limit of moderator to fuel ratio is determined purely from structural considerations. With 1 1/2 inch tubes, the min. spacing between tubes for V_m/V_f ratio of one is only 0.52 inches. It was felt that mechanical strength would be seriously impaired if the holes were spaced closer, though in the LMFR design a 0.833 V_m/V_f ratio is proposed with 2 inch tubes.

All flow rates were based on a temperature rise of 500°F in the core. While this is high compared to the 300° proposed in the LMFR, there are certain definite reasons why, in the proposed design, a higher temperature rise is feasible. In the LMFR, the temperature rise is limited by mass transfer in the heat exchanger tubes, and this problem does not exist in the direct fluid contact cooled reactor. The factors limiting temperature rise are the lower temperature limit, set by the melting point of the fused salt coolant and the upper limit set by structural strength limitations or corrosion. In the core itself temperature is limited only by the uranium- carbon reaction at about 1000°C*. At this temperature corrosion in the jet for any structural material other than graphite would probably be excessive, and it may not be feasible to use graphite with the high jet velocities required. For the temperature rise of 433°F, the upper fuel temperature is still over 1400°F, which is surely near an upper temperature limit for any structural material other than graphite.

---

*F. T. Miles, personal communication.

As shown previously, breeding ratio is improved by higher fuel concentrations and thus smaller core sizes. A compromise was, therefore, required between a small core to give better breeding and a large core to decrease pressure drop. From Figure 7, it is seen that pressure drops become excessive when core diameter is below about 6 feet. At this diameter, breeding ratio is still nearly 1.0, so for reference design this diameter was chosen. At the design conditions of 1 1/2 inch fuel tubes and 6 inch diameter, pressure drop through the core is about 12 psi. This includes losses in the cross-over header below the core.

It is quite likely that it is not advantageous from an economic viewpoint to build a two-region breeder of this power capacity. At a lower power, the core could be made smaller and breeding ratio improved considerably. One alternative, as proposed for the LMFR, is to make the core height less than the diameter to increase leakage to the blanket for breeding and still retain sufficient flow area for low pressure losses

3.4 Fission Product Poison Fraction

For critical core concentration calculations, a poison fraction of 0.05 was assumed. This is defined as absorption in fission product poisons per absorption in fuel. Continuous contacting of the fuel with coolant keeps fused salt soluble fission products very low. The bulk of the poisoning is due to the coolant insoluble fission products. A fuel processing cycle of 173 days will keep the poison fraction below 0.05. Coolant is processed on about a 20 day cycle to remove the soluble fission products.

3.5 Poison Effect of Entrained Coolant

Any coolant entrained in the fuel solution will constitute a serious poison problem in the core because of the high nuclear cross section. A

Figure 7
Core Velocity and Pressure Drop Versus Core Diameter

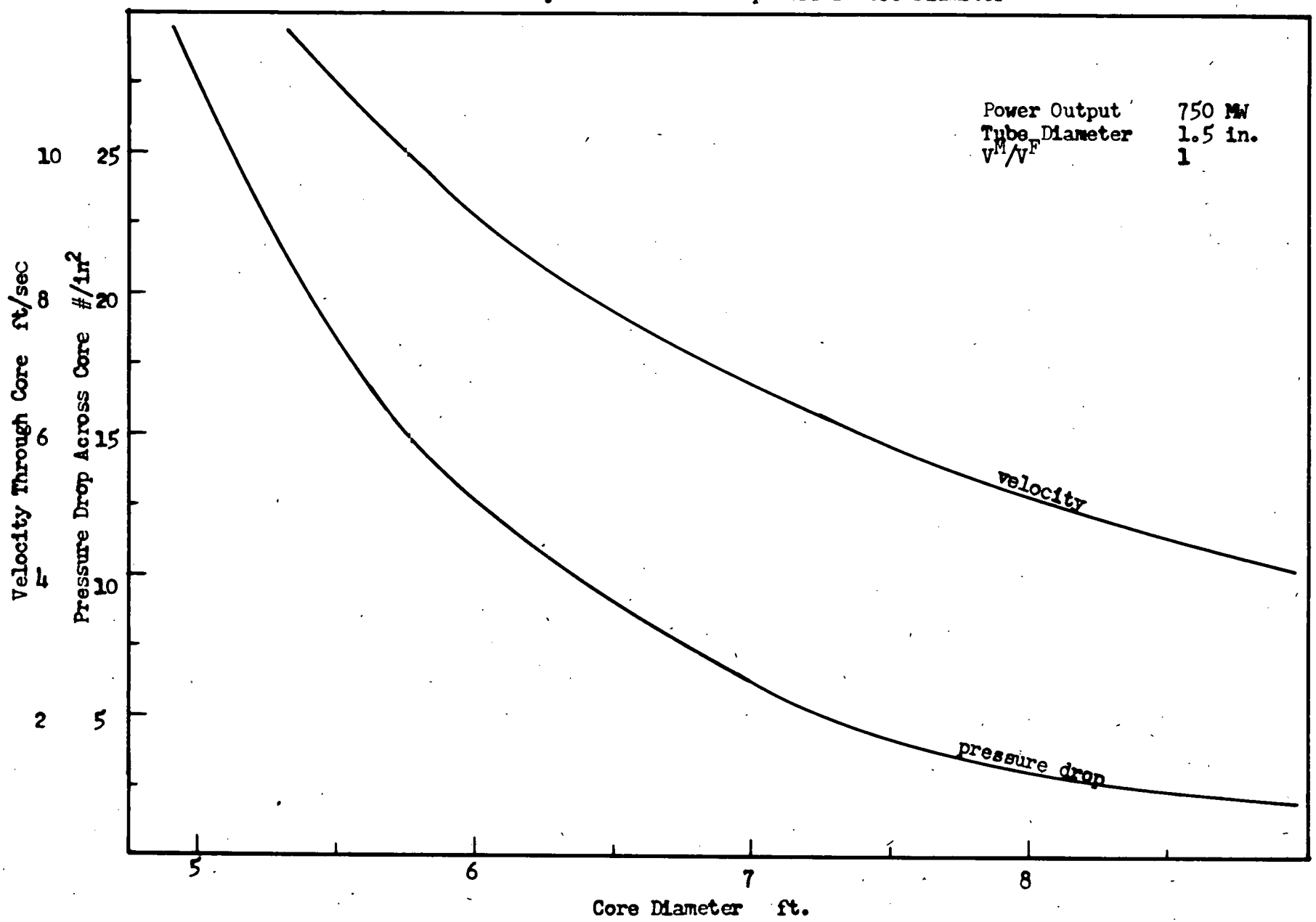

ORNL-LR-Dwg.-10183
UNCLASSIFIED

volume fraction of only 8×10^{-5} constitutes the same poisoning effect as the assumed 0.05 fission product poisoning. It would be quite optimistic to predict that entrained coolant could be kept at or below this figure. Only experimental evidence could fully determine how serious the problem might be. Experience with chemical processing studies at Brookhaven National Laboratory have shown qualitatively, at least, that phase separation is quite rapid. Actual laboratory studies are needed to produce quantitative evidence of the complete separation required.

Even if it were shown that entrained coolant could not be kept below the required figure, the proposed design might prove feasible using a fused salt with lower cross section. As pointed out previously, the only reason for choosing the LiCl-KCl eutectic for the coolant was that experience at BNL had shown this to be compatible with the U-Bismuth fuel solution. If the $NaF-BeF_2$ eutectic could be used as coolant, entrainment could be 64 times as high and still give a poison fraction of only 0.05.

4.0 BREEDING BLANKET

4.1 General Considerations - Blanket Configuration

Because of the complexity of the immiscible liquid cooling of the core solution, the only feasible means of breeding is in the external blanket of a two-region reactor. As pointed out previously, the proposed reactor core is probably too large for economic breeding in an external blanket, but no practical one-region reactor design could be envisioned which still utilized the basic idea of immiscible liquid cooling.

It was arbitrarily decided to remove the heat from the blanket in a conventional shell and tube heat exchanger, utilizing the heat for superheating

to improve steam conditions since the blanket bismuth stream is about 230°F hotter than the fused salt stream in the boiler.

In the limited time available, no attempt was made to complete the blanket flow design. On the side and bottom of the core, no difficulties would be encountered in locating the breeding solution flow passages. On top of the core where the core entrance and exit lines take up a good fraction of the total volume, location of flow passages and headers might prove more difficult. The flow passages were presumed to be similar to those in the core, circular holes in graphite blocks.

The proposed breeding solution is the one developed at Brookhaven for the LMFR, a dispersion of thorium in bismuth. They have found that a concentration of 10% thorium by weight is the maximum that can be conveniently pumped. At this concentration, the viscosity of the dispersion is about 10 times that of pure bismuth.

The effect on nuclear homogeneity was checked by calculating the mean free path for absorption of resonance neutrons, which is about 200 cm. Thus, there can be little flux depression of resonance neutrons in the flow passages and resonance escape can be calculated from a homogeneous model. In the thermal region flux depression has little effect on thermal utilization, because the macroscopic cross section of the moderator is only in the order of 5% of the total absorption cross section.

4.2 Two-Group Study of Blanket Variables

While the critical mass of the core and effect of core size on breeding could be estimated with sufficient accuracy from the modified one-velocity nuclear model used for the core parametric study, this model is of

little use for a study of blanket variables, such as thickness, carbon/breeding-slurry volume ratio and U^{233} concentration. The main factors of interest were the power generation in the blanket and the breeding ratio.

Reactors with 16 different blanket configurations were calculated on the ORACLE, using the two-group, two-region code in spherical symmetry. Results obtained were: (1) critical core concentrations, (2) fast and thermal flux plots, and (3) complete neutron balances. The variables studies were blanket thickness from 2 to 4 feet, U^{233} concentration from 100 to 300 ppm, and moderator/blanket-slurry ratios of 1 and 2.

From Figure 8 it is seen that the power generation in the blanket is affected only by the U^{233} concentration, and is essentially independent of blanket thickness and carbon to slurry ratios.

Breeding ratio also proves to be an important function of only one variable--blanket thickness. In Figure 9 a sharp drop in breeding ratio is noted for blanket thickness below three feet while above three feet breeding ratio increases very slowly with thickness. Increasing the carbon to slurry ratio from 1 to 2 decreases the breeding ratio by less than 1%. This decrease is due to increased absorption of neturons in graphite, but is partially offset by a decrease in fast leakage as shown in Figure 10. At the higher carbon/slurry ratios, the increased amount of carbon aids in thermalization of fast neutrons.

In choosing a blanket design, chemical processing cycles had to be considered since uranium concentration is controlled by the cycle time. The basic aim of the reactor design--minimization of fuel holdup--was also an important factor.

UNCLASSIFIED
ORNL-LR-DWG. 8620

45

Figure 8

Power Fraction in Blanket Versus Blanket Thickness at Various Blanket Concentrations

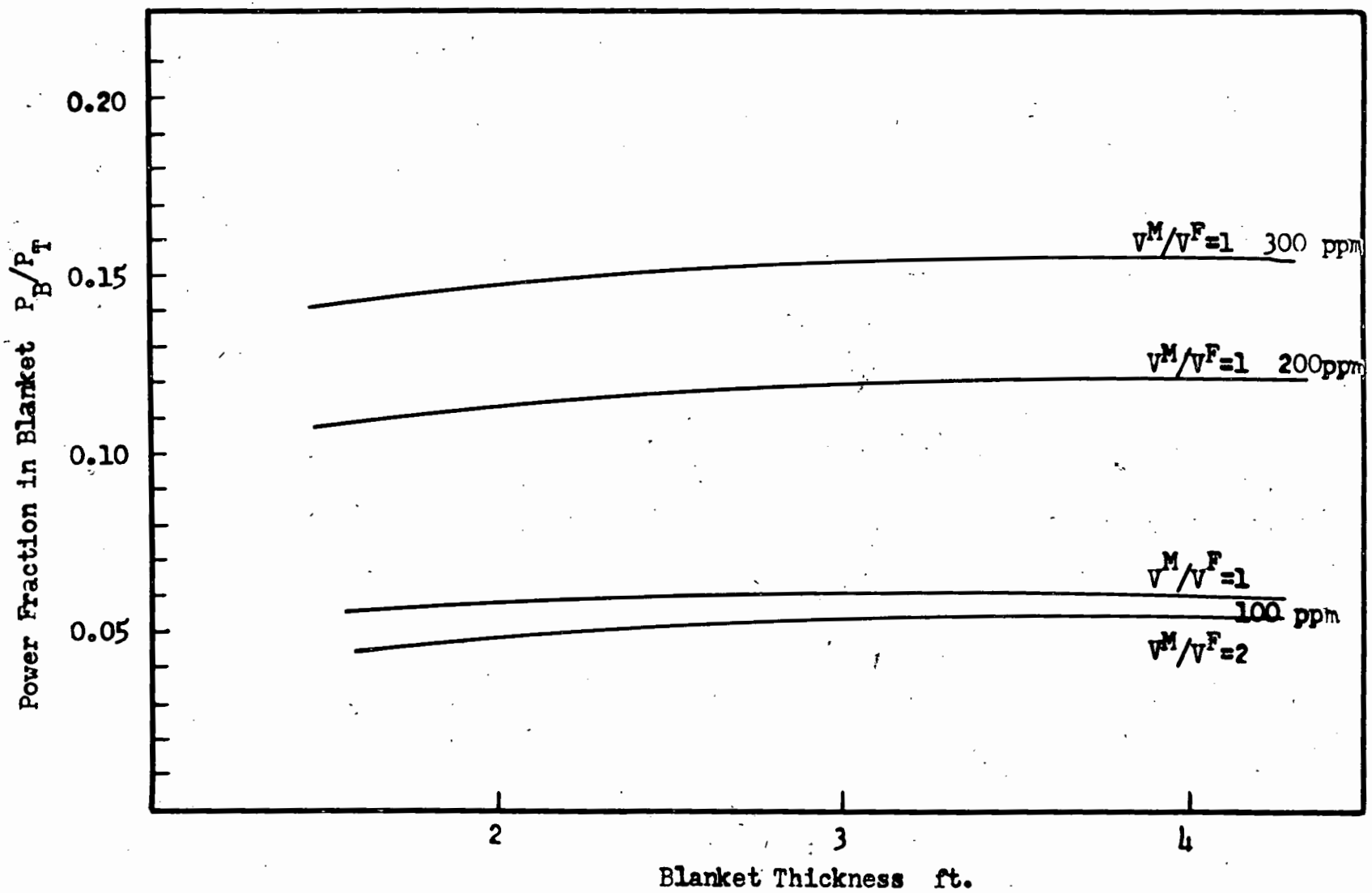

UNCLASSIFIED
ORNL-LR-DWG. 8622

Figure 9 46

Breeding Ratio Versus U^{233} Concentration in Blanket for Various Blanket Thicknesses and Moderator to Bismuth Ratios

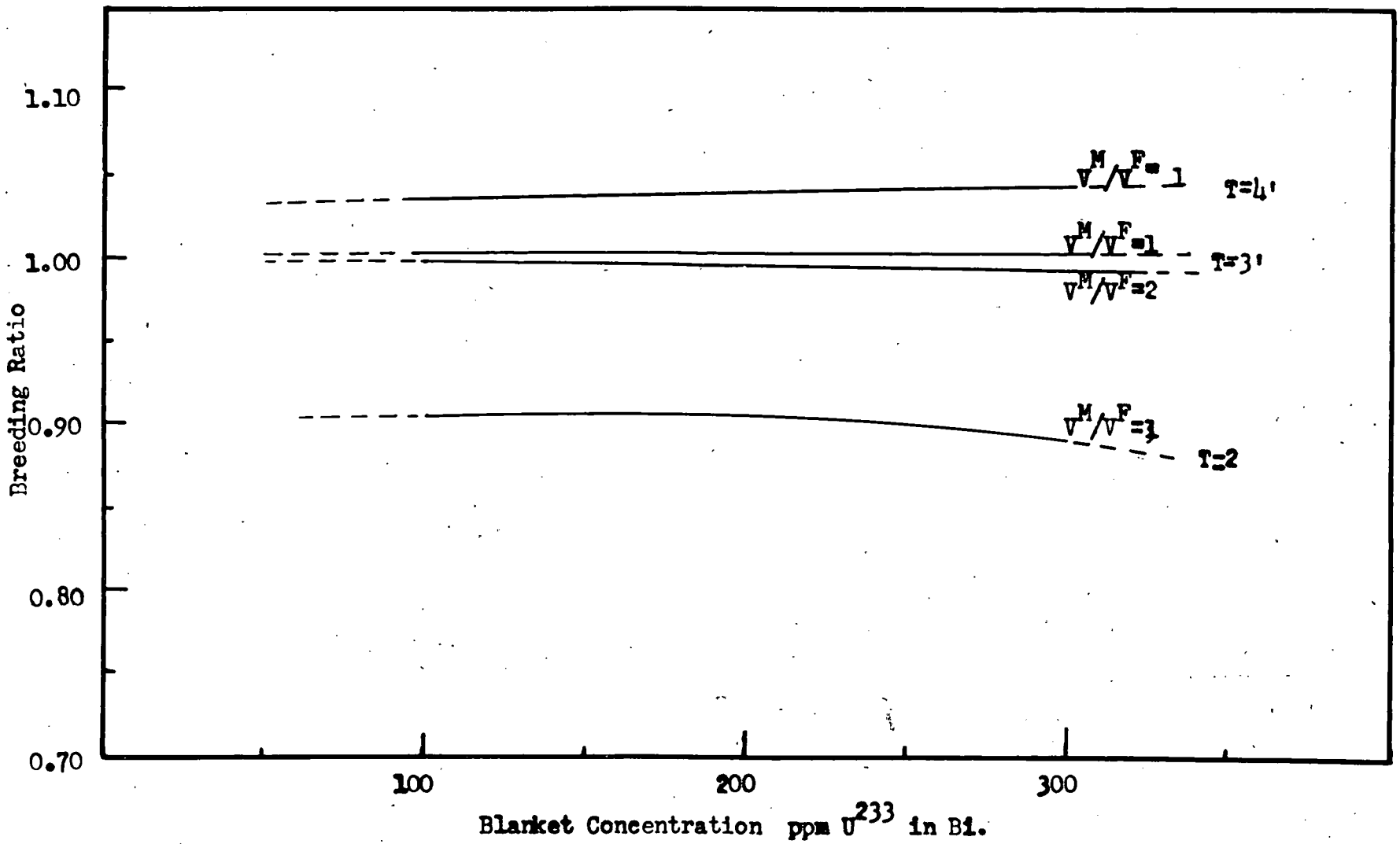

ORNL-LR-Dwg.-10184
UNCLASSIFIED

Figure 10
FAST AND THERMAL LEAKAGE FROM BLANKET VERSUS BLANKET
THICKNESS FOR VARIOUS FUEL CONCENTRATIONS AND MODERATOR RATIOS

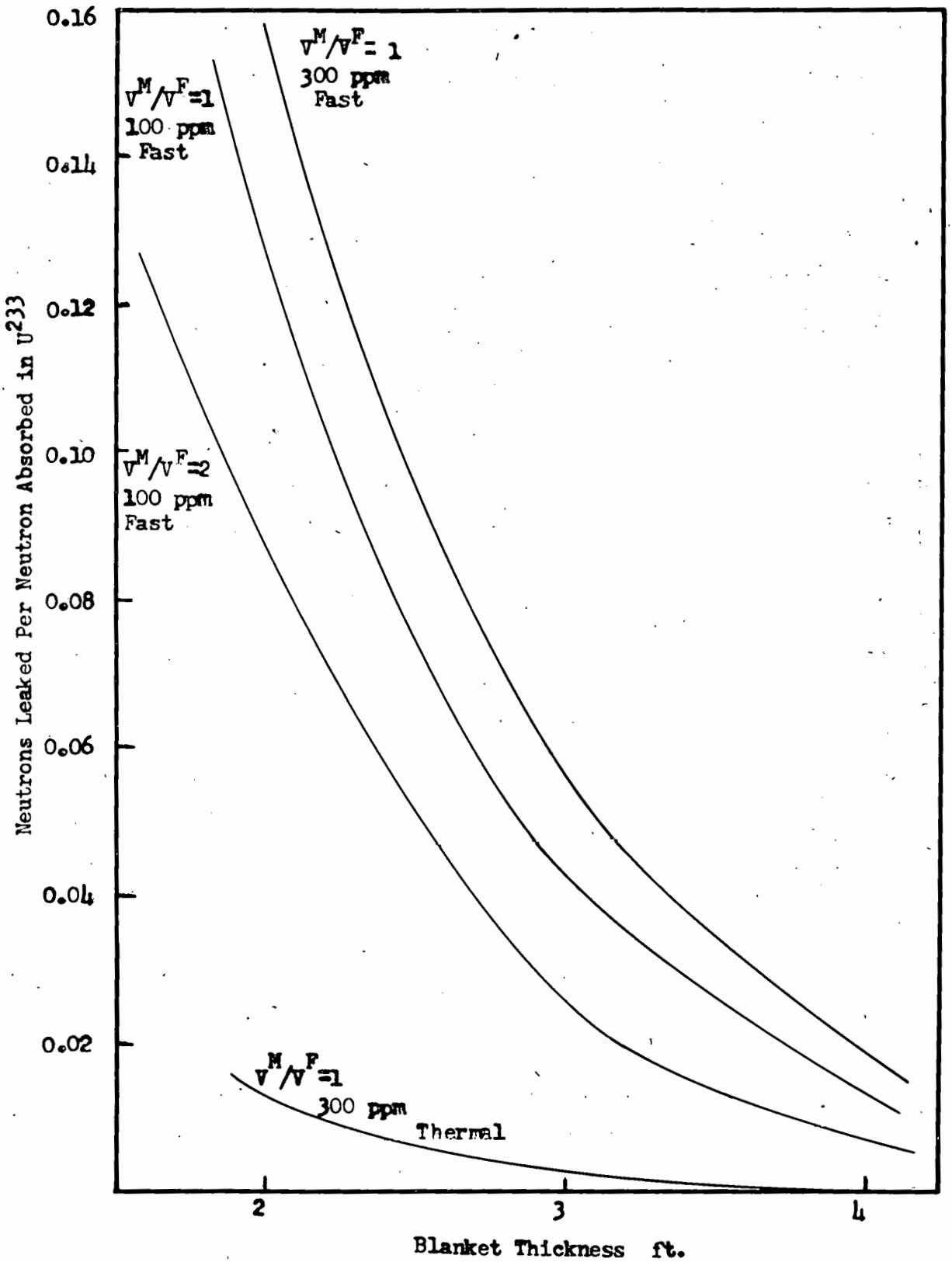

As a first approximation, the volume of slurry processed per unit time for recovery of U^{233} is inversely proportional to U^{233} concentration in the slurry. Thus, the flow rate through the chemical processing plant is only about 1/3 as great with a U^{233} concentration at 300 ppm as with 100 ppm. For this reason, the highest concentration calculated was chosen. It is conceivable there would be advantages in going to even higher concentrations to further reduce processing rates. As the concentration increases, the fast leakage also increases, and this adversely affects breeding. However, at a concentration of 300 ppm, the breeding ratio is only about 0.005 less than at a concentration of 100 ppm. To minimize bismuth and uranium holdups, the 2:1 carbon to slurry ratio was chosen for the blanket design. Again, this variable was not studied over wide enough ranges to determine limiting conditions, but it is apparent that breeding ratio would continue to drop as the ratio increased. A blanket thickness of 3 feet was deemed adequate. Slightly higher breeding ratio could be attained by going to a four feet blanket at the expense of increasing the blanket volume 67 per cent.

At the reference design conditions of 300 ppm uranium concentration, 3 feet thickness and carbon to slurry ratio of 2, 15.6 per cent of the reactor power is generated in the blanket, with an average thermal flux (in the blanket) of 1.29×10^{14} and an average fast flux of 3.5×10^{14}. Complete flux plots for the reference design reactor are shown in Figure 11. It should be noted that approximately one-half of the fissions in the blanket take place in the fast range (above 0.065 ev) indicating a serious deviation from a true thermal reactor. The two-group model used for these calculations in not really adequate for a reactor deviating this far from a thermal system, so some of

UNCLASSIFIED
ORNL-LR-DWG. 8621

Figure 11

Spatial Flux Distribution for Reference Design Reactor

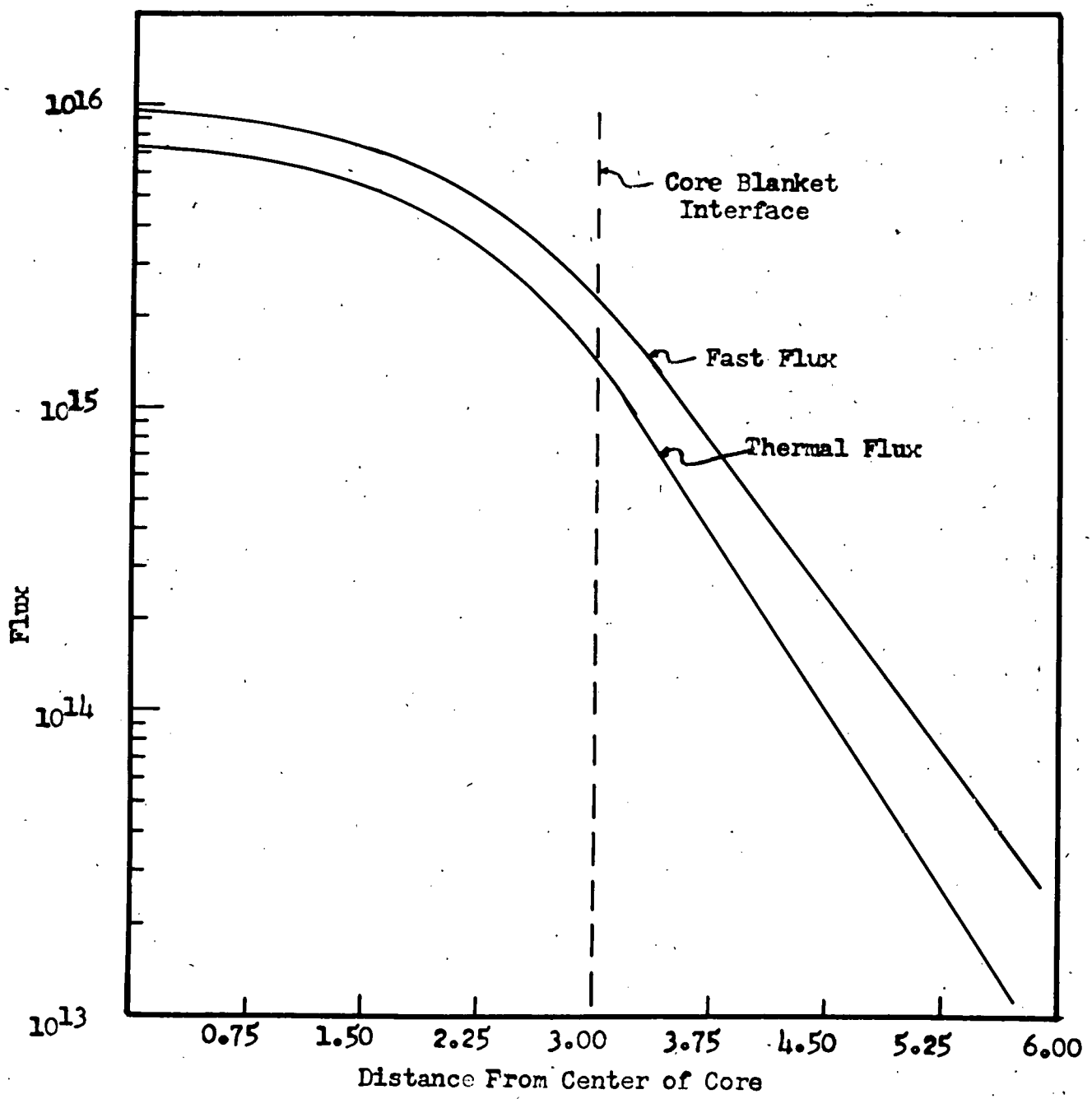

the absolute values may be in error. However, all trends should be predicted with sufficient accuracy.

4.3 Neutron Losses In Proactinium and Fission Products

In making the above calculations a poison fraction of 0.05, which included protactinium plus fission product losses, was assumed. From the average flux, and slurry volume, a processing cycle of 34.7 days is required to maintain the 300 ppm U^{233} concentration. This corresponds to a processing flow rate of 0.068 gpm. From this cycle the concentration of Pa poison fraction due to Pa and loss by neutron capture was calculated. The poison fraction due to Pa is 0.07, which is higher than the total assumed poisons in the blanket, so a correction was made to the calculated breeding ratio by substracting the captures in Pa per capture in U^{233} atoms from the breeding ratio. This decreased the breeding ratio 1.5 percent. Removal of fission products from the bismuth recycle stream in the blanket processing cycle could be easily adjusted to maintain a poison fraction of 0.05. Since data was not available on the split of fission products between the uranium and bismuth streams (see Section 6.2), in the processing system, exact cycle conditions cannot be calculated.

4.4 Higher Uranium Isotope Build-Up

Due to captures in U^{233} a series of higher uranium isotopes grow in with time. These follow a complex pattern until equilibrium is reached, as shown graphically by Stoughton.[14] As U^{234} builds up the poisoning effect increases, then goes through a maximum and sharply decreases as U^{235} grows in and starts fissioning. For a time the fissioning of U^{235} actually overshadows the poisoning effect of U^{234} and the higher isotopes contribute more neutrons than they absorb. Then, U^{236} grows in and poisoning levels out at a poison fraction of 0.001 for our case after several years operation.

The effect on neutron economy is seen to be quite small. However, for a liquid bismuth fuel which has a limited uranium solubility the most important effect is the greatly increased total uranium concentration. Equilibrium isotope concentrations are:

U^{233} = 285 ppm
U^{234} = 160 ppm
U^{235} = 21 ppm
U^{236} = 324 ppm
Total = 790 ppm

Isotopes beyond U^{236} may be neglected with little loss in accuracy.

4.5 Overall Neutron Balance

For the reference design reactor, overall neutron economy is shown in the following table. Note that in the calculations, the factor η (neutrons produced per absorption in U^{233} atoms) was assumed constant with energy. There is reason to believe that η actually decreases somewhat in the range above thermal energy. This decrease would tend to lower breeding ratio, but this tendency would be partially offset by the higher critical mass required in the core which would raise the breeding ratio. In any case, the effect is small.

Table 3

Neutron Balance for Reference Reactor

Neutrons absorbed in U^{233} in core	= .843	
Neutrons absorbed in U^{233} in blanket	= .157	
Total neutrons absorbed	= 1.0	
Neutrons produced	= 2.31	
Absorption in:		
U^{233}	= 1.000	
Carbon in core	= .047	
Bismuth in core	= .135	
Thorium in blanket	= .992	
Carbon in blanket	= .016	
Bismuth in blanket	= .023	
Fission products	= .050	
Higher uranium isotopes	= .001	
Proactinium	=(0.015)*	Not included in two-group nuclear calculation
Fast leakage	= .039	
Thermal leakage	= .014	
Total	2.31	
Net breeding ratio	= 0.992-0.015 = 0.977	

5.0 DIRECT LIQUID CONTACT HEAT EXCHANGER

The removal of heat from a liquid fuel by direct contact with an immiscible liquid coolant medium was the basis for a preliminary design of a spray type heat exchanger at Brookhaven National Laboratory[4].

In the present study two types of heat exchangers were considered in which direct contact of fuel and coolant is utilized for heat removal and for pumping the fuel. The fuel consists of U^{233} dissolved in molten bismuth; a suitable coolant is the LiCl-KCl eutectic. The relative density ratio of fuel to coolant of 6 to 1 favors prompt separation of these immiscible liquids. In both exchangers the transfer of momentum from the coolant provides the circulating fuel with the required head. The disc type jet pump exchanger, selected for the reference design, is essentially a co-current exchanger, whereas, the peripheral jet centrifugal exchanger achieves partial counter current flow. In both types conditions which enhance the pumping performance do not necessarily make for desirable performance in heat transfer and separation.

5.1 Proposed Objectives of Direct Contact Exchanger

The proposed objectives of exchanging heat and momentum by direct liquid contact are as follows:

a. To eliminate temperature drop across the tube wall in the process of heat transfer.

b. To decrease the fuel volume holdup (and hence, the fuel investment) in the primary heat exchanger.

c. To reduce the size and cost of the exchanger.

d. To decrease the external radiation level of the primary exchanger by reducing the holdup of active materials therein.

e. To reduce the holdup of fuel in the processing system by extracting some of the fission products during the heat transfer process.

f. To simplify the pumping of reactor fuel liquid with respect to maintenance and radiation hazard.

g. To reduce the magnitude of certain difficulties which are amplified by the presence of heat exchanger tubing, i.e., radiation damage; plugging of tubes due to mass transfer; thermal stress failure; large active area for corrosion.

5.2 Disc Type Jet Pump Exchanger

Figure 12 shows a scaled drawing of the disc type jet pump exchanger which has been chosen for the reference design. The exchanger is to be located three ft. above the top of the core. This orientation is preferable to that at the core-blanket interface because of the serious poison effect of the fused salt coolant and because the jet pump structure is more accesible and in a lower radiation field. However, the external holdup of fuel and the shielding requirements are increased thereby.

A survey of the literature on liquid-liquid jet pumps indicated that no simple theoretical analysis exists by which the action of jet entrainment and mixing may be adequately described (5), (6), (7). The gross behavior has been investigated using a modification of a method given by Folson (5). It appears that even in the case of the latter, no suitable experimental data have been obtained for investigating the accuracy of the equations when two immiscible liquids of different densities are involved. Thus, the need for an experimental investigation is obvious. In the time available, two highly simplified experiments were performed by the group. These served only to provide a qualitative appreciation of problems expected and to emphasize that additional experimental work was warranted and quite feasible.

UNCLASSIFIED
ORNL-LR-DWG. 8278

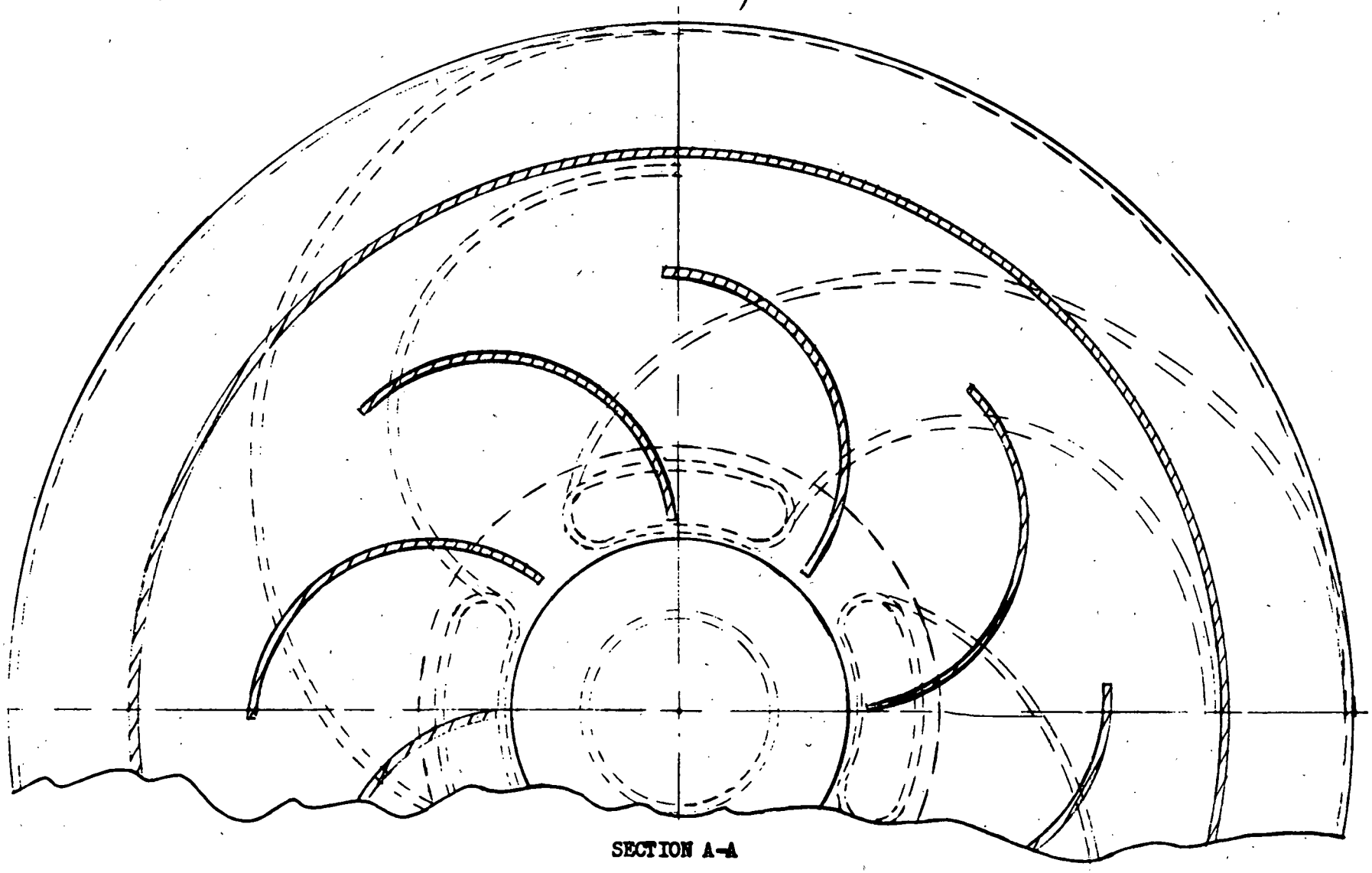

SECTION A-A

UNCLASSIFIED
ORNL-LR-DWG. 8277

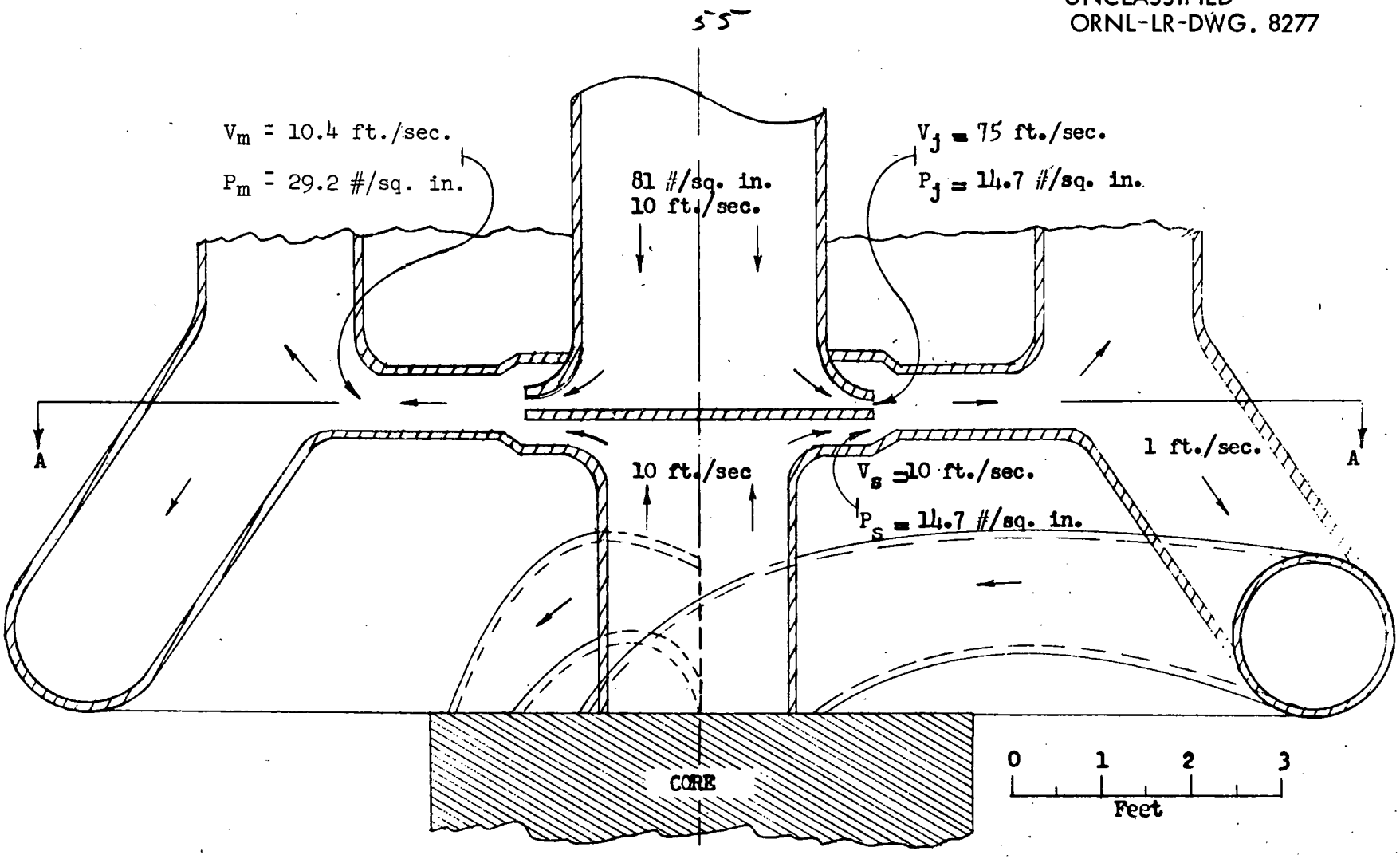

Figure 12

Jet Pump Heat Exchanger

The design of the jet pump is based on certain arbitrary assumptions together with a parametric study of the pumping, heat transfer, and separation performances. It is essential that those specifications indicated by the study which provide adequate pumping must also be compatible with the flow conditions required for proper heat transfer and separation.

The radial disc type of jet pump has been chosen in lieu of a number of linear jet pumps, symmetrically located, on the basis of simpler construction and assembly of the radial type and the associated piping.

5.21 Disc Type Jet Pump - Pumping Performance

Although there appears to be no method with which to adequately describe the behavior of the liquid-liquid jet pump in the mixing chamber, it is probably that four elementary processes are taking place therein:

(1) Acceleration of the particles of the fluid fuel by the direct impact of particles from the jet fluid.

(2) Entrainment of the fluid fuel by viscous friction at the periphery of the primary jet.

(3) Degradiation of the mechanical energy of both liquids resulting in the production of heat.

(4) Diffusion of elementary particles of both fluids where variations in density exist which produce concentration gradients.

Method of Calculation - The method of calculation, described in detail in Appendix has been to determine the change in pressure across the mixing tube for various jet velocities and coolant temperature drops, assuming a linear jet with a cylindrical mixing tube (5). Thus, the area of the linear jet is related to the area of the radial disc type jet and the velocity and pressure adjusted accordingly. Since the calculation is at best an approximation of gross behavior, further refinements to account for certain losses were not

carried out. These losses include: boundary layer losses, eddy current losses, and losses due to incomplete mixing.

On the basis of prelinimary calculations, estimated materials characteristics, and from purely arbitrary considerations certain quantities were fixed for the final calculation. These are:

Velocity of the suction liquid at the jet nozzle	10 fps
Pressure of suction and driving liquids just outside the jet	14.7 psia
Coolant velocity in the downcomer	20 fps
Ratio of jet disc radius to downcomer radius	1.5
Horizontal radius to the end of the mixing tube	4 feet
Reactor power generation (heat)	750 Mw
Temperature drop in the fuel	500°F

Those parameters which were varied in the final calculation are:

Coolant jet velocity	50 - 100 fps
Coolant temperature rise	125 - 500°F

The results of the calculations are presented graphically in Figures 13 and 14. The heat gained by the fuel vs. jet velocity is plotted in Figure 13 for various ratios of fuel to coolant change in temperature. Pressure drop through the core, including a small gain due to thermal pumping, is about 12 psi. At high volume rates of coolant flow, the required head may be developed at a relatively low jet velocity. However, the high volume rates of flow reduce the exchanger holdup time and hence, affect heat transfer and separation adversely. On the other hand, the low coolant flow rates require a much higher jet velocity to impart the required head to the fuel. Thus, a design condition is selected which will develope the required

UNCLASSIFIED
ORNL-LR-DWG. 8283

Figure 13

Typical Jet Pump Performance

Head Gained by Fuel in Jet Pump vs Jet Velocity

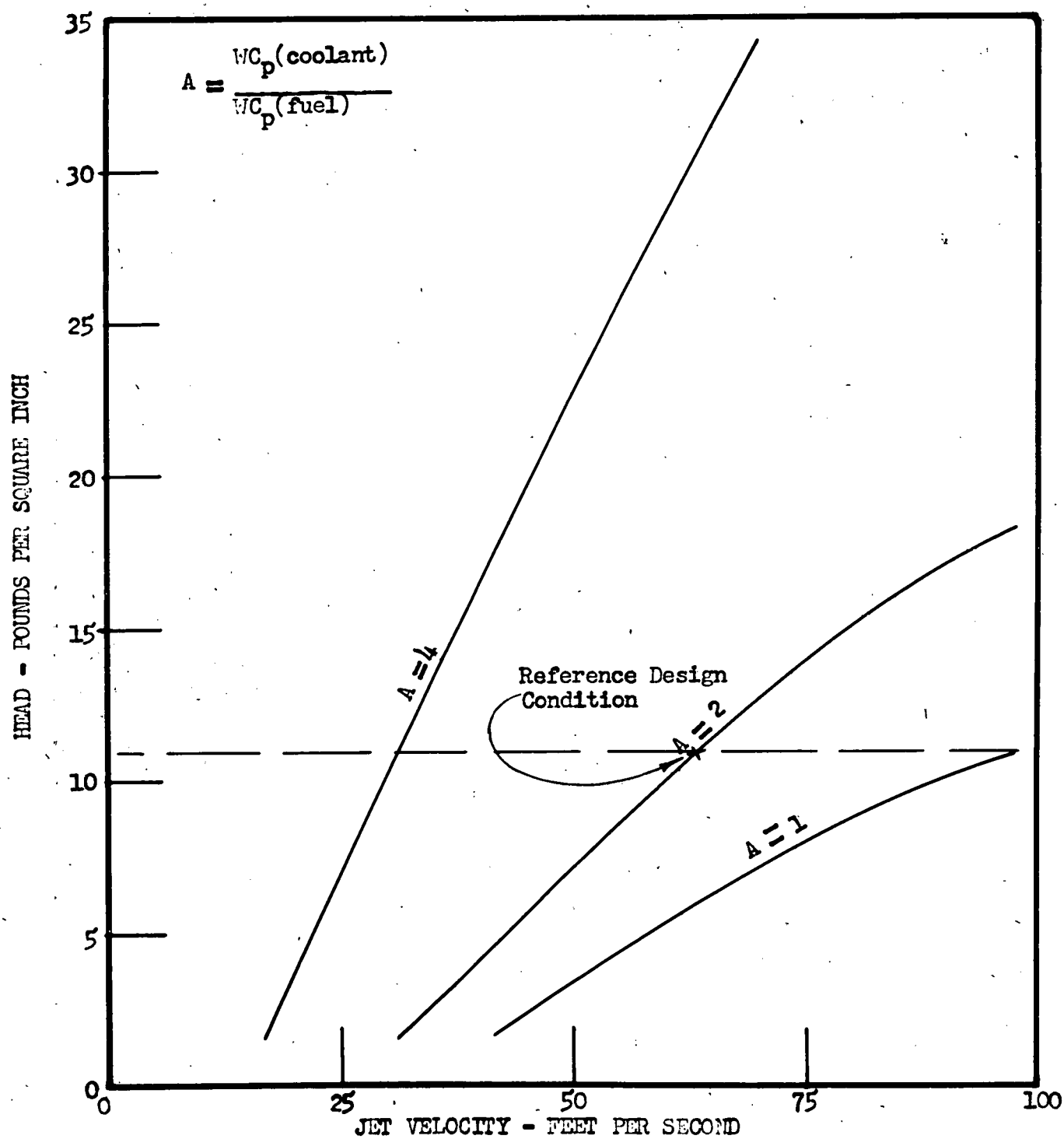

UNCLASSIFIED
ORNL-LR-DWG. 8285

Figure 14

Typical Jet Pump Performance

Theoretical Jet Pump Efficiency vs Jet Velocity

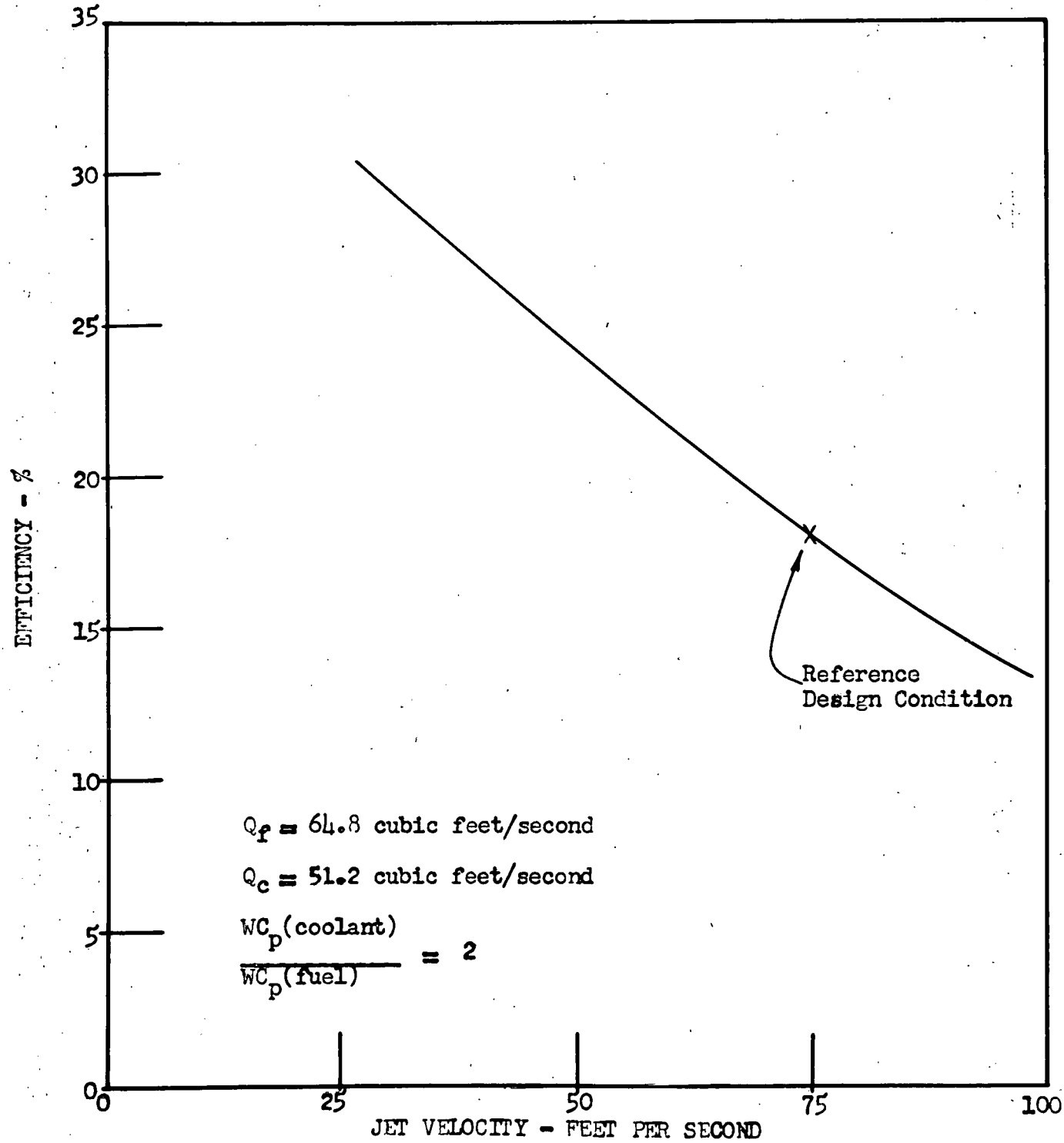

fuel head at the lowest coolant flow rate and the lowest feasible jet velocity. The configuration selected has the following characteristics:

Temperature change in the coolant	250°F
Coolant to fuel volume flow rate	1.58
Jet velocity	75 fps
Jet height	0.0113 pt
Velocity at exit of mixing tube	10.3 fps
Total head gained by fuel	2119 psf
Theoretical mechanical efficiency	20%
Fuel Holdup	2105 gal

The theoretical mechanical efficiency, defined as the rate mechanical energy is added to the fuel divided by the rate mechanical energy is lost from the drive fluid, is plotted vs. jet velocity for various fuel to coolant change in temperature ratios in Figure 14.

Experimental Work

In a very simplified experiment mercury under atmospheric pressure was pumped by a linear jet with water as the driving fluid. The jet pump was fabricated of glass and was on a very reduced scale. In view of the lack of correspondence between the proposed model and the glass jet pump, only general qualitative observations are reported.

a. Flow in the mixing tube was quite turbulent.

b. No pumping difficulty was observed with a relatively high jet velocity and high coolant volume rate of flow. (Note that fuel to coolant density ratio is 13.6 to 1.)

c. The mercury in the dispersed phase appeared to be very small drops, of the order of 0.02 inches in radius.

d. Little separation was noted at the end of the mixing tube. For this reason a centrifugal swirling chamber and a settling chamber were joined to the end of the linear mixing tube to enhance operation.

e. The separation performance appeared to be satisfactory although it did indicate that in a mercury water system some carryover of finely dispersed particles of mercury could be anticipated in the water exit stream.

Additional Characteristics of the Design Pump Exchanger

The disc type jet pump exchanger has the following characteristics some of which may prove limiting in the light of additional experimental investigation:

a. The design pump has no moving parts.

b. The design pump has an inherently low mechanical efficiency.

c. The coolant pumping power required for the jet pump exchanger is 474 kw.

d. Erosion of the jet by the high velocity coolant may or may not be a limiting factor in the design; this conclusion must be substantiated experimentally.

e. The large temperature gradient across the jet induces high thermal stresses. For certain materials of construction this stress may be relieved by plastic flow.

f. Since the fuel flow and the coolant flow rates are not always proportional, it is essential that the coolant mass rate of flow be maintained nearly constant in order to maintain fuel circulation. Thus, it may be necessary to bypass some of the coolant around the secondary heat exchanger when the load is varied in order to maintain constant throttle steam conditions.

5.22 Disc Type Jet Pump - Heat Exchange Performance

The co-current heat exchange performance has been calculated by an adaptation of the Gurney-Lurie chart for a solid sphere in unsteady state with the surrounding medium at constant temperature. Briefly, the method consists in using the chart to calculate for a given size fuel drop and a given heat transfer coefficient, the temperature difference between the fuel drop and the surrounding coolant after a specified time interval. The fact that the coolant medium is not at constant temperature is accounted for in the calculation by taking the average of two values obtained by assuming the coolant medium constant at an upper and lower value. The details of the calculation and an explantory sketch are presented in the appendix. An exact method for analyzing this type of unsteady heat transfer is given in Reference 11.

The parameters varied in the study are:

Fuel drop radius, inches	0.02 - 0.1
Heat transfer coefficient, BTU/hr.sq.ft.F	1000 - infinity
Contact time, seconds	0.1 - 0.5

A heat transfer coefficient of 2500 was used as a suitable value for design calculations[4]. On the basis of the turbulence anticipated and on the basis of a calculation for moving spheres presented in the Appendix, 2500 is considered to be conservative. The latter calculation gives a value of 3300.

In Figure 15, the temperature difference between fuel and coolant vs. fuel drop size is plotted for various contact times. If the maximum allowable temperature difference is prescribed at 100°F, it is observed that, within the range of the plot shown, the maximum tolerable drop size is r_m=.044",

UNCLASSIFIED
ORNL-LR-DWG. 8289

Figure 15

Co-Current Heat Exchange

Fuel–Coolant Exit Temperature Difference vs Fuel Drop Radius

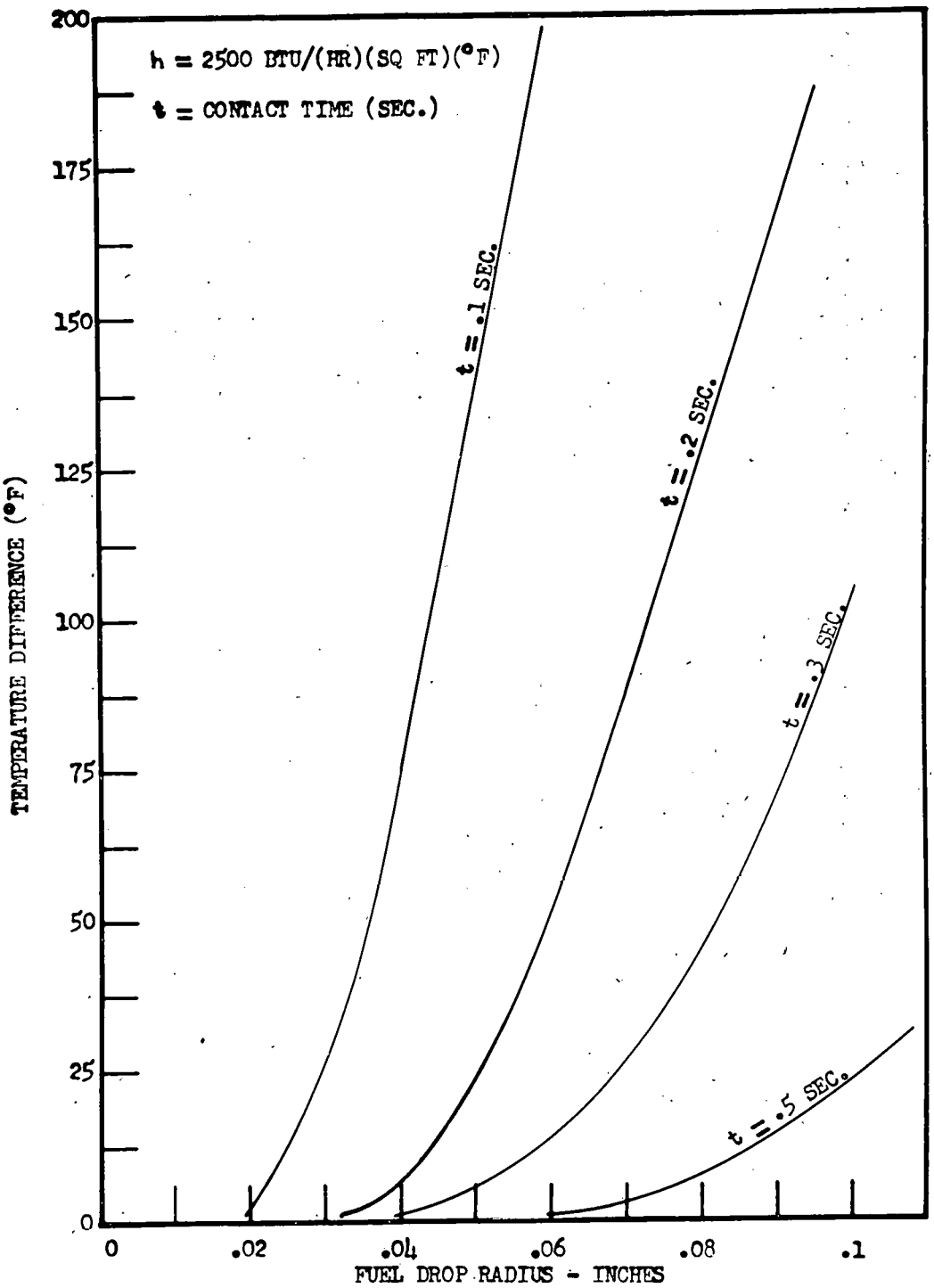

UNCLASSIFIED
ORNL-LR-DWG. 8290

Figure 16

Co-Current Heat Exchange

Fuel—Coolant Exit Temperature Difference vs Heat Transfer Coefficient

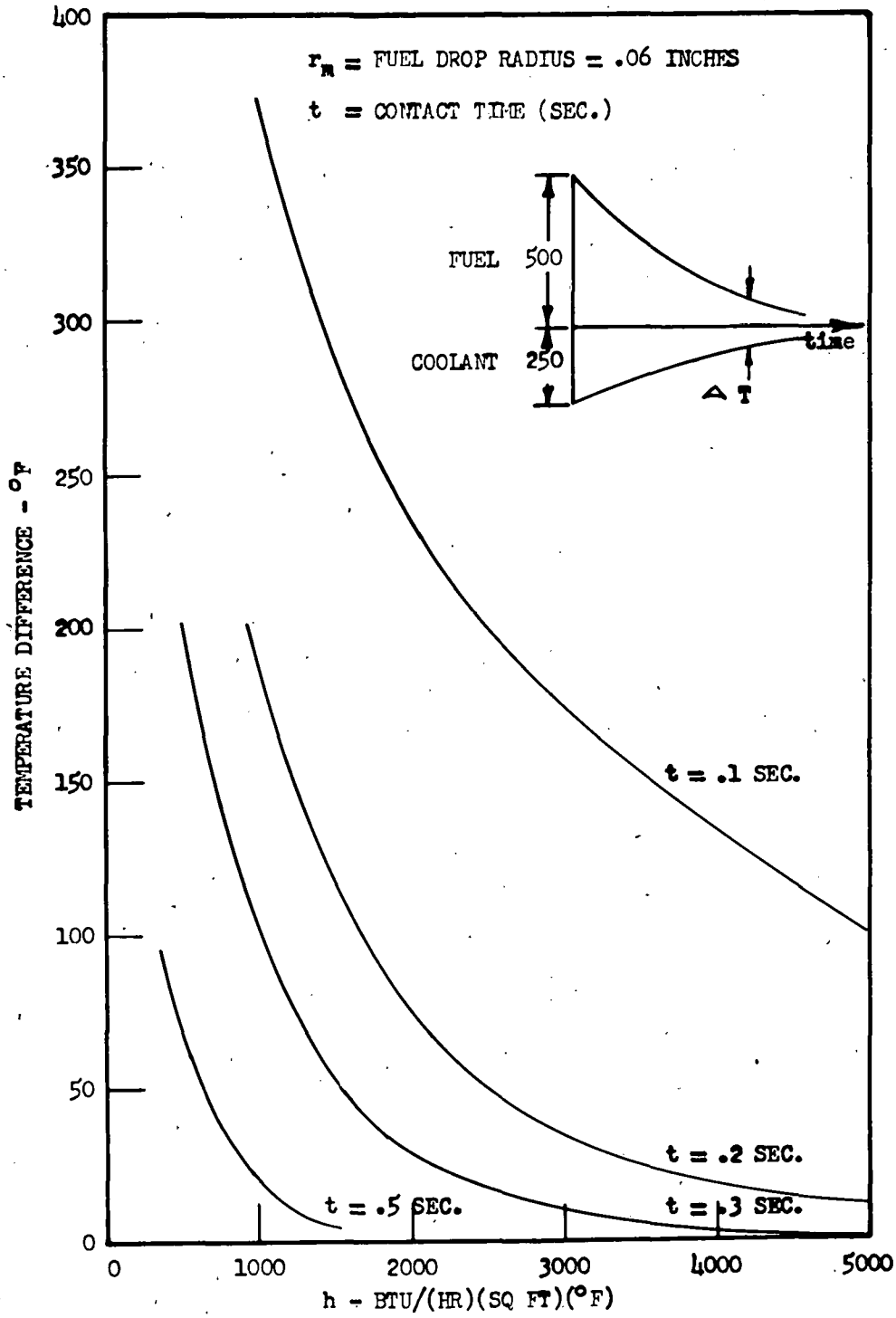

or a minimum tolerable contact time if 0.3 seconds. From a consideration of the total volume rate of flow and the volume of effective heat transfer, the average contact time is estimated to be 0.2 seconds.

A drop size, rm=0.62", considered to be conservative, is arbitrarily specified for the design condition. Thus, with a heat transfer coefficient of 2500, the calculated temperature difference between fuel and coolant is 57°F. The temperature difference expected will be less than this value for three reasons: (1) increased value of heat transfer coefficient due to turbulence; (2) drop size smaller than that specified is probable; (3) the average drop temperature will be about 20% less than the temperature of the drop center which was used as a basis for entry to the Gurney-Lurie chart.

Figure 16 presents the variation of the temperature difference with the value of heat transfer coefficient for a drop size, rm=0.06", with contact time as a parameter.

In Figure 17 temperature difference vs. contact time is plotted for several drop sizes, assuming that h = 2500. The area of uncertainty is indicated by plotting upper and lower values corresponding to assumed upper and lower initial temperature differences between fuel and constant temperature coolant. It is seen that for the drop size and contact time of interest, the result obtained is not strongly dependent upon the assumed initial temperature difference and hence, taking the average of the upper and lower values in the calculation appears reasonable.

5.23 Disc Type Jet Pump - Separation Characteristics

Considering the fuel as the dispersed liquid, the first step in analyzing the separation of fuel and coolant is to calculate the terminal velocity for fuel drops of various sizes falling through a medium of fused

ORNL-LR-Dwg.-10185
UNCLASSIFIED

Figure 17
CO-CURRENT HEAT EXCHANGE

FUEL-COOLANT EXIT TEMPERATURE DIFFERENCE vs CONTACT TIME

FOR THREE DROP SIZES

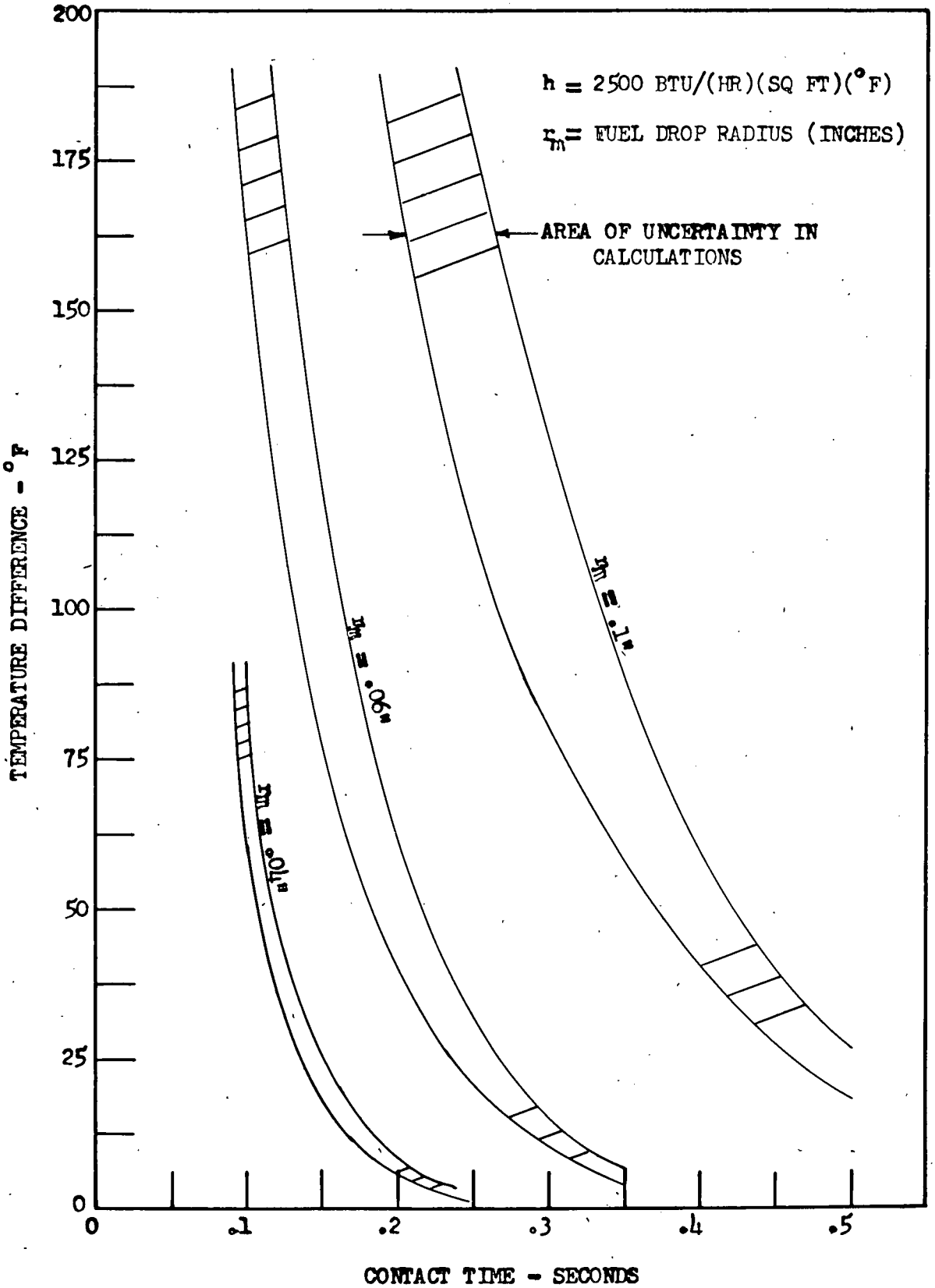

salt in a standard gravitational field. The calculation is given in detail in the Appendix. Results for several drop sizes are as follows:

r_m	Terminal Velocity, ft/sec
0.02"	1.3
0.04"	1.8
0.06"	2.2
0.10"	2.8

In considering the mixing tube proper the question to be determined is whether or not the various drops of fuel will fall through a height required for separation of the phases by the time they have transited the mixing tube longitudinally. As a first estimate turbulence has been neglected and the drops have been assumed to move in space along the resultant of two velocity vectors, one vertical due to gravity and one horizontal of magnitude equal to the average longitudinal velocity of fuel through the mixing tube. It has been further assumed that the average velocity of fall is one half the calculated terminal velocity. The height of the mixing tube for the design jet pump exchanger is .64 feet. Based on the relative volume flow rates the estimated height of the fused salt layer when settled out is .39 feet. With these values and the above assumptions, a drop of radius .062" at the mixing tube entry (which has the longest transit time) is considered, to determine if it will fall through a height of 0.39 feet in the estimated transit time of 0.2 seconds. A simple calculation shows that the drop will fall 0.22 feet in the allotted time.

The case considered is quite optimistic from the standpoint of separation. Thus, if in <u>this</u> case the drop will not settle out, it is most

unlikely that separation would be achieved in the actual design where turbulent flow conditions exist through the mixing tube.

Because of the serious poison effect of fused salt in the core, it is mandatory that separation be complete and hence, additional means must be provided for this purpose. Figure 12 shows the means selected (1) vanes and a swirling chamber have been added to the mixing tube discharge to obtain a greater effective gravitational field; (2) an enlarged separation chamber has been added to the swirling chamber to provide additional settling time. The orientation and size of the latter has been calculated so that coolant drops of radius .062" or larger will rise in the fuel settling chamber faster than the fuel is descending (1 ft/sec). See Appendix.

The configuration of the design settling chamber may be conservative from the standpoint of insuring separation. However, this conservatism results in a substantial increase in the external holdup of fuel. See below. The extent to which the size of the settling chamber might be reduced by an improved design, as well as the determination of carryover of fuel and coolant for various designs, can only be determined with any degree of certitude by detailed experimentation.

Fuel Hold-Up Volumes

Proposed Disc Type Jet Pump Exchanger	2105 gals.
Brookhaven Spray Type Exchanger (scaled to 750 MW heat)	4760 gals.

5.3 Fluid Contacting Centrifugal Pump Exchanger

An alternate design to that of Section 5.2 which has the same proposed objectives in shown in Figure 18. In the configuration chosen the coolant enters at a velocity of 65 feet per second through four tangential

UNCLASSIFIED
ORNL-LR-DWG. 8279

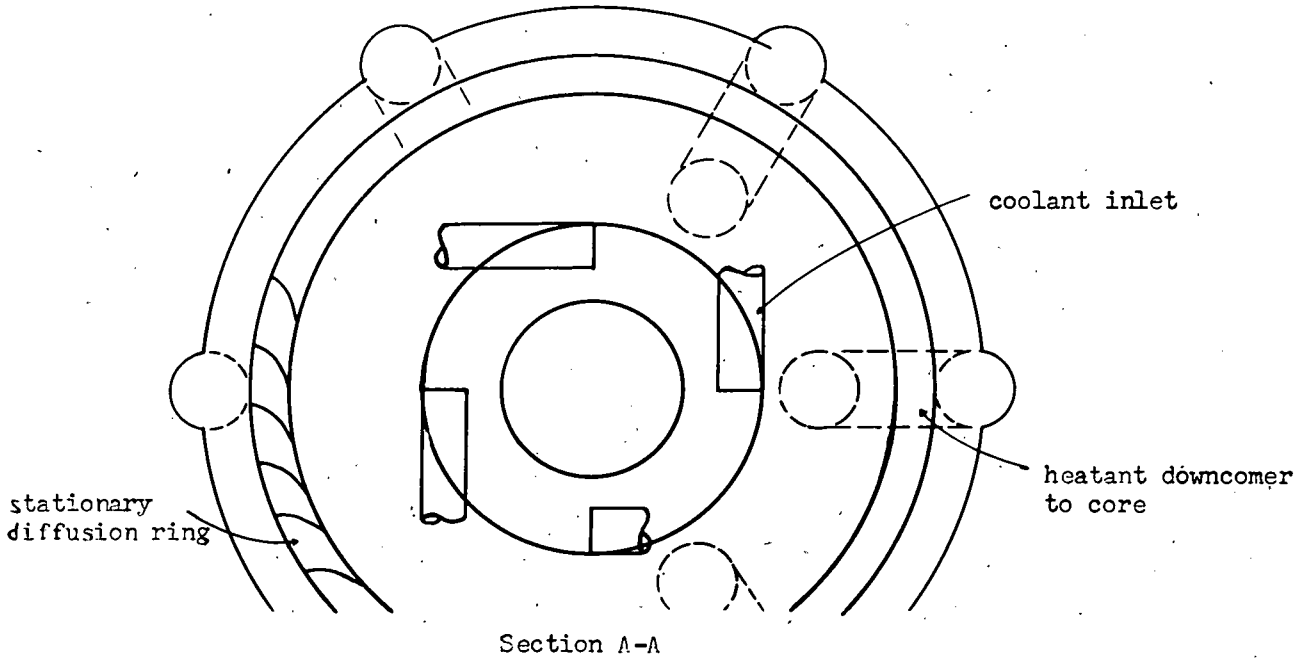

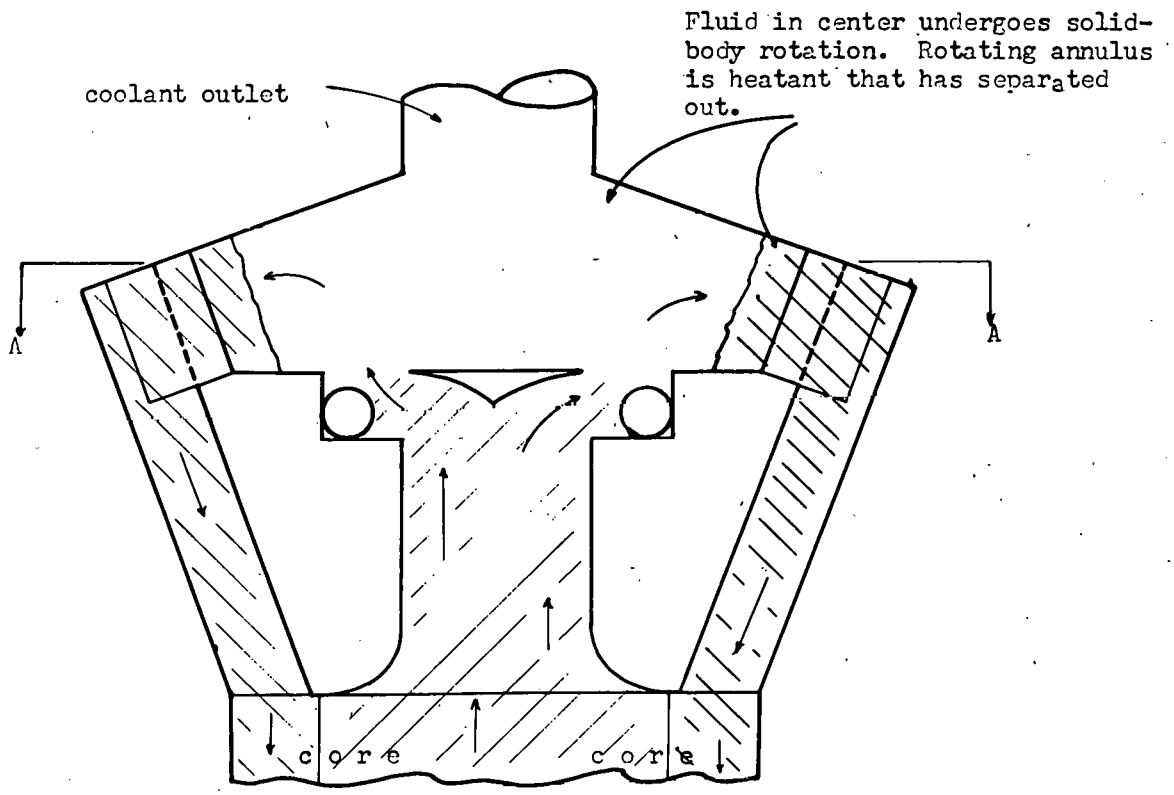

Figure 18

Fluid Contacting Heat Exchanger

jets, symmetrically located at the base of the exchanger. A swirling and rising motion is imparted to the liquid fuel entering at a low velocity from the core riser. The centrifugal action and the upward component imparted cause the heavier liquid (the fuel) to move from the central region to the periphery where it moves upward and outward through diffuser vanes. The lighter coolant moves from the periphery to the central region and upward to the discharge. The flow patterns obtained are complicated and not readily examined analytically; from the standpoint of heat exchange, it is believed that the flow will be preponderantly counter current.

5.31 Centrifugal Pump Exchanger - Pumping Performance

The gross pumping behavior was analyzed on the assumption that the coolant enters the chamber at high velocity and transfers part of its momentum to the liquid fuel. It is further assumed that momentum is conserved on the gross scale; entry losses, mixing losses, and eddy current losses are neglected. The mixing process is envisaged to be completed in a short distance after which fuel and coolant attain a common linear motion. The detailed calculation is given in the Appendix.

The head gained by the fuel is assumed to be that due to a change in velocity head and to the centrifugal head, the latter considered as a gain in pressure head. It has been assumed for simplification that 100% of this head so gained by the fuel is recoverable; in view of viscous losses and other losses inherent in such a complex flow pattern, the gain in fuel velocity head will not be fully recoverable.

Figure 19, a plot of head developed in the fuel vs. jet velocity, shows the results of the calculation for various values of fuel to coolant volume flow rates. Throughout the calculations it was assumed that the rotating annular shell of fuel was six inches thick. The characteristics of the

UNCLASSIFIED
ORNL-LR-DWG. 8284

Figure 19

Characteristics of a Fluid Contacting Centrifugal Pump

("Head" includes contributions from kinetic energy and centripetal force)

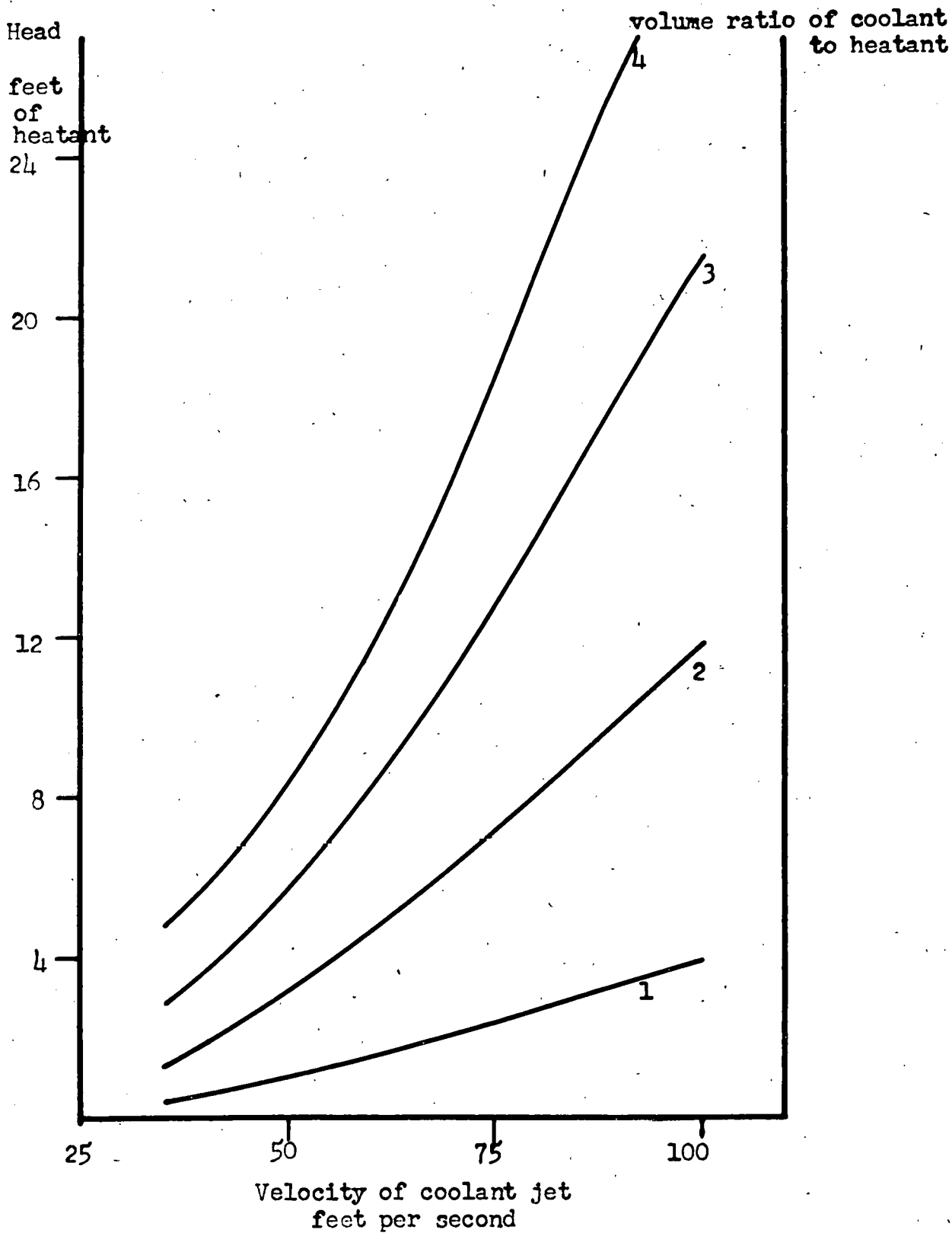

design centrifugal pump exchanger are:

Jet velocity	65 fps
Ratio of fuel to coolant volume rates of flow	1/2
Gain in fuel head	5.5 ft

The theoretical mechanical efficiency, defined as the rate mechanical energy is added to the fuel divided by the rate mechanical energy is lost by the coolant, is calculated in the Appendix and is plotted against the ratio of coolant to fuel mass flow rates in Figure 20. The efficiency for the design condition is 20%. Thus, the pumping power required for the coolant is of the same order of magnitude as that required in the disc type jet pump exchanger.

It is believed that the consequences of going to higher coolant flow rates are more deleterious in the centrifugal type than in the disc type exchanger from the aspect of separation performance.

In addition to transferring momentum to the fuel the coolant must retain sufficient head at the exchanger discharge to move through the secondary heat exchanger and external piping. Here again, as in the disc type jet, for a given jet velocity and mass flow rate, the coolant head available at the exchanger discharge may be increased by operating the core under a higher pressure. This assumes that the secondary loop pump is located in the cold leg. An alternative is to locate the pump in the hot leg of the secondar loop so that the coolant discharging from the primary exchanger may be raised to the required head.

Operating of the core with the fuel under the slightly higher pressure required to raise the level of the coolant head at the exchanger

ORNL-LR-Dwg.-10186
UNCLASSIFIED

Figure 20

THEORETICAL EFFICIENCY OF A FLUID CONTACTING CENTRIFUGAL PUMP AT FIXED HEAD

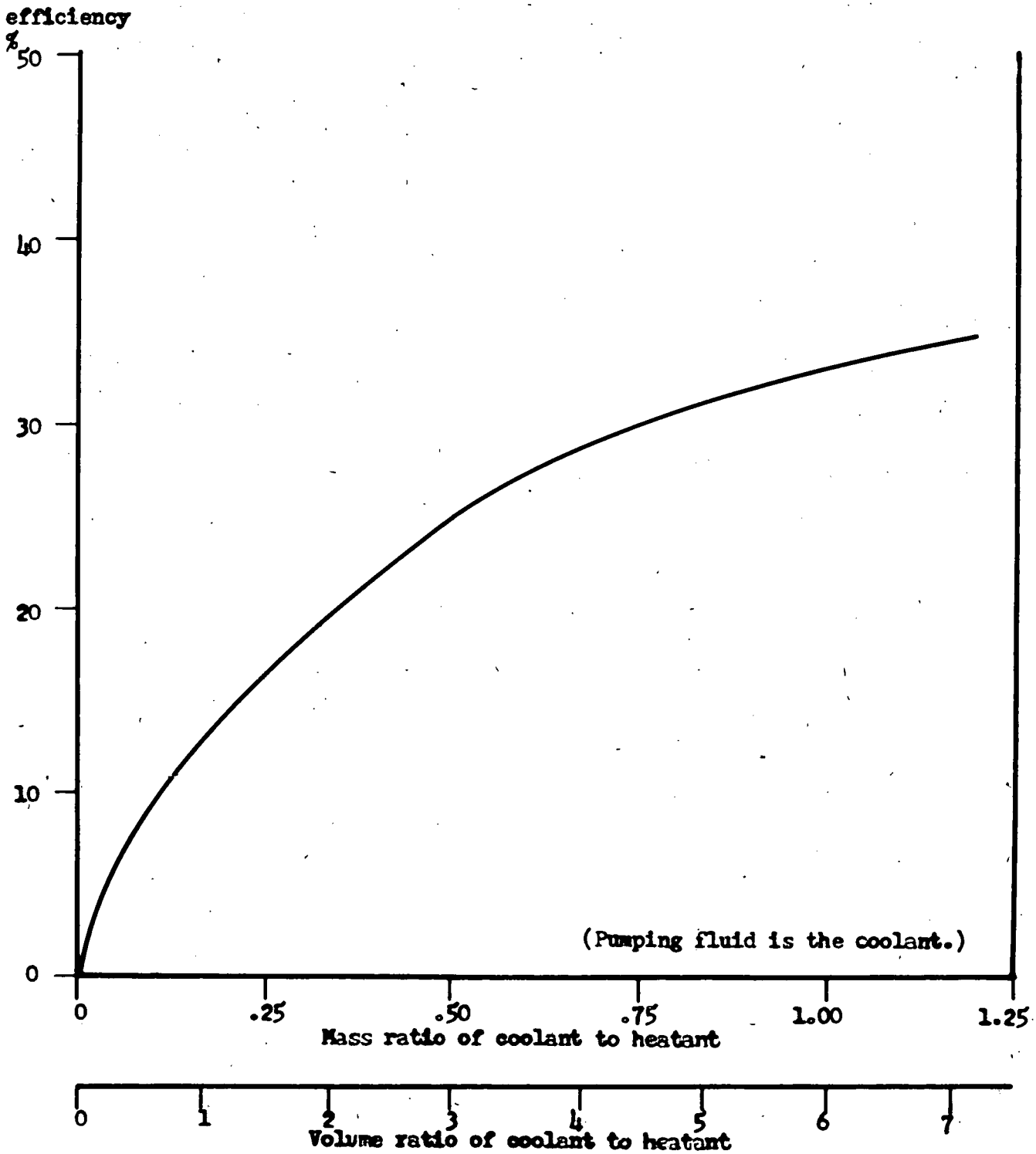

discharge is not considered a serious limitation in core construction since even with atmospheric pressure at the top of the core, as in the reference design, the pressure at the core base due to statistic head is about 26 psig. In order to prevent oxygen from leaking into the core and oxidizing the uranium operation of the core under a pressure greater than atmospheric is desirable. From the standpoint of preventing leakage of active core fluids to the external environment, it is desirable to operate the core at a pressure below atmospheric.

In this type of exchanger, as well as in the disc type jet exchanger, for a given configuration the volume rates of flow of coolant and fuel are not always proportional. Thus, the flow rate of the coolant must be maintained nearly constant. As has been indicated in Figure 19, the head developed in the fuel increases with the coolant flow rate. However, in the case of the centrifugal exchanger the adverse effect of high coolant rates upon separation and heat transfer performance is more severe than in the disc type jet exchanger. This is due to the fact that despite the gain of a linear velocity head by a fuel mass, it may never reach the rotating annulus. At certain values of coolant flow rate, the radial drag force acting on a fuel mass may reach a magnitude such that the effective centrifugal force is not sufficient to throw the fuel toward the periphery at a rate consistent with the specified fuel rate of flow.

5.32 Centrifugal Pump Exchanger - Heat Exchange

Since the exact nature of the flow patterns of coolant and fuel is unknown, a simplified model has been assumed in which fuel at the center moves toward the periphery in the dispersed state through the concentric surrounding medium of fused salt, which is displaced toward the center. Only the radial components of coolant and fuel velocity are considered. The method

of heat transfer calculation, given in the Appendix, consists in treating the problem as a steady state case similar to that encountered in a shell and tube heat exchanger. The log mean temperature driving potential is determined for several values of drop size, heat transfer coefficient, and contact times. With that quantity determined, the difference in temperature between the fuel outlet temperature and the coolant inlet temperature may be calculated. An exact method for this problem in heat transfer is given in Reference 4. For the case of a contact time of 2 seconds, heat transfer coefficient of 2500, and a drop radius of 0.0985", the approximate method gives a value of 22 F as compared to 19 F, given by the exact calculation.

In Figure 21, temperature difference vs. drop size is plotted for three contact times with k taken as 2500 BTU/hr.sq.ft F. If 100 F is prescribed as the maximum temperature difference, then, within the range of the plot, the maximum drop size is $r_m = 0.12"$.

Figure 22 shows the effect of the heat transfer coefficient on the temperature difference for a given drop size and for various contact times.

From the standpoint of heat exchange, the fluid contacting centrifugal exchanger is considered superior to the disc type jet exchanger in that the former is subject to much lower thermal stress across the coolant inlet and in that for the same heat removal rate and average core temperature, the maximum temperature of the fused salt coolant will be higher in the countercurrent type.

5.33 <u>Centrifugal Pump Exchanger - Separation</u>

The fact that the holdup of fuel appears to be less for the centrifugal exchanger is misleading in that the calculations, which have been highly idealized in view of the complex flow characteristics, do not take into account

UNCLASSIFIED
ORNL-LR-DWG. 8288

Figure 21

Counter Current Heat Exchange

Temperature Difference vs Fuel Drop Radius for Three Contact Times

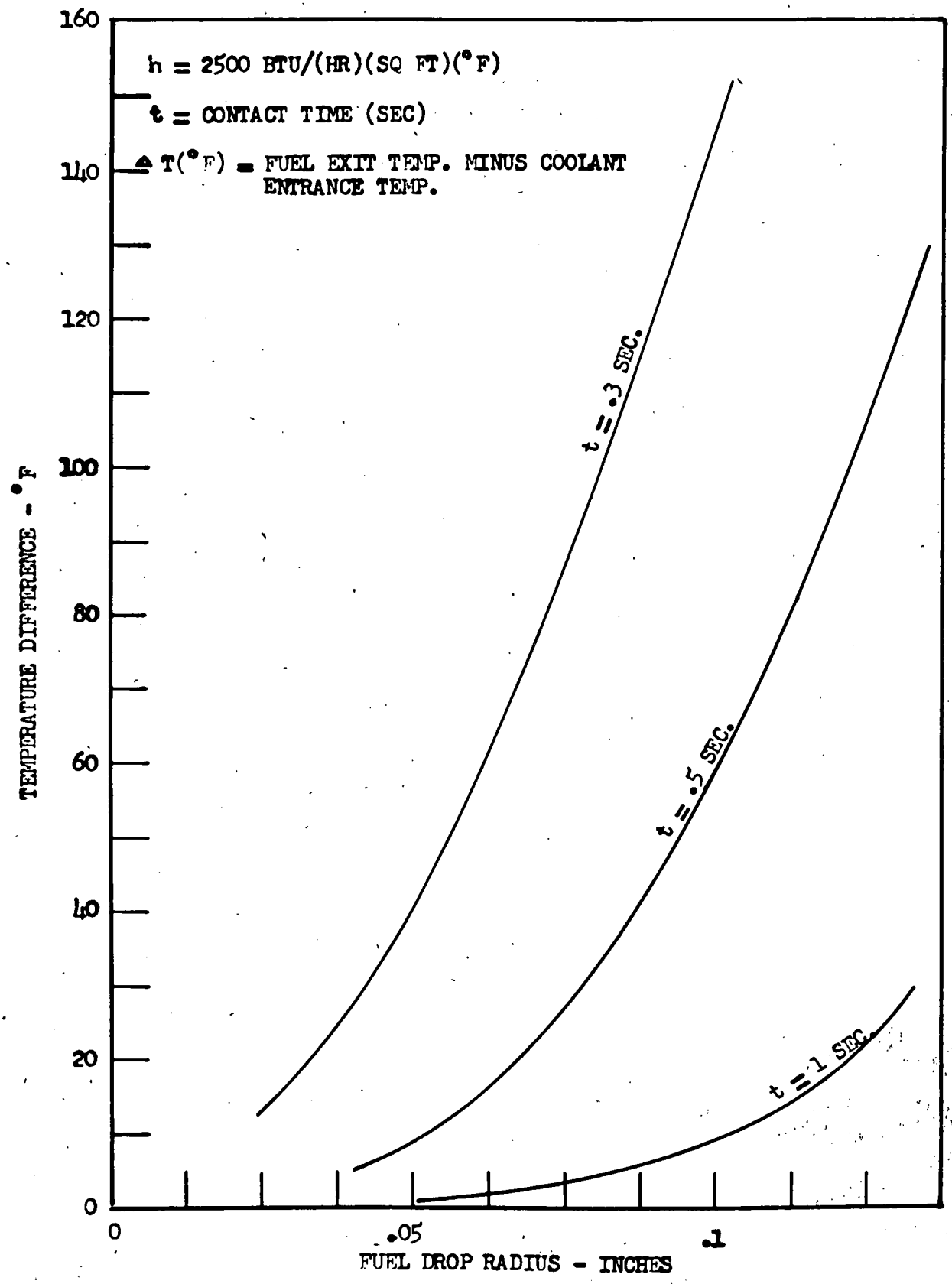

UNCLASSIFIED
ORNL-LR-DWG. 8291

Figure 22

Counter Current Heat Exchange

Temperature Difference vs Heat Transfer Coefficient for Three Contact Times

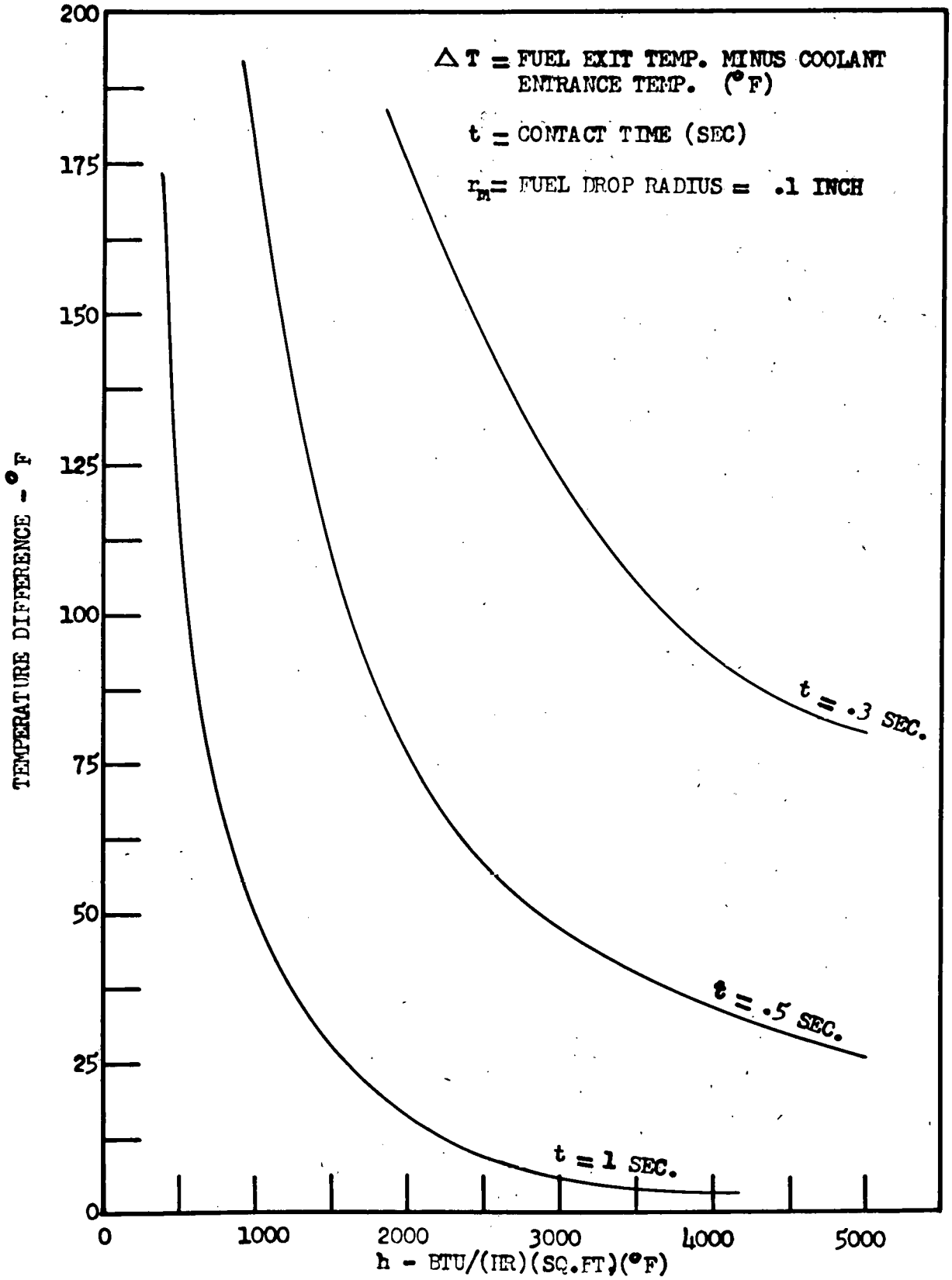

the radial drag for various geometries and coolant flow rates cannot be predicted with any certainty, and hence, experimentation will be required to determine whether or not the separation characteristics are satisfactory. It is to be noted that because of this drag force anticipated, the effective centrifugal field cannot be increased merely by increasing the head gained by the fuel. Thus, it may well be that additional holdup volumes and times may be required in the form of settling chambers.

5.4 Summary Evaluation of Two Exchangers

a. More efficient heat exchange - centrifugal pump exchanger.

b. Minimum thermal stress problem - centrifugal pump exchanger.

c. More effective separation at the flow rates involved - disc type jet exchanger.

d. More uncertainty in the calculations and overall estimate of performance - centrifugal pump exchanger.

6.0 CHEMICAL PROCESSING

The processing scheme proposed for this reactor is basically one of the systems proposed for the Liquid Metal Fuel Reactor with modifications where required. No attempt was made to develop new processing methods, but the processing cycle times are changed to achieve some advantage from the fuel-coolant contact in the primary heat exchanger.

6.1 Core Processing

For the proposed direct liquid contact cooled reactor, the chemical processing scheme must be modified, because the direct contact of fuel and coolant comprises one essential step of the core processing system. To achieve the greatest advantage this fuel-coolant contact affords, the system referred to as Fuel Processing Scheme A[3] was chosen for this reactor system. Two

alternate schemes for processing are outlined in the above report.

For this system, the fission products can be divided into three classes: (1) volatile fission products; (2) fused salt soluble fission products, referred to as fps; and (3) fused salt insoluble fission products, designated fpn. The chemical processing system can be broken down into three separate sections, each for the removal of one of the above classes of fission products.

6.11 Volatile Fission Product Removal

Volatile fission products, the most important of which is Xenon-135, are removed in the LMFR Scheme A by spraying the fuel system into a space above the core maintained at about 1 micron pressure where the gases diffuse out of the fuel solutions. This scheme requires a holdup of several core volumes to give sufficient holdup time for gas removal. It is possible that the requirements for the direct contact cooled reactor are much simpler. Fission gases could conceivably be removed when the fuel is finely dispersed in the heat exchanger and collected and removed from the fused salt system. No experimental evidence to justify this method is available, but distinct advantages are obvious if the scheme proved feasible.

6.12 Salt Soluble Fission Products

When proper oxidizing conditions are maintained in the fused salt through addition of $BiCl_3$ about 50 weight per cent of the fission products, including the alkali, alkaline earth, and rare earth metals, are extracted by the salt phase. Stoichiometric quantities of $BiCl_3$ must be used since an excess will cause uranium to be extracted with the fission products.

While in the LMFR scheme, this phase of processing is carried out on a side stream from the fuel loop; in the present design the fuel-coolant

contact comprises the first step, and a side stream from the salt will be processed to concentrate the fission products for ultimate disposal. Figure 23 shows the basic steps required to do this, and Table 4 lists the approximate flow rates and stream concentrations. The side stream from the salt loop is contacted with fresh bismuth to remove traces of uranium. The fission products are then extracted from the salt with Pb containing an excess of calcium. The fused salt is returned to the main circuit, and the fission products extracted in a small volume of salt for disposal.

In the early stages of this study, it was thought that the chemical processing scheme would be greatly simplified by means of the direct contact cooling procedure. However, it can now be seen that this step is a rather small part of the salt soluble fission product removal system which in itself removes only certain of the fission products. The chemical processing plant on the whole is essentially the same for both systems.

6.13 Salt Insoluble Fission Products

The salt insoluble fission products, including zirconium and polonium, must be removed from a side stream of the fuel solution. Uranium is first removed from the fuel by contacting with fused salt containing an excess of $BiCl_3$ to oxidize the uranium. The bismuth stream is then contacted with NaOH, containing small amounts of $NaNO_3$, to remove zirconium and magnesium. This salt stream is then discarded. The remaining fission products and polonium are extracted by molten zinc, concentrated by vacuum stripping of the zinc stream and discarded. The purified bismuth is used to remove uranium from fused salt streams, is then enriched to the proper U^{233} concentration and returned to the core.

81

UNCLASSIFIED
ORNL-LR-DWG. 8292

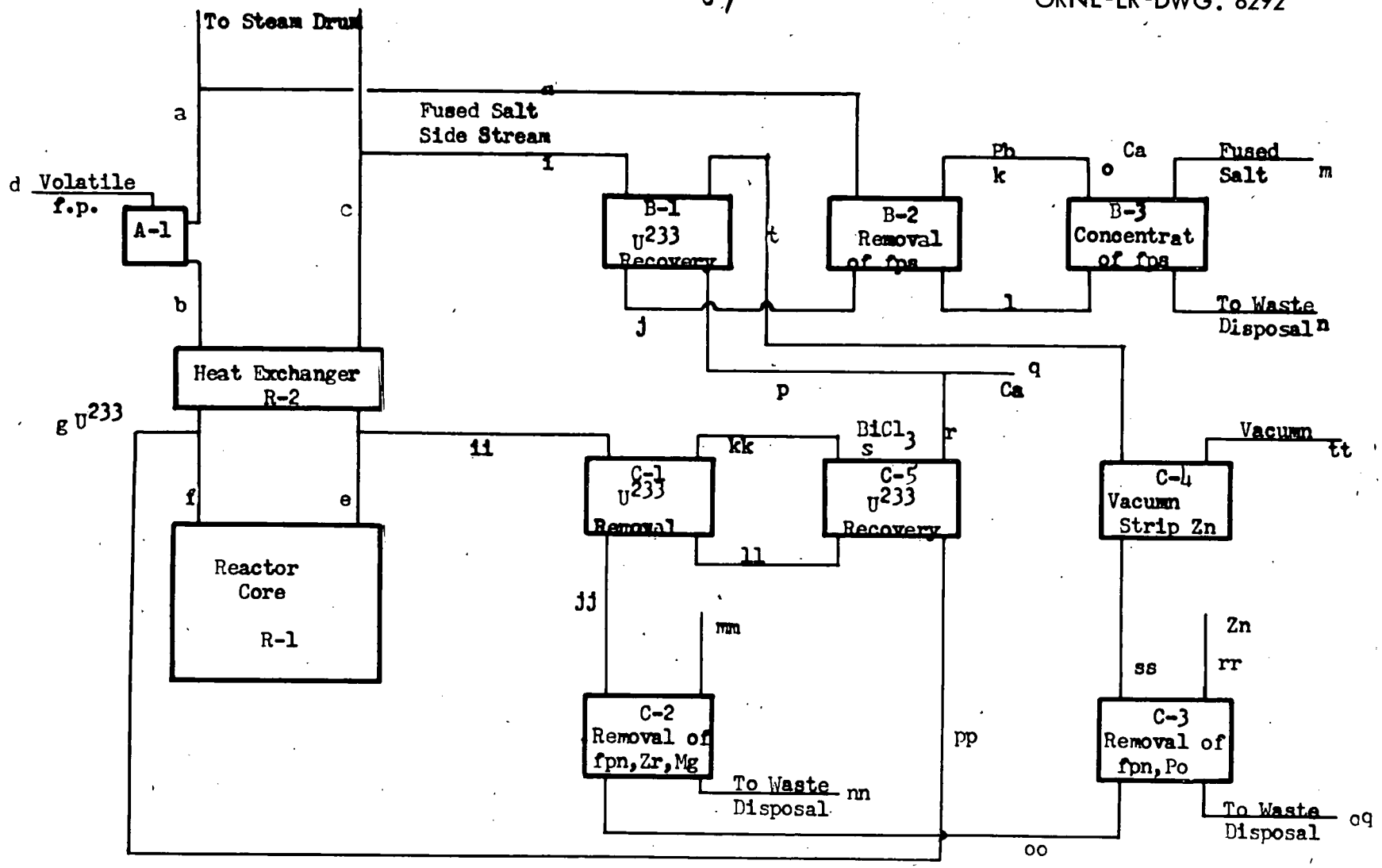

Figure 23

Simplified Core Process Flowsheet

TABLE 4

Composition and Flow Rates for Core Chemical Processing Cycle (Refer to Figure 23)

Stream	Composition	Approx. Flow Rate
a, b, c	Fused Salt Coolant (KCl + LiCl + tps)	3.78×10^7 #/hr
d	Volatile Fission Products	--
e, f	U-Bi Reactor Fuel (285 ppm U^{233} in Bi)	1.42×10^8 #/hr
g	U^{233} Make-Up	19 g/day
h, i, j	Fused Salt Side Stream for Processing	600 #/hr
k, l	Pb Stream for fps Removal	2300 #/hr
m, n	Fused Salt for fps Concentration and Disposal	5 #/hr
o, q	Ca Make-Up	20 g/hr
ii, jj, oo ss, t, p, pp	U-Bi Side Stream for Processing	60 #/hr
ll, kk	Fused Salt Stream for U Extraction	--
mm, nn	NaOH + 0.17 $NaNO_3$ for Zr, Mg, + fpn removal	4 #/hr
rr, gg	Zn for removal of fpn + Po	6 #/hr

6.14 Processing Cycles and Poison Level

In the nuclear calculations, a poison fraction of 0.05 was assumed, and the cycle times were calculated to maintain this poison fraction with no effort being made to optimize cycle times against poison fraction because of the incomplete processing cost data available.

The poison fraction assumed was arbitrarily split, assigning 0.01 to the fused salt insoluble group. As stated above, insufficient information is available to adequately design and estimate the performance of the volatile fission product removal system. The 0.01 value was used in LMFR designs.

Extraction of the soluble fission products by the fused salt is essentially complete. The fission product equilibrium concentration ratio is in the order of 100+, in favor of the salt phase. The conditions determining the allowable concentration of fission products in the coolant salt are not clearly defined. To decrease processing rates, it is advantageous to allow high concentrations, but these in turn, allow poisons to accumulate in the bismuth phase. Using the equilibrium ratio of 100, at a concentration of 50 ppm in the salt phase, poison fraction due to this group of fission products is only of the order of 0.002 and processing rates are less than 1 gpm. Whether a concentration this high, or even higher, is permissible depends to a large extent on safety considerations and emergency cooling requirements. It appears that under no reasonable conditions will the soluble fission products contribute a significant poison fraction.

To maintain the insoluble fission products at a poison fraction of 0.04 at the reference design core flux of and total volume of 2840 gallons of fuel solution, a cycle of 173 days corresponding to a processing flow rate of 0.0114 gpm is required. The economic optimum processing rate is probably considerably higher, but could not be determined from the available cost data.

6.2 Blanket Processing - U^{233} Removal

For the proposed two region reactor, U^{233} produced in the blanket will be removed by the same scheme devised for the LMFR and returned to the core. The processing cycle is extremely simple in principle though several steps need experimental evidence to prove feasibility. Brookhaven National Laboratory has proposed other schemes which might prove more successful. Figure 24 shows the basic steps in the blanket processing scheme.

A side stream from the blanket slurry is diluted with an equal volume

+ F. T. Miles - personal communication.

UNCLASSIFIED
ORNL-LR-DWG. 8286

Figure 24

Simplified Thorium Breeder Blanket Processing Flowsheet

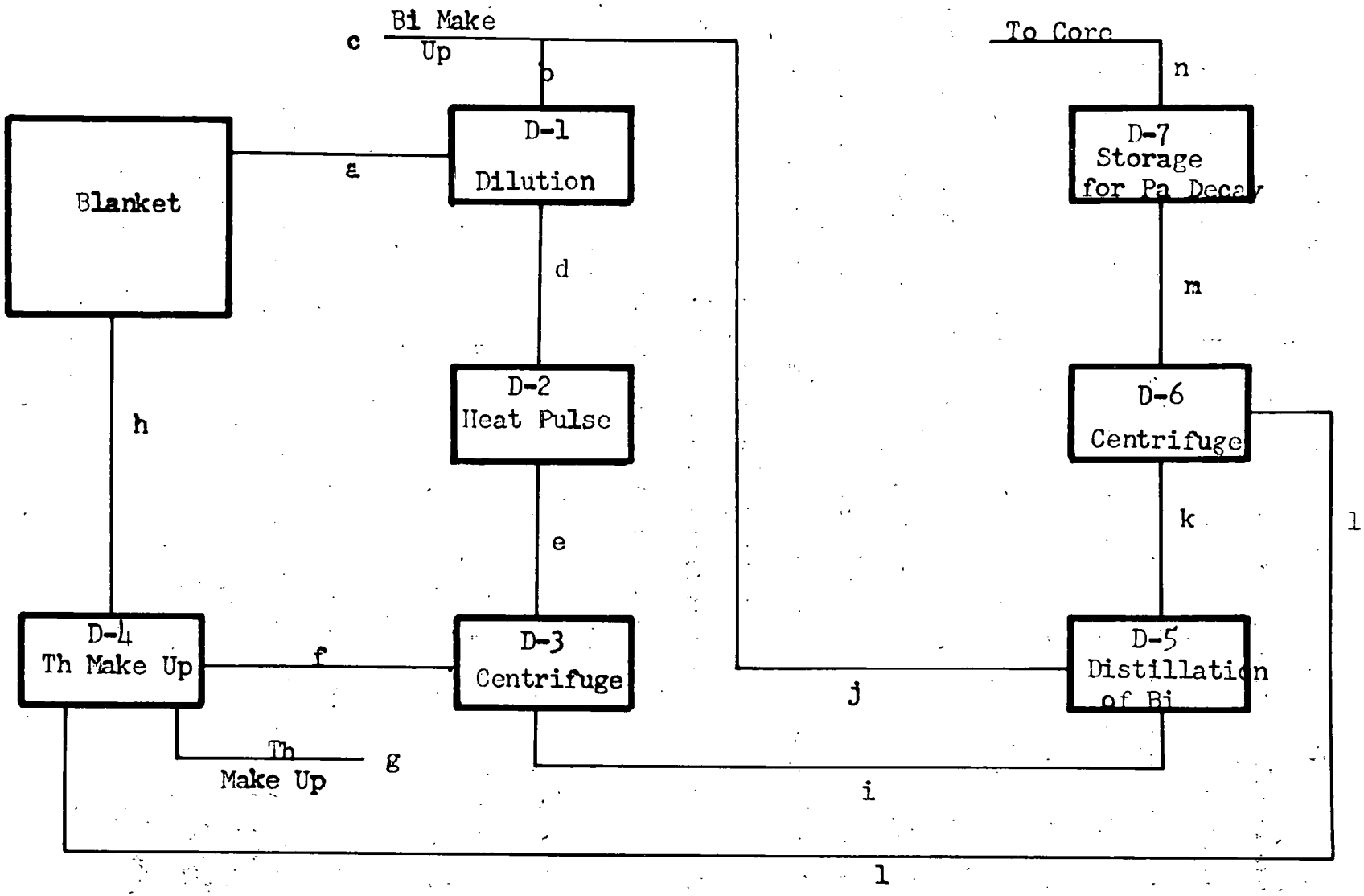

TABLE 5

Composition and Flow Rates for Blanket Processing Cycle
(Refer to Figure 24)

Stream	Compsition	Flow Rate
a,h	Bi + U + Th slurry	275 #/hr
b	Bi for dilution	275 #/hr
c	Bi make-up	13 #/hr
d,e	Bi + U + Th slurry	555 #/hr
f	Bi + Th slurry	275 #/hr
g	Th make-up	820 #/day
i	Bi + U to U recovery + dissolved Th	275 #/hr
j	Bi from distillation	262 #/hr
h	Bi + U + Th slurry	13 #/hr
l	Bi + Th to Th make-up	0.15 #/hr
m,n	Bi + U + Pa to core	13 #/hr

of bismuth and subjected to a heat pulsing dissolution step. In this operation, the temperature is cycled between 350°C and 850°C until 60% of the thorium in the slurry is dissolved. The remaining solids, mainly thorium, are centrifuged from the stream, mixed with recovered bismuth from a subsequent step and returned to the blanket.

The solids free stream from the centrifuge is reduced to 1/20 the original volume by distilling excess bismuth. This precipitates dissolved U^{233}, Pa, and some fission products, which are then centrifuged from the stream. The solids are then stored for about 160 days for decay of Pa to U^{233} before return to the core.

No provision is made in the system for poison removal. All fission products which follow the U^{233}-Pa stream will subsequently be moved in the core processing steps. If required, the bismuth stream from the distillation step could be processed to prevent excessive fission product buildup within the blanket processing system.

7.0 STEAM CYCLE

Three criteria were used in the design of the stream cycle:

1. Since the heat exchangers to the steam will be radioactively hot, the heat exchangers will be difficult or impossible to repair after they have been in service. They should be cheap to replace. Therefore, the steam pressure should be low.

2. The fuel cost will be between 2 and 2 1/2 mills per kilowatt hour. Since this is not negligible compared to a coal cost of 2 1/2 to 4 mills, the thermal efficiency must be fairly high.

3. Since the "hot" heat exchangers will require shielding, the volume of the heat exchangers must be minimized. This can be done by reducing the amount of superheating and reheating. For example, rather than reheat, the steam can be expanded to a higher moisture content.

4. Temperature is limited by the corrosion in the blanket loop. The maximum steam temperature is 1000°F.

The following table gives the thermal efficiency for a number of different cycles. These are ideal cycles without regenerative feed water heating.

The cycle chosen was the 1450 psia, 100°F non-reheat cycle. With regenerative feed water heating the thermal efficiency is 39.0%. Thirty-two per cent of the heat is added in superheating. For a complete description of the steam cycle see Figure 25.

87

Figure 25

STEAM CYCLE

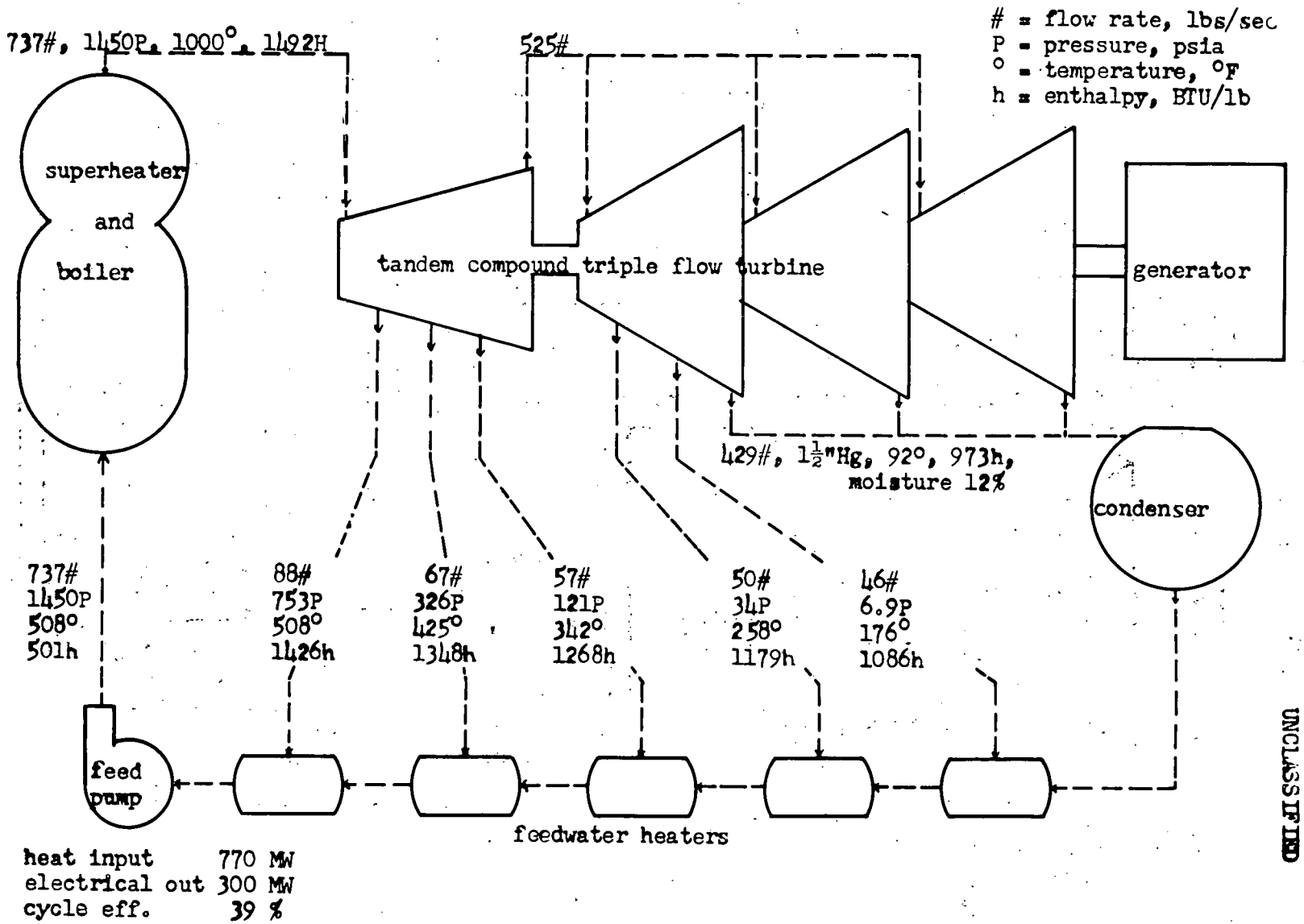

ORNL-LR-Dwg.-10187
UNCLASSIFIED

UNCLASSIFIED
ORNL-LR-DWG. 8618

Figure 26

Over-all Cycle

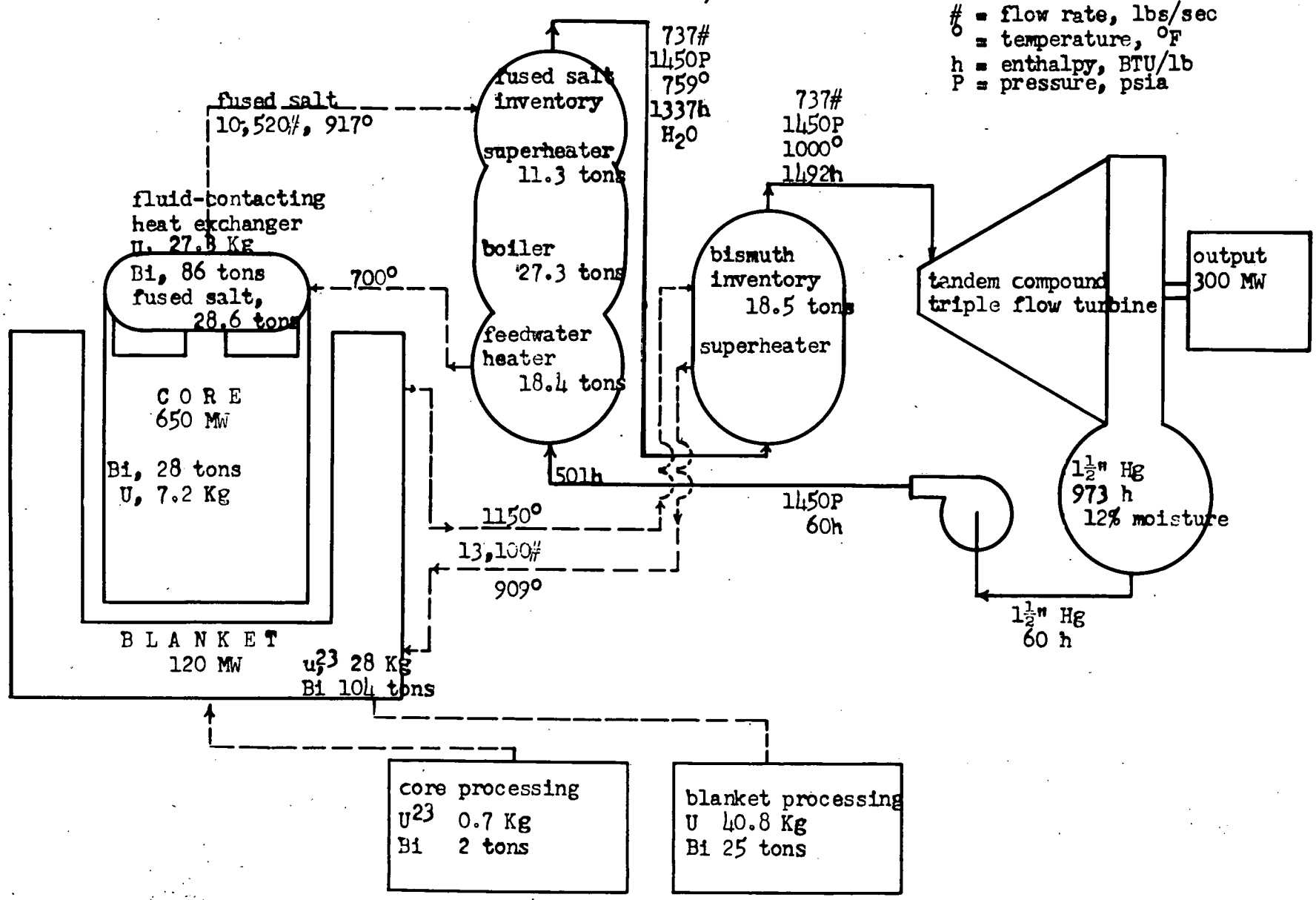

TABLE 6

Thermal Efficiencies for Various Steam Cycles

THROTTLE		REHEAT				
press. psia	temp. °F	press. psia	temp. °F	% exhaust moisture	thermal efficiency	% heat in superheat and reheat
700	1000			18	33.9	21.5
1250	1000			11 1/3	35.8	22
1250	1000	700	1000	8	36.9	26.3
1450	1000			12 1/3	36.2	22.4
1450	1000	700	1000	8	37.0	27.1
1800	1000			14	36.8	23.3
1800	1000	700	1000	8	37.8	29.5
2015	975	640	975	8	38.1	30.7

Selection of the steam cycle was somewhat arbitrary due to the multiplicity of unknowns. Among parameters on which greater knowledge is required are: (1) cost of heat exchangers as a function of steam pressure, (2) cost of shielding versus amount of superheating and reheating, and (3) turbine cost for different throttle steam conditions.

Overall Cycle - The overall cycle is shown in Figure 25. To make the system as simple as possible, the steam is heated directly by the radioactively hot fluid. There is no danger of a leak in the heat exchangers contaminating the turbine, since any leak will be from the high pressure steam side to the low pressure heatant side.

Note that the UBi from the blanket transfers heat to steam and not to water. Therefore, in case of a leak, low density steam would enter the UBi rather than water. Any chemical or physical reactions would thus be less violent.

The fraction of reactor heat taken from the blanket was not determined from a thermodynamic analysis but is rather the result of fixing core and blanket fuel concentrations.

8.0 CONTROL OF THE REACTOR AND POWER OUTPUT

Design of the reactor control system progressed only to the point of calculating a temperature coefficient of reactivity and devising a possible scheme for maintaining constant steam conditions to the turbine for varying load conditions.

With the calculated temperature coefficient of 9×10^{-5} per degree C, the reactor should be completely self-regulating, and no control rods are required for stable operation. For any given fuel concentration, there is only one temperature at which the reactor is exactly critical. Thus, the <u>average</u> steady state temperature is constant and independent of load. This temperature is fixed by the fuel concentration.

The flow rates of the fuel and coolant are interdependent, though not necessarily proportional, due to the jet pump action. This system is therefore, not well adapted to handling load changes by varying flow rates. For this reason, the coolant and fuel mass flow rates will be maintained constant for all power levels.

With a constant fuel flow rate, and a constant average fuel temperature in the core, the temperature rise of the fuel in the core will be proportional to the power level. The fuel inlet and outlet temperature (in the core) will vary with load as shown below.

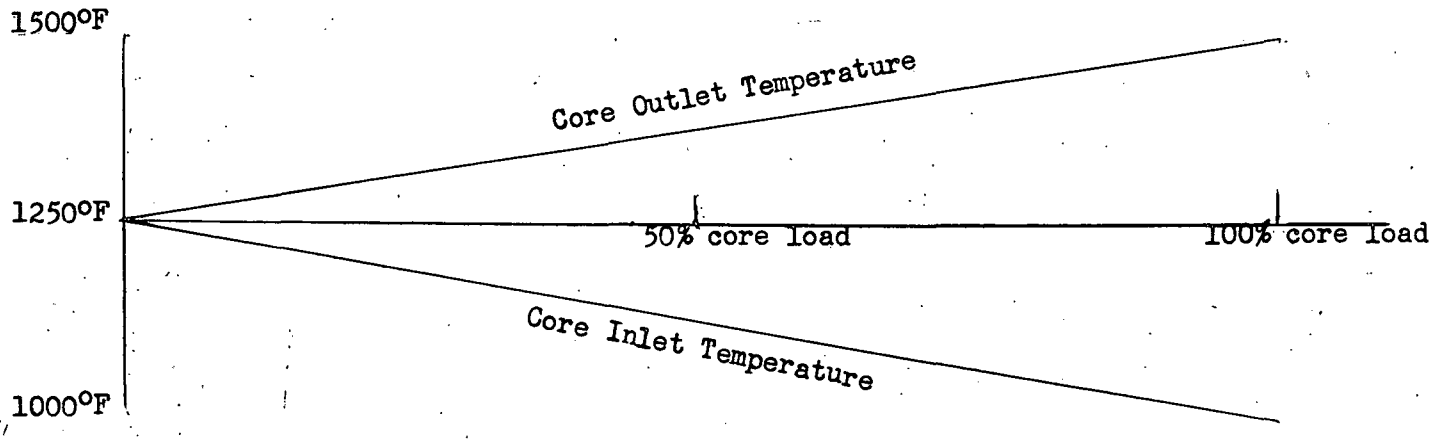

Co-current heat exchange in the jet pump heat exchanger implies that as the coolant leaves the heat exchanger, it is approaching the fuel inlet temperature. As this temperature increases with decreased load, the coolant temperature will also increase. Also, the coolant temperature rise in the primary heat exchanger is proportional to the power. The net result is that the fused salt coolant temperature varies with load as shown below:

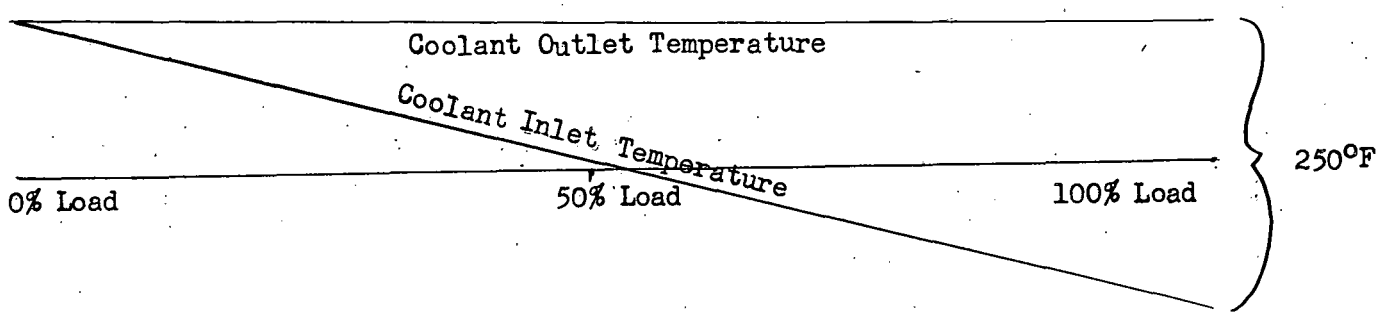

The average as well as the maximum coolant temperature is therefore increased as the load is decreased. For this reason, temperature of the steam leaving the boiler tends to increase as the load decreased. To offset this effect part of the coolant is by-passed around the boiler to maintain the steam temperature constant leaving the boiler.

Superheating of the steam is done by circulating the blanket fluid directly to the superheater. As this fluid is pumped with conventional pumps, it is proposed that the superheated-steam temperature be maintained constant by varying the blanket fluid flow rate as the power level varies.

Summary of Control Requirements - This reactor is self-regulating due to the negative temperature coefficient in the core. The operating temperature of the core is fixed by the concentration of U^{233} in the fuel solution.

As the load on the generator is decreased, the steam flow rate is decreased, maintaining throttle conditions the same. Since the primary coolant and blanket solution temperatures vary with power level, the following two

controls are required to maintain throttle conditions.

1. The temperature of the steam leaving the boiler is regulated by automatically by-passing part of the coolant around the boiler at reduced loads. At full load, no coolant is by-passed.

2. The throttle temperature of the steam is held constant by controlling the pump rate of the blanket fluid through the blanket and superheater.

9.0 MATERIALS OF CONSTRUCTION

Due to the low solubility of uranium in bismuth, critical mass must be kept low and thus nuclear poisons in the core must be minimized. For this reason, graphite is to be the only structural material in the core and blanket. Other desirable properties of graphite are:

1. Ability to retain structural qualities at temperatures of 1500°F.
2. Good moderator.
3. No mass transfer problem.
4. Relatively inexpensive.
5. Impervious to molten bismuth.
6. Not subject to corrosion and erosion by molten U-Bi flowing at 10 ft/sec at temperature of 1500°F.
7. Ability to withstand moderate pressures.
8. Fabricable.

Although more development work is required before the large core tank can be fabricated of graphite, this is not felt to be an insurmountable problem. (See page 304 of reference 3.)

The construction of the jet pump heat exchanger presents many problems, due to the fluids, temperatures, velocities, and desired lifetime involved. As a long-term prospect, molybdenum appears to be the most

promising material of construction. Molybdenum is compatible with both molten bismuth and the proposed fused salt eutectic. It has the necessary high temperature strength characteristics, and is very resistant to corrosion and mass transfer. Unfortunately, at the present state of development, the fabrication problems and high cost associated with molybdenum are prohibitive.

Graphite is another possibility as a material of construction for the jet pump heat exchanger, providing it can be shown that erosion is not too severe at the velocities involved.

Graphite would certainly be less costly than molybdenum, but considerable development needs to be done in the field of fabrication and leak-proof seals (graphite to graphite and graphite to metal).

If the jet pump heat exchanger were to be constructed of materials presently available and at a sufficiently advanced stage of development, it would likely be made as follows:

> All parts which are in contact exclusively with U-Bi would be made of 446 stainless steel. This would include the riser from the core, the lower part of the settling chamber, and the return line to the core. The lines containing the fused salt eutectic would be made of Inconel. The mixing chamber, which must come in contact with both U-Bi and fused salt, could be made of an intermediate alloy such as 316 stainless steel.

However, it is expected that corrosion and mass transfer problems would be severe in such an arrangement, and it is therefore not likely that a sufficiently long lifetime could be attained to produce economic electric power. For this reason, this reference design must be regarded as a long range project, with much development work to be done.

To minimize corrosion the boiler should be made of Inconel, but the cost is prohibitive. The 400 series stainless steels order to contain the the fused salt will contain the fused salt, but for a reduced lifetime.

The superheater could be made of Croloy - 5 - Si, a low chromium steel. A carbon steel pressure vessel will surround the entire reactor.

10.0 ECONOMICS OF THE PROPOSED REACTOR

The reactor proposed in this reference design is similar in many respects to the LMFR. For this reason all capital and operating costs were estimated by extrapolating from the figures published in Reference 3. Extrapolations were made by multiplying the LMFR figures by the ratio of the net KW outputs raised to the 0.6 power. As our chemical processing scheme very closely resembles the one designated as Scheme A in the above report, figures from that report were used.

Interest rates used in computing capital cost were as follows:

1. All depreciating capital investment charges, with one exception, were computed at 16% which corresponds to an expected life of 20 years. The one exception is the Chemical Process Operating Equipment which was computed at 21%, corresponding to a life of 10 years.

2. Liquid metal inventories were considered to be non-depreciating and were computed at 12% per year.

3. The U-233 inventory was charged at 4% per year--based on the latest AEC regulations.

As shown in the following table, these figures result in a final cost of power of approximately 6 mills per KWH.

TABLE 1

Item	Investment $	Interest Rate %/yr	Yearly Cost %/hr	Unit Cost Mils/Kwh
1. Plant Investment Not Including Chem. Processing, Reactor or Boiler	28,000,000	16	4,480,000	2.13
2. Reactor and Boiler Investment	18,000,000	16	2,880,000	1.37
3. Chemical Processing Investment Business	3,000,000	16	480,000	.23
4. Lab and Operating Equipment	3,800,000	21	800,000	.38
4. Chem. Processing and Operation	---	---	2,600,000	1.24
5. Station Operation and Maintenance	---	---	69,000	.03
6. U-233 Makeup(Breeding Ratio 0.98)	---	---	1,100,000	.52
7. U-233 Inventory	1,650,000	4	66,000	.03
8. Bismuth Inventory	1,040,000	12	125,000	.06
			TOTAL	5.99

Note: Items 1,2,3,4, and 5 above were obtained by extrapolating the figures given in B and W AED-501. Extrapolation was made by using the ratio of the net KW outputs of the two reactors raised to the 0.6 power.

The above table shows a lower final cost than that obtained for the LMFR due mainly to the fact that our design is based on a larger power output which results in a lower unit cost on capital equipment.

One of the major objectives in this project was to reduce the inventory of uranium and bismuth. However, it can be seen from the tabulated figures that the inventory charges are of such small magnitude that no appreciable saving in power cost is possible.

Slight reduction in net unit cost may be achieved due to the possibility that our primary heat exchanger may be less costly to fabricate than the conventional shell and tube heat exchanger which it replaces. Any savings here would probably be offset by the increased cost of the boiler which might require higher alloy steels to contain the fused salt.

APPENDIX - TABLE OF CONTENTS

	Page Number
1.0 Physical Properties of Materials Used	99
2.0 Physical Constants In Core	101
2.1 Bismuth Flow Rate In Core	101
2.2 Flow Area and Number Of Tubes Per Pass	101
2.3 Bismuth Flow Velocity	101
2.4 Pressure Drop Across Core	101
3.0 Nuclear Calculations	102
3.1 Preliminary Nuclear Calculations	102
3.11 Breeding Ratio	102
3.12 Critical Mass and Core Radius	103
3.13 Heterogeneity Calculations	105
3.2 Fission Product Poisoning Calculations	107
3.21 Volatile Fission Products	107
3.22 Non Volatile, Fused Salt Soluble Fission Products	107
3.23 Non Volatile, Fused Salt Insoluble Fission Products	107
3.3 Isotope and Pa Build Up	108
3.31 Blanket	108
3.32 Isotope Build Up In Core	109
3.4 Final Nuclear Calculations	110
3.41 Fermi Age Calculations	111
3.42 Resonance Escape Probability	112

Page Number

3.43 Estimation Of Fast Fission Factor 112

3.5 Temperature Coefficient Calculations 113

3.6 Reference Reactor Calculations 115

3.61 Reference Reactor Data 115

3.62 Oracle Results 115

3.63 Power Generation in Blanket 115

3.64 Breeding Ratio 116

3.65 Blanket Processing Cycle 116

3.66 Protactinium Build-up In Blanket 117

3.67 Isotope Build Up-up Core 117

3.68 Fission Product Poisoning in Core & Processing Cycle 118

4.0 Direct Contact Exchanger Performance 119

4.1 Pumping Performance of a Disc Type Liquid Jet Pump 119

4.2 Heat Transfer in the Co-current Flow of Two Immiscible Liquids 123

4.3 Prediction of Heat Transfer Coefficients for Moving Spheres 125

4.4 Calculation of the Terminal Velocity of a Fuel Drop Falling Through a Medium of Fused Salt 126

4.5 Calculation of the Diameter and Angular Orientation of the Fuel Settling Chamber 127

4.6 Heat Transfer in the Countercurrent Flow of Two Immiscible Liquids 128

4.7 Pumping Performance of a Fluid Contacting Centrifugal Heat Exchanger 130

		Page Number
5.0	Heat Exchanger Design	132
5.1	Superheater Design	132
5.2	Water heater, Boiler and First Primary Superheater	132
6.0	Proposed Reactor Systems	136
6.1	Proposed Sodium-Water Cooled System with Stationary Uranium-Bismuth Liquid Fuel	136
6.2	Powered Fluid Contacting Heat Exchanger	138

1.0 PHYSICAL PROPERTIES OF MATERIALS USED

Bismuth

Melting Point	520 °F
Boiling Point	2691 °F
Specific Heat (842 °F)	0.036 Btu/#°F
Thermal Conductivity	8.95 Btu/hr ft °F
Viscosity	1.28 cp.

Density g/cc	Temperature °F
10.07	520
9.84	842
9.66	1112

Graphite

Density	1.78 g/cc
Specific Heat	0.402 Btu/# °F

Fused Salt

Density	103 #/ft^3
Specific Heat	0.27 Btu/# °F
Viscosity	1.6 cp

Thermal Conductivity Btu/hr °F	Temperature °F
9.66	286
8.89	700

Thermal Neutron Cross Sections (590 °C)

Material	σ_a	σ_f	σ_s
U^{233}	305	278	8.2
Bi^{209}	0.0167	--	9
C^{12}	0.00167	--	4.8
Th^{232}	3.65	--	13
U^{234}	48	--	
U^{235}	358	302	
U^{236}	3.13		
Pa^{233}	52		
Th^{233}	1043		
Fission Products			
S_1	19.285		
S_2	13.24		
N_1	113.6		
N_2	1.62		

2.0 PHYSICAL CONSTANTS IN CORE

2.1 The bismuth flow rate through the core is a function of power output and temperature rise across the core. For 750 MW of heat and a 500 °F rise across the core, the flow rate is given by:

$$(750\ \text{MW})(3.413\frac{\text{Btu/hr}}{\text{MW}})(\frac{1}{0.036}\ \text{Btu/\#}^{\circ}\text{F})(\frac{1}{500}\ ^{\circ}\text{F}) = 1.422 \times 10^{8}\ \text{\#/hr}$$

2.2 The flow area and number of tubes required per pass for the two pass arrangement with moderator to fuel ratio of 1 is calculated from core diameter and fuel channel diameter.

$$\text{Flow area per pass} = (1/4)(\pi)(R^2) = (\pi)(3^2)/(4) = 7.069\ \text{ft}$$

$$\text{Number of tubes in core per pass} = (7.069\ \text{ft}^2)(144\ \text{in}^2/\text{ft}^2)(4/\pi 1.5^2)$$

$$= 576\ \text{tubes}$$

2.3 The bismuth flow velocity is now calculated from the above parameters.

$$\text{Velocity} = (1.422 \times 10^{8}\ \text{\#Bi/hr})(\frac{1}{612\text{\#/ft}^3})(\frac{1}{3600\text{sec/hr}})(\frac{1}{7.069\text{ft}^2})$$

$$= 9.13\ \text{ft/sec}$$

2.4 The total pressure drop across the core consists of three major factors which are the density difference in the two passes which produces a negative drop, the friction losses including exit and entrance losses at the top of the reactor, and the turning losses in the bottom header. The equation for the pressure drop across the core is given below:

$$\Delta P = -D_c \Delta\rho \frac{g}{g_c} + \frac{\rho v^2}{2g_c}\left[\frac{f\,L}{D^1} + K_c + K_e\right] + 2\rho C v^{2.25}$$

D_c = core height = 6 ft.

ρ = density difference in two passes of core = 7 lb/ft^3

v = flow velocity in core = 9.13 ft/sec

f = friction factor in fuel channel = 0.0031

L = total flow length = 14 ft.

K_c and K_e = contraction and expansion coefficients

= 0.04 and 0.16 respectively

C = turning loss coefficient = 0.008

$$\Delta P = -\frac{(7)(6)}{144} + \frac{(612)(9.13)}{(2)(144)(32.17)}\left[\frac{(0.0031)(14)}{1.5/12} + 0.04 + 0.16\right] + \frac{(2)(612)(0.008)(9.13^{2.25})}{144}$$

$\Delta P = 12.59\ lb/in^2$

3.0 NUCLEAR CALCULATIONS

3.1 Preliminary Nuclear Calculations

3.11 Breeding Ratio -- For the preliminary calculations of the effect of moderator to fuel ratio on the breeding ratio, a simple one-group method was used. For this case the breeding ratio may be expressed as:

$$B.R. = \left[\eta - 1 - a\right] f_b$$

η = neutrons released per absorbtion in U^{233}

$$a = \frac{\sum_a^{total} - \sum_a^{U^{233}}}{\sum_a^{U^{233}}}$$

f_b = U^{233} atoms produced (net) per neutron leaking from core

Example

U^{233} concentration = 600 ppm in Bi.

$V_C / V_{Bi} = 1.0$

$\overset{U}{a} = 0.002364$

$\overset{C}{a} = 0.000746$

$\overset{Bi}{a} = 0.0002363$

$\eta = 2.31$

$$B.R. = \left[2.31 - 1 - \frac{(0.002364 \quad 0.000746)}{(0.002364)}\right] f_b$$

$$B.R. = 1.179\ f_b$$

NOTE:

Although f_b is known only approximately these calculations show a trend in B.R. with V_C/V_{Bi}.

3.12 Critical Mass and Core Radius -- The preliminary calculations for the effect of the moderator to fuel ratio on the critical mass at constant breeding ratio and to determine the effect of fuel concentration on core radius were based on a modified one-velocity, two region model. These calculations were performed for spherical geometry with the core size for the actual right cylindrical reactor determined by equating the bare core bucklings.

The model employed can be expressed by the following relations:

Material Buckling

$$\frac{\nu \Sigma_f}{\Sigma_a^T} p_c \epsilon \left[1 + B^2(L_c^2 + \tau_{th.})\right]^{-1} = 1 \qquad \text{(function of core only)}$$

Geometric Buckling

$$D_c(BR_s\cot(BR_s) - 1) = -D_b\left[K_bR_s\coth K_b(\tilde{R}'_s - R_s) + 1\right]$$

$$K_b = \frac{\Sigma_{2b}}{D_{2b}}$$

For calculation of R_s

$$(\pi/R_s)^2 = (\pi/R_{cyl})^2 + (\nu/2h_{cyl})^2$$

$$R_s = R_{cyl}/0.917 \qquad \text{where } h = R_{cyl}$$

To calculate the critical mass as a function of the moderator to fuel ratio at constant breeding ratio, the fuel concentration for various moderator to fuel ratios corresponding to a given B.R. were picked from Fig 9. The critical mass was then calculated using the model explained above. Also the critical core radius for various fuel concentrations (at $V_c/V_{Bi} = 1$) were determined.

Example:

U^{233} concentration = 600 ppm in Bi

$V_C/V_{Bi} = 1$

$p_c = 1$ (assumed)

$\tau_{th} = 644\ cm^2$

$L_c^2 = 364\ cm^2$

$\nu = 2.54$

$\Sigma_a^T = 0.002675$

$\Sigma_f = 0.002158$

$K_b = 0.0825\ cm^{-2}$

$D_b = 0.925\ cm$

$D_c = 0.975\ cm$

$(R'_s - R_s) = 91.5\ cm$

$$B^2 = \frac{\nu\Sigma_f - \Sigma_a^T}{\Sigma_a^T(L_c^2 + \tau_{th})} = \frac{(2.54)(0.002158) - (0.002675)}{(0.002675)(364 + 644)}$$

$B = 0.03225$

R_s assumed to be 85.5

$$BR_s\cot(BR_s) = \frac{D_b}{D_c}\left[K_bR_s\coth K_b(\tilde{R}_s' - R_s) + 1\right] + 1$$

$BR_s\cot(BR_s) = -6.64$

$BR_s = 2.75$

$R_s = 85.5$ (check)

3.13 Heterogeneity Calculations -- The reference design considered for evaluation consisted of a graphite block with cylindrical holes which are filled with the (U + Bi) fuel solution. It was desired at the start to determine the effect of this arrangement on the nuclear homogeneity of the system. Since the most important effect of the homogeneity of the system is on thermal utilization this effect was evaluated by comparing the thermal utilization of the given heterogeneous system with the system homogenized. On the basis of diffusion theory, the thermal utilization of the heterogeneous system can be expressed by the following relation:

$$1/f = E\,\frac{V^{Bi}\Sigma_a^{Bi} + V^{C}\Sigma_a^{C}\,F}{V^{F}\Sigma_a^{F}}$$

The exact expressions for F and E involve the modified Bessel functions, but it was found that greater calculational accuracy could be obtained by use of the approximate expressions for R and E.

$$E = 1 + \frac{\varkappa_1^2R_1^2}{2}\left[\frac{R_1^2}{R_1^2 - R_o^2}\ln\frac{R_1}{R_o} - \frac{3}{4} + \frac{R_o^2}{4R_1^2}\right]$$

$$F = 1 + \frac{1}{2}\left[\frac{\mathcal{M}_o R_o}{2}\right]^2 - \frac{1}{12}\left[\frac{\mathcal{M}_o R_o}{2}\right]^4 + \frac{1}{48}\left[\frac{\mathcal{M}_o R_o}{2}\right]^6 - \frac{1}{180}\left[\frac{\mathcal{M}_o R_o}{2}\right]^8$$

R_o = tube radius

R_1 = cell radius

$\mathcal{M}_{o,1} = \left(\sqrt{3\Sigma_a \Sigma_{tr}}\right)_{o,1}$

These relations were used to evaluate the thermal utilization of the reactor which was then compared with a homogenous thermal utilization.

Example:

U^{233} concentration = 0.02 % vol.

$\Sigma_a^F = 0.0033905$	$\Sigma_a^{C^o} = 0.0001492$
$\Sigma_{tr}^F = 0.25393$	$\Sigma_a^{U^o} = 14.59$
$\mathcal{M} = 0.050822$	$\Sigma_a^{Bi^o} = 0.0004726$
$\Sigma_{tr}^{C^o} = 0.4049$	$V_M/V_F = 1$
$\Sigma_{tr}^{U^o} = 0.3910$	$R_o = 1.905$ cm
$\Sigma_{tr}^{Bi^o} = 0.2539$	$R_1 = 2.694$

Substitution of the above data into the above equations gives:

$E = 1.000036$

$F = 1.0011712$

$$1/f = 1.000036 + \frac{(0.0004726) + (1.0011712)(0.0001492)}{(0.002990)}$$

$f = 0.828$ (by homogeneous calculation $f = 0.824$)

As can be seen by the above results, the nuclear calculations may be made by homogenizing the reactor.

3.2 Fission Product Poisoning Calculations

The method of calculating the fission product poisoning used for this report is the same as was employed by BNL in their LMFR design.[3] For this method, the total fission products are divided into three separate groups; volatile, non volatile fused salt soluble, and non volatile fused salt in-soluble. The following fission product data have been taken from B & W -AED - 501.

3.21 Volatile Fission Products -- An arbitrary value of 1% Xe^{135} poisoning was assumed.

3.22 Non Volatile, Fused Salt Soluble Fission Products (fps)

(a) s_1 group cross sections greater than 1000 barns

$y_{s1} \cong$ 10 millimoles

$\bar{\sigma}_{s1} \cong$ 37,000 b. (0.025 ev.) 19,285 b. (590 °C)

$\overline{MW}_{s1} \cong$ 149.2

(b) s_2 group cross sections less than 1000 barns

$y_{s2} \cong$ 1042.3 millimoles

$\bar{\sigma}_{s2} \cong$ 25.4 b. (0.025 ev) 13.24 b. (590 °C)

$\overline{MW}_{s2} \cong$ 113.4

3.23 Non Volatile, Fused Salt Insoluble Fission Products (fpn)

(a) n_1 group cross sections greater than 100 barns

$y_{n1} \cong$ 59.5 millimoles

$\bar{\sigma}_{n1} \cong$ 218 b. (0.025 ev) 113.6 b. (590 °C)

$\overline{MW}_{n1} \cong$ 100

(b) n_2 group cross section less than 100 barns

$y_{n2} \cong 594.5$ millimoles

$\bar{\sigma}_{n2} \cong 3.1$ b. (0.025 ev) 1.62 b. (590 °C)

$\overline{MW}_{n2} = 97.8$

For these calculations, the following expression for poison fraction was used: (this formula neglects fission product decay, but except for very small processing times can be neglected.)

$$p = \frac{\gamma \bar{\sigma} \Phi t_c}{1 + \bar{\sigma} \Phi t_c}$$

$\bar{\sigma}$ = average cross section for fission product group

$\gamma = y \times 10^{-3}$ moles

t_c = chemical processing cycle time (sec)

3.3 Isotope and Pa Build Up

3.31 Blanket

(a) Pa and U^{233} build up -- The decay chain for the production of U^{233} in the blanket can be simplified to

$$\begin{array}{ccccc} Th^{232}(n,\gamma)\ Th^{233} & \xrightarrow{\lambda} & Pa^{233} & \xrightarrow{\lambda_b} & U^{233} \\ \downarrow (n,\gamma) & & \downarrow (n,\gamma) & & \\ Th^{234} & & Pa^{234} & & \end{array}$$

It was assumed with negligible error that as a thorium-232 atom captured a neutron it immediately becomes a protactinium-233 atom. For this condition, the steady-state build up of Pa and U^{233} become:

$$\frac{N_{13}}{N_{02}} = \frac{\sigma_c(02)\,\Phi}{\sigma_c(13)\,\Phi + \lambda_{13} + (1/t_b)a}$$

$$\frac{N_{23}}{N_{02}} = \frac{\sigma_c(02)\,\Phi\,\lambda_{13}}{\left[\sigma_c(13)\,\Phi + \lambda_{13} + (1/t_b)a\right]\left[\sigma_a(23)\,\Phi + (1/t_b)b\right]}$$

Φ = average thermal flux over blanket and external system

λ_b = decay constant for Pa^{233} nuclei

t_b = chemical processing cycle time

a,b = accounts for the type of processing scheme in which some of the Pa and U^{233} is fed back to the blanket.

(b) Isotope build-up -- At steady state and with continuous chemical processing, the build-up equations for uranium isotopes U^{234}, U^{235} and U^{236} can be written as:

$$\alpha_{43} = \frac{N_{24}}{N_{23}} = \frac{\sigma_c(23)}{\sigma_a(24) + a/\Phi t_b}$$

$$\alpha_{53} = \frac{N_{25}}{N_{23}} = \frac{N_{24}}{N_{23}}\,\frac{\sigma_a(24)}{\sigma_a(25) + a/\sigma t_b}$$

$$\alpha_{63} = \frac{N_{26}}{N_{23}} = \frac{N_{25}}{N_{23}}\,\frac{\sigma_c(25)}{\sigma_a(26) + a/\sigma t_b}$$

3.32 Isotope Build Up In Core -- The isotope build-up in the core will depend on whether the uranium feed to the core is 100% U^{233} or the composition as produced in the blanket.

(a) For the case of 100% U^{233} feed, the isotope build-up equations at steady state become:

$$\frac{N_{24}}{N_{23}} = \frac{\sigma_c(23)}{\sigma_a(24)}$$

$$\frac{N_{25}}{N_{23}} = \frac{\sigma_c(23)}{\sigma_a(25)}$$

$$\frac{N_{26}}{N_{23}} = \frac{\sigma_c(23) \times \sigma_c(25)}{\sigma_a(25) \times \sigma_a(26)}$$

(b) For the case of feed with uranium of the blanket composition, the isotope build-up equations become at steady state:

$$\frac{N_{24}}{N_{23}} = \frac{\sigma_c(23) + \alpha_{43}\sigma_a(23)}{\sigma_a(24)}$$

$$\frac{N_{25}}{N_{23}} = \frac{\sigma_c(23) + \sigma_a(23)\left[\alpha_{43} + \alpha_{53}\right]}{\sigma_a(25)}$$

$$\frac{N_{26}}{N_{23}} = \frac{N_{25}}{N_{23}} \frac{\sigma_c(25)}{\sigma_a(26)} + \alpha_{63} \frac{\sigma_a(23)}{\sigma_a(26)}$$

3.4 Final Nuclear Calculations (two group treatment)

After determining the core parameters by the simple preliminary calculations it was desired to investigate the following blanket parameters.

(1) Blanket thickness versus breeding ratio

(2) Blanket U^{233} concentration versus power ratio

(3) Blanket V_C/V_{Bi} versus power ratio

It was realized that this could only be done adequately by a two group treatment. The two group method employed was based on the following differential equations:

CORE $$-D_{1c}\nabla^2\phi_{1c} + \Sigma_{Rc}\phi_{1c} = \nu\Sigma_{f_{2c}}\phi_{2c}\epsilon_c \qquad \Sigma_{Rc} = D_{1c}/\tau_c$$

$$-D_{2c}\nabla^2\phi_{2c} + \Sigma_{2c}\phi_{2c} = p_c\Sigma_{Rc}\phi_{1c}$$

BLANKET $$-D_{1b}\nabla^2\phi_{1b} + \Sigma_{Rb}\phi_{1b} = \nu\Sigma_{f_{2b}}\phi_{2b}\epsilon_b \qquad \Sigma_{Rb} = D_{Rb}/\tau_b$$

$$-D_{2b}\nabla^2\phi_{2b} + \Sigma_{2b}\phi_{2b} = p_b\Sigma_{Rb}\phi_{1b}$$

These equations can be solved on the ORACLE at ORNL in spherical geometry. From this method critical fuel concentrations, flux distributions, (fast and slow), and complete neutron balances were obtained directly.

3.41 Fermi Age Calculations -- To determine the age from fission to thermal energies for the nuclear calculations, the method in Glasstone & Edlund was used. Assuming a flux distribution of 1/E the Fermi Age becomes:

$$\tau_{u_{th}} = \int_0^{u_{th}} \frac{D(u)}{\xi\Sigma_t(u)}\, du$$

For the purpose of calculation, the region between fission and thermal was broken into three parts; then the appropriate constants evaluated for each region. Using this method, the Fermi Age equation becomes:

$$\tau_{th} = \frac{D_1}{\xi\Sigma_t^1}\Delta u_1 + \frac{D_2}{\xi\Sigma_t^2}\Delta u_2 + \frac{D_3}{\xi\Sigma_t^3}\Delta u_3$$

D_i = diffusion coefficient for region i

Σ_t^i = total macroscopic cross section for region i

$\bar{\xi}$ = average gain in lethargy per collission

3.42 Resonance Escape Probability -- To determine the resonance escape probability, the method from Glasstone & Edlund for homogeneous mixtures was used. Assuming a flux distribution of 1/E; the resonance escape probability becomes:

$$p = e^{\int_0^{u_{th}} \frac{\Sigma_a(u)}{\xi\, \Sigma_t(u)}\, du}$$

For the purpose of calculations, the energy region between fission and thermal energies was broken into three parts; then the appropriate constants evaluated for each region. By this method, the resonance escape probability equation becomes:

$$p = \exp\left[-\frac{\Sigma_a^1 \Delta u_1}{\bar{\xi}\, \Sigma_t^1} - \frac{\Sigma_a^2 \Delta u_2}{\bar{\xi}\, \Sigma_t^2} - \frac{\Sigma_a^3 \Delta u_3}{\bar{\xi}\, \Sigma_t^3} \right]$$

Σ_a^i = total macroscopic absorption cross section for region i

Σ_t^i = total macroscopic cross section for region i

$\bar{\xi}$ = average gain in lethergy per collision

3.43 Estimation of Fast Fission Factor -- For the purpose of estimating the fast fission factor, the model for a bare reactor with fast leakage and monoenergetic fission neutrons was used. The expression for the fast fission factor for this model may be given as:

$$\epsilon = \frac{\int_0^{u_{th}} \gamma(u)\, P(0\to u)\, e^{-B^2 \tau(0\to u)}\, du + \dfrac{\Sigma_x^{th}\, P(0\to u^{th})\, e^{-B^2 \tau(0\to u^{th})}}{\Sigma_a^{th}\,(1+L^2B^2)}}{\Sigma_x^{th}\, P(0\to u^{th})\, e^{-B^2 \tau(0\to u^{th})}\, \left[\Sigma_a^{th}(1+L^2B^2)\right]^{-1}}$$

$$\gamma(u) = \frac{\Sigma_f(u)}{\xi \Sigma t(u)}$$

For the purpose of calculational simplicity, the interval to u_{th} were broken up into three groups, and average cross sections for each group used. From this the fast fission factor is given by:

$$\epsilon = \frac{\gamma_1 P(0\to u_1) e^{-B^2\tau(0\to u_1)} \Delta u_1 + \gamma_2 P(0\to u_2) e^{-B^2\tau(0\to u_2)} \Delta u_2 + \gamma_3 P(0\to u_3) e^{-B^2\tau(0\to u^3)} \Delta u^3 + \frac{\Sigma_f^{th} \rho^{th} e^{-B^2\tau^{th}}}{\Sigma_a^{th}(1+L^2B^2)}}{\Sigma_f^{th} \rho^{th} e^{-B^2\tau^{th}} \left[\Sigma_a^{th}(1+L^2B^2)\right]^{-1}}$$

3.5 Temperature Coefficient Calculation

For the purpose of determining the temperature coefficient of the reference reactor, the simple one-group bare model approximation was employed. The multiplication equation for this can be expressed by:

$$k = \nu \frac{\Sigma_f}{\Sigma_a} p\ g\ P_{NL} \epsilon$$

then the temperature equation becomes:

$$\frac{\delta k}{\delta T} = k\left[\frac{1}{\Sigma_f}\frac{\delta \Sigma_f}{\delta T} - \frac{1}{\Sigma_a}\frac{\delta \Sigma_a}{\delta T} - \frac{1}{1+L^2B^2}\frac{\delta(1+L^2B^2)}{\delta T} + \frac{1}{p}\frac{\delta p}{\delta T} + \frac{1}{g}\frac{\delta g}{\delta T} + \frac{1}{\epsilon}\frac{\delta \epsilon}{\delta T}\right]$$

where

(1) $(1/g)(\delta g/\delta T) = \tau(\delta B^2/\delta T) + B^2(\delta\tau/\delta T)$

(2) $(1/p)(\delta p/\delta T) = \Delta u(\delta\beta/\delta T) + \beta(\delta\Delta u/\delta T)$ $\qquad (\delta\beta/\delta T) = 0$

(3) $(\delta\Sigma_a/\delta T) = \sum_{n=1}^{m} N_i(\delta\sigma_a^i/\delta T) - (3N_i\sigma_a^i/\ell)(\delta\ell/\delta T)$

(4) $(\delta\Sigma_f/T) = N_U(\delta\sigma_f/\delta T) - (3N_U\sigma_f/\ell)(\delta\ell/\delta T)_{Bi}$

(5) $\left[\delta(1+L^2B^2)/\delta T\right] = B^2(\delta L^2/\delta T) + L^2(\delta B^2/\delta T)$

(6) $(1/\epsilon)(\delta\epsilon/\delta T) = 0$ (assumed)

(7) $(\partial B^2/\partial T) = -2B^2\alpha_c$

(8) $(\partial \ell/\partial T) = \alpha \ell_o$

(9) $(\partial \tau/\partial T) \doteq (\tau_o/\Delta u_o)(\partial \Delta u/\partial T)$

(10) $(\partial \Delta u/\partial T) = 1/CT$

(11) $(\partial \sigma_a/\partial T) = -(\sigma_a/2T)$

EXAMPLE: Reference Reactor

Material	$\alpha = (1/\ell)(\partial \ell/\partial T)$
Carbon	$6 \times 10^6/\,^oC$
Bismuth	$15 \times 10^6/\,^oC$
U^{233}	0 (assumed)
$L^2 = 502.3$	$\Sigma_f^U = N_U \sigma_f^U = 0.001553$
$\tau = 566$	$B^2 = 0.000985$

By use of the above equations,

(1) $(1/g)(\partial g/\partial T) = 65.2 \times 10^{-6}$

(2) $(1/p)(\partial p/\partial T) = 21.3 \times 10^{-6}$

(3) $(\partial \Sigma_a/\partial T) = -1.243 \times 10^{-6}$

(4) $(\partial \Sigma_f/\partial T) = -0.9698 \times 10^{-6}$

(5) $\partial(1+L^2B^2)/\partial T = -5.94 \times 10^{-6}$

$$\frac{\partial k}{\partial T} = \frac{-0.9698\times10^{-6}}{0.001553} + \frac{1.2436\times10^{-6}}{0.002015} + \frac{5.94 \times 10^{-6}}{1+(502.5)(0.000985)}$$

$$-21.3 \times 10^{-6} - 65.2 \times 10^{-6}$$

$(\partial k/\partial T) = -9 \times 10^{-5}$

3.6 Reference Reactor Calculations

3.61 Reference Reactor Data

(1) V_C/V_{Bi}(core) = 1

(2) a = 3 ft.

(3) T (blanket thickness) = 3 ft

(4) $V_C/V_{fuel\ sol}$(blanket) = 2

(5) U^{233} conc. in Bi (blanket) = 300 ppm

(6) Th conc. in Bi (blanket) = 10% by weight

(7) Power (total) = 770 MW (heat)

(8) Poison Fraction in Core and Blanket = 0.05 (assume)

3.62 Oracle Results

(1) U conc. in Bi (core) = 285 ppm

(2) Resonance Abs. in Blanket = 2.968

(3) $A^F_{2B} = 0.6225$

(4) $A^T_{2B} = 3.593$

(5) $A^F_{2C} = 3.463$

(6) $\epsilon_B = 1.445$

(7) $\epsilon_C = 1.4035$

(8) $\phi_B = 1.49 \times 10^{14}$

(9) $\phi_C = 2.71 \times 10^{15}$

3.63 Power Generation in Blanket

$$\frac{P_B}{P_C} = \frac{A^F_{2B}\epsilon_B}{A^F_{2C}\epsilon_C} = \frac{(0.6225)(1.445)}{(3.463)(1.4035)} = 0.185$$

$P_B/P_T = 15.6$

$P_B = 120$ MW

3.64 Breeding Ratio: (Neglecting Pa Loss)

$$B.R. = \frac{A_{res}\epsilon_B - (\epsilon_B - 1)A_{2B}^{23} + A_{2B}^{Th}}{A_{2C}^{23}\epsilon_C + A_{2B}^{23}\epsilon_B}$$

$$(A_{2C}^{23}) = (A_{2C}^{F})/(1.05) = (3.463)/(1.05) = 3.30$$

$$(A_{2B}^{23}) = (A_{2B}^{F})/(1.05) = (0.6225)/(1.05) = 0.593$$

$$(A_{2B}^{Th}) = (A_{2B}^{T} - A_{2B}^{F}) \frac{\sum_a^{Th}}{\sum_a^{Th} + \sum_a^{C} + \sum_a^{Bi}}$$

$$(A_{2B}^{Th}) = (3.593 - 0.463)(0.928) = 2.755$$

$$B.R. = \frac{2.968 - (1.455)(0.593) + 2.755}{(3.30)(1.4035) + (0.593)(1.445)}$$

$$B.R. = 0.997$$

3.65 Blanket Processing Cycle

$P_B = 120$ MW Assume: 10 Liters/MW of heat

$V_B = 10.8 \times 10^6$ cc $V_{H.E.} = 2.20 \times 10^6$ cc

$V_B/(V_B + V_{H.E.}) = 0.905$

$\Phi_{(B+H.E.} = \Phi_B(0.905) = (1.49 \times 10^{14})(0.905) = (1.35 \times 10^{14}$

$(N^{23}/N^{02}) = 2.69 \times 10^{-3}$

$$\frac{N^{23}}{N^{02}} = \frac{\sigma_a(02)\Phi\lambda_{13}}{(\sigma_a(13)\Phi + \lambda_{13} + a/t_B)(\sigma_a(23)\Phi + b/t_B)}$$

$$\frac{N_{23}}{N_{02}} = \frac{(3.65 \times 10^{-24})(1.35 \times 10^{14})(2.93 \times 10^{-7})}{[(52)(1.35)\times10^{10} + 2.93\times10^{-7} + 0.28/t_B][(305)(1.35)\times10^{-10} + 0.285/t_B]}$$

$$\frac{N_{23}}{N_{02}} = \frac{14.45 \times 10^{-17}}{(3\times10^{-7} + 0.28/t_B)(0.412\times10^{-7} + 0.285/t_B)}$$

Assuming t_B until $N_{23}/N_{02} = 2.69 \times 10^{-3}$

$t_B = 34.7$ days $(3 \times 10^6$ sec)

3.66 Protactinium Build-up In Blanket:

$$\frac{N_{13}}{N_{23}} = \frac{\sigma_a(23)\Phi + b/t_B}{\lambda_{13}}$$

$$\frac{N_{13}}{N_{23}} = \frac{(305\times10^{-24})(1.35\times10^{14}) + (0.285)/(3\times10^6)}{2.93 \times 10^{-7}}$$

$(N_{13}/N_{23}) = 0.464$

P (abs. in Pa/abs in U in blanket) $= (N_{13}\sigma_{13})/(N_{23}\sigma_{23})$

$= (0.464)(52/305) = 0.0792$

P' (abs in Pa/abs in U_{C+B}) $= (0.0792)(0.156) = 0.012$

3.67 Isotope Build-up In Core

$(N_{24}/N_{23}) = \sigma_c(23)/\sigma_a(24) = 27/48 = 0.563$

$N_{25}/N_{23} = \sigma_c(23)/\sigma_a(25) = 27/358 = 0.0754$

$N_{26}/N_{23} = \sigma_c(23)\sigma_c(25)/\sigma_a(25)\sigma_a(26) = (27)(55)/(358)(3.1)$

$= 1.335$

$P_{24/23} = N_{24}\sigma_a(24)/N_{23}\sigma_a(23) = (0.563)(48)/(305) = 0.0885$

$$P_{25/23} = \frac{N_{25}}{N_{23}} \frac{\sigma_a(25) - \nu\sigma_f(25)}{\sigma_a(23)} = (0.0745/305)(358 - 2.50\times303)$$

$= -0.101$

$P_{26/23} = N_{26}\sigma_a(26)/N_{23}\sigma_a(23) = 1.135(3.1)/(305) = 0.0137$

$P_{net} = 0.0012$

3.68 Fission Product Poisoning in Core & Processing Cycle

Assumed:

(1) Volatile fission products $P_1 = 0.01$

(2) Soluble fission products $P_2 = 0.00$

(3) Insoluble fission prodicts $P_3 = 0.04$

Required Processing Cycle

$\Phi_c = 2.71 \times 10^{15}$ $V_c/V_T = 0.241$

$\Phi = 6.55 \times 10^{14}$

$$P_3 = 0.04 = \frac{\gamma_{n1}\bar{\sigma}_{n1}\Phi_c t_c}{1+\bar{\sigma}_{n1}\Phi_c t_c} + \frac{\gamma_{n2}\bar{\sigma}_{n2}\Phi_c t_c}{1+\bar{\sigma}_{n2}\Phi_c t_c}$$

$$0.04 = \frac{(0.0595)(113.6\times10^{-24})(6.55\times10^{14})\ t_c}{1+(113.6\times10^{-24})(6.55\times10^{14})\ t_c} + \frac{(.5945)(1.62)(6.55)\times10^{10}}{1+(1.62)(6.55)\times10^{-10}}$$

$$0.04 = \frac{4.42 \times 10^{-9}\ t_c}{1\ \ 74.5 \times 10^{-9}\ t_c} + \frac{0.63 \times 10^{-9}\ t_c}{1\ \ 1.06 \times 10^{-9}\ t_c}$$

Assuming t_c until $P_3 = 0.04$

$t_c = 174$ days $(1.5 \times 10^7$ sec)

4.0 DIRECT CONTACT EXCHANGER PERFORMANCE

4.1 Pumping Performance of a Disc Type Liquid Liquid Jet Pump.

The basic equation employed is that for a linear liquid liquid jet pump with cylindrical mixing tube (5).

$$1/g\left[W_jV_j + W_sV_s - (W_s + W_j)V_t\right] = A_t\left[(p_t + Z_t) - (p_s + Z_a)\right]$$

Q is volume rate of flow, cu ft/sec

W is weight rate of flow, lb/sec

V is average fluid velocity, ft/sec

A is area of mixing tube cross section, ft^2

p is pressure, lbs/ft^2

g is acceleration due to gravity, ft/sec^2

Z is elevation of measuring section above arbitrary datum, ft

a refers to entrance end of cylindrical mixing tube

j refers to drive jet (fused salt)

s refers to suction fluid (fuel)

t refers to the outlet end of the mixing tube

Assumed constant values:

V_s -- 10 ft/sec

Ps -- 14.7 psia

V_d -- 20 ft/sec (coolant velocity in downcomer)

$r_m = 4$ ft. (radius to mixing tube exit)

$r_d = 1.28$ ft (radius of drive line downcomer)

$Z_t - Z_a = 0$

$\Delta T_f = 500^\circ F$ (fuel temperature drop across exchanger)

$P = 750$ MW (reactor power generation, heat; core)

Sample calculation for a coolant temperature rise of 250°F and a jet velocity of 75 ft/sec.

$$W_s = (750 \text{ MW})(10^3 \text{ KW/MW})(3413 \text{ BTU/KW HR})(\text{LB}^\circ\text{F}/.036 \text{ BTU})(1/500^\circ\text{F}) \times (\text{HR}/3600 \text{ sec})$$

$$Q_s = W_s / \rho_s$$

$W_s = 40{,}000$ LB/sec $\qquad W_j = 10{,}560$ LB/sec

$Q_s = 64.8$ cu ft/sec $\qquad Q_s = 102.4$ cu ft/sec

Assume that $r_j = 1.5\ r_d = 1.92$ ft (radius to disc jet nozzle).

Now considering one-half of the jet pump it is seen that

$A_s = 3.24$ ft^2 (Cross sectional area of suction exterior to jet)

$A_j = 0.68$ ft^2 (Cross sectional area of jet)

$A_t = 3.92$ ft^2 (Cross sectional area of mixing tube at entrance(and exit), assuming a cylindrical mixing tube for one-half the total flow)

V_t' may now be determined for the hypothetical cylindrical tube.

$V_t' = 21.3$ ft/sec

With the basic formula for the linear jet the change in pressure across the cylindrical mixing tube is calculated to be

$\Delta p' = + 451$ psf

The cylindrical mixing tube is now related to the actual radial mixing tube by expanding the exit area of the former to equal the corresponding exit area of the latter. The velocity at the exit of the radial mixing tube is then determined by the use of the actual area of one-half the total area of the mixing tube exit for the design jet pump.

$$A_t = A_t' \, (r_m / r_j) = 8.1 \text{ ft}^2$$

$$V_t = 83.6 \text{ ft}^3/\text{sec} \; (1/ 8.1 \text{ ft}^2) = 10.3 \text{ ft/sec}$$

The decrease in velocity resulting from the expansion of the mixing tube exit is accounted for as an increase in pressure across the mixing tube, $\Delta p''$.

$$\frac{V_t'^2 - V_t^2}{2\,g} \times \rho_m = 1610 \text{ psf}$$

where ρ_m is the estimated average density at the mixing tube exit calculated from the ratios of volumetric flow rates on the assumption that complete mixing has occurred.

Thus the actual rise in pressure across the mixing tube equals

$$\Delta p' + \Delta p'' = 2061 \text{ psf}$$

Since the change in velocity and pressure across the mixing tube has been determined, the total change in head for each liquid may be readily calculated.

Change in coolant head

due to velocity change	=	8830 psf	(loss)
due to pressure change	=	2061 psf	(gain)
Net change		6769 psf	(loss)

Similarly, the net gain in fuel head is 2119 psf.

The theoretical mechanical efficiency is defined as the rate at which mechanical energy is added to the suction fluid divided by the rate mechanical energy is lost by the drive fluid. Thus

$$\text{eff.} = 100 \times \frac{W_s \times \text{gain in fuel head}}{W_j \times \text{loss in coolant head}}.$$

For the above example the efficiency is calculated to be 20 %.

4.2 Heat transfer in the co-current flow of two immiscible liquids -- Gurney-Lurie Approximation.

Consider drops of Fuel as spheres surrounded by a coolant medium at constant temperature. For a given drop size, initial temperature difference, and contact time determine the proper solution to the unsteady state heat transfer problem by employing the proper Gurney-Lurie chart (9).

In actuality the coolant medium is not at constant temperature but is warming from zero contact time. The assumption is made that the actual temperature difference after a specified contact time will be the average of the two values obtained by taking the initial temperature difference to be 500°F and 750°F as shown in the sketch below.

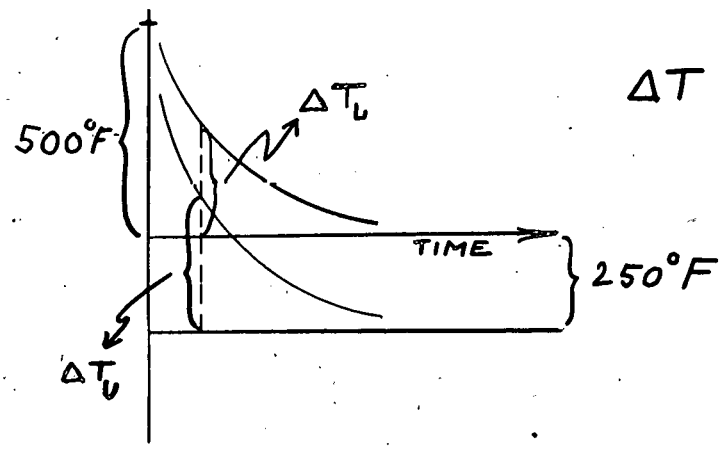

$$\Delta T \cong \frac{\Delta T_u + \Delta T_u}{2}$$

Sample calculation:

Consider the case where

contact time is 0.2 sec (0.556×10^{-4} hr)

r_m, drop radius is 0.06"

h is 2500 BTU/ HR SQ FT °F

drop center is reference point for temperature.

The chart abcissa, X, is evaluated by the formula

$$X = \frac{k \times \text{contact time}}{\text{density} \times C_p \times r_m^2} = 0.902$$

$k = 8.95$ BTU/HR FT °F

$C_p = 0.036$ BTU/LB °F

density is 614 LBS/FT^3

This value of X together with a value of n equal to zero and a value of the "resistance ratio" of 0.716 is used to enter the chart. The corresponding value of Y, the ordinate, is 0.08. Note that the resistance ratio, m, is defined as

$$\frac{\text{thermal conductivity of the sphere material}}{\text{drop radius} \times \text{heat transfer coefficient}}$$

Thus 0.08 equals the final temperature difference divided by the temperature difference at zero contact time.

For an initial temperature difference of 750°F Δ T(upper) is 60°F. ΔT(lower), corresponding to an initial ΔT of 500°F, is 40 °F.

Therefore T at t equal 0.2 sec is 50°F.

4.3 Prediction of Heat Transfer Coefficients for Moving Spheres.

The basic formula used is

$$St \cong 0.236 \; Re^{-0.3} \; Sc^{-0.6}$$ see reference (10).

$$St \cong h/\text{density} \times C_p \times \text{Velocity}$$

$$Sc \cong \text{viscosity} \times C_p / k$$

$$Re \cong \text{drop diameter} \times \text{Velocity} \times \text{density} / \text{viscosity}.$$

Salt properties:

C_p -- 0.27 BTU/LB°F density -- 100 LB/FT^3

k -- 0.75 BTU/HR FT°F viscosity -- 3.87 LB/HR FT

Note that the value of h depends upon the drop size of the fuel and the properties of the coolant.

For a fuel drop 0.1" in radius and a relative velocity of 2 FT/SEC, Re equals 3100, Sc equals 1.40. The solution of the basic formula for h gives a value of 3300 BTU/HR FT^2 °F.

4.4 Calculation of the Terminal Velocity of a Fuel Drop Falling Through a Medium of Fused Salt.

At the terminal velocity, drag force equals driving force.

Drag force = C_D x salt density x r^2 x $V^2/2$

where C_D is taken as 0.44.

Driving force = 4/3 x r^3 x salt-fuel density difference x g.

Thus V, the terminal velocity, may be expressed as

$$V = 8.99 \times (r, \text{inches})^{\frac{1}{2}} \times (\text{no. of g's})^{\frac{1}{2}}$$

For the case in which the drop radius equals 0.062 " and the gravitational acceleration equals 32.2 FT/SEC^2, the terminal velocity is 2.24 FT/SEC.

In like manner the following expression for the terminal velocity of a salt drop falling through a medium of fuel may be derived:

$$V = 3.67 \times (r, \text{inches})^{\frac{1}{2}} \times (\text{no. of g's})^{\frac{1}{2}}$$

4.5 Calculation of the Diameter and Angular Orientation of the Fuel Settling Chamber.

The calculation for the reference design yielded a velocity of 10.3 FT/SEC at the mixing tube exit. It is assumed that the linear velocity is converted to a velocity of 10 FT/SEC in circular motion at an average radius of five feet. Thus the centrifugal acceleration developed is 20 FT/SEC^2. The resultant acceleration, as show by the following sketch is 1.18 g's at an angle of 58 degrees with the horizontal.

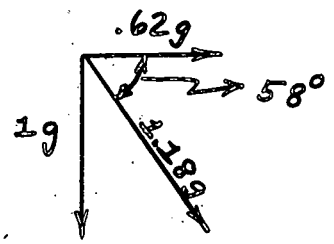

By use of the formula developed in part 4.4 of the Appendix the terminal velocity of a coolant drop rising in the fuel is 1.0 FT/SEC (drop radius equal to 0.062"). Thus the critical downward velocity of the fuel is taken as 1.0 FT/SEC so that, under the simplified assumptions made, the coolant will not be carried into the core if the coolant drops are larger than the given value.

With a total fuel flow of 64.8 FT^3/SEC the area of the top of the fuel settling ring corresponding to a normal flow velocity of 1 FT/SEC is calculated. The thickness of the ring at its top is 1.6 FT, measured normal to the tube wall.

Although not indicated in Fig. 12, for the downward velocity to be constant at 1 FT/SEC, the ring thickness must be reduced as the inner radius increases.

4.6 Heat Transfer in the Countercurrent Flow of Two Immiscible Liquids -- Modified Heat Transfer Coefficient Method.

Consider a parcel of fuel fluid which is subject to a temperature driving force which varies with time. The problem is treated as a steady state case by using a log mean temperature driving force. The basic equation is $Q/\Theta = U A \Delta T_{lm}$ where

- Q is the heat in BTU which is available in the fuel drop, or some fraction of that heat.
- Θ is the contact time in seconds
- U is an effective coefficient of heat transfer
- A is the outside area of drop
- ΔT_{lm} is the log mean temperature driving force.

a. Calculate the average area of heat transfer.

$$A_M = \frac{\int_0^R 4\pi r^2 \times 4/3 \; r^3 \, dr}{\int_0^R 4/3\pi r^3 \, dr} = 8/3\pi R^2$$

b. Calculate the average path for heat transfer by conduction.

$$l_M = \frac{\int_0^R 4/3\pi r^3 (R - r) \, dr}{\int_0^R 4/3\pi r^3 \, dr} \doteq 1/5 \; R$$

c. Calculative the effective coefficient of heat transfer.

$$1/U = 1/h + \frac{l_M \; 4\pi R^2}{k \times 8/3\pi R^2} = 1/h + (l_M/k)\,(3/2)$$

For a value of h equal to 2500 BTU/HR SQ FT°F, a value of k equal to 8.95 BTU/HR FT °F, a contact time of 0.3 sec., and a drop radius of 0.10" the following quantities are obtained:

$$A = 8.73 \times 10^{-4} \text{ FT}^2$$

$$U = 1470 \text{ BTU/HR SQ FT}^{\circ}\text{F}$$

$$Q = 0.0268 \text{ BTU} \quad (\text{ based on a } 500^{\circ}\text{F temperature drop })$$

$$\Delta T_{lm} = 250^{\circ}\text{F}$$

d. Evaluate outlet fuel temperature less inlet coolant temperature given that the temperature drop in the fuel is 500°F and the temperature drop in the coolant is 250°F.

$$\Delta T_{lm} = \frac{(T_{F1} - T_{C2}) - (T_{F2} - T_{C1})}{\ln \dfrac{(T_{F1} - T_{C2})}{(T_{F2} - T_{C1})}}$$

$$T_{F2} - T_{C1} = 145^{\circ}\text{F}$$

4.7 Pumping Performance of a Fluid Contacting Centrifugal Heat Exchanger.

The basic equation assumed is $M_c V_c + M_f V_f = (M_c + M_f) V_t$

where

M_c is the mass rate of flow of coolant, LB/SEC

M_f is the mass rate of flow of fuel, LB/SEC

V_c is the velocity of the incoming coolant, FT/SEC

V_f is the velocity of the incoming fuel, FT/SEC

V_t is the velocity of fuel and coolant after mixing.

If V_f is taken to be zero and the above equation solved for the velocity of the incoming coolant, the result is

$$V_c = (1 + M_f/M_c) V_t$$

In this derivation it has been assumed that there is little change in the pressure due to mixing. If the fuel liquid is considered to be rotating in an annular ring at the Velocity V_t (losses neglected), the number of g's of centrifugal acceleration is given by

V_t^2/rg where r is a properly averaged radius of the annular ring. This number of g's may be thought of as the fuel pressure head in feet in a standard gravitational field which is equivalent to one foot of fuel pressure head in a gravitational field equal to the centrifugal acceleration given above. Denote this quantity by H. Thus $V_t^2/rg = H$.

If this equation is solved for V_t and the result substituted in the expression for V_c given above, the result is

$$V_t = (H \times r \times 32.2 \text{ FT/SEC}^2)^{\frac{1}{2}} \quad \text{and}$$

$$V_c = (1 + M_f/M_c)(H \times r \times 32.2 \text{ FT/SEC}^2)^{\frac{1}{2}}$$

Sample Calculation:

Assume that V_c equals 65 FT/SEC and that the ratio of coolant flow rate to fuel flow rate is 2. Thus M_c/M_f equals 1/3. V_t is then calculated to be 16.2 FT/SEC.

If it is further assumed that the rotating ring of fuel is 0.5 FT in thickness then the pressure head developed in the fuel because of the centrifugal acceleration is 0.5 x H where H is calculated from V_t by the expression previously given and a value of r determined by the geometrical configuration of the exchanger. If r is taken as 3 FT, from the alternate design exchanger, then 0.5 x H equals 1.4 feet of pressure head.

The velocity head gained by the fuel is 4.1 FT under the assumptions made and hence the total gain of head by the fuel is 5.5 FT. It is believed that something of the order of 50% of the gain in velocity head and essentially all of the centrifugal pressure head gained may be recovered.

The theoretical mechanical efficiency, defined as the rate that mechanical energy is added to the fuel divided by the rate it is lost to the coolant, may be approximated by the following formula in which changes in centrifugal head are neglected:

$$\text{eff.} = \frac{\text{fuel weight rate of flow x gain in fuel velocity head}}{\text{coolant weight rate of flow x loss in velocity head}} \times 100$$

For the case examined above the ratio of fuel to coolant weight rates of flow is 3 and the loss in the coolant velocity head is 61.5 FT. An estimate of the theoretical mechanical efficiency is then 20%.

5.0 HEAT EXCHANGER DESIGN

5.1 Superheater design

Data: Blanket power = 120 MW.

Tubes--O. D. = 0.95", I. D. = 0.70", k = 15 BTU/hr-ft^2-$^\circ$F

Material	U-Bi	Steam
T_{in}	1150°F	759°F
T_{out}	909	1000
T_{avg}	1034	880
C_p	0.036 BTU/lb-$^\circ$F	0.63
Density	610 lb./ft^3	2
Viscosity		2.35 x 10^{-5} lb/sec-ft
Velocity	10 ft/sec	100
Mass flow	13,100 lb/sec	737
Thermal cond.		34.8 x 10^{-3} BTU/hr-ft^2-$^\circ$F

Flow areas:

U-Bi $\quad A = \dfrac{W_{Bi-U}}{v} = \dfrac{13,100}{(10)(610)} = 2.15 \text{ ft}^2$

Steam $\quad A = \dfrac{(737)}{(100)(2)} = 3.68 \text{ ft}^2$

Heat transfer coefficients (h)

$h_{Bi} = 2500$ BTU/hr-ft^2-$^\circ$F

Steam $\quad \dfrac{hD}{k} = 0.023\left(\dfrac{Dv\rho}{\mu}\right)^{0.8}\left(\dfrac{C_p\mu}{k}\right)^{0.4} \qquad h_s = 580$

Overall heat transfer coefficient = 383

Area and number of tubes:

$Q = 113{,}800$ BTU/sec $\qquad T = 150^{\circ}F$

$$A = \frac{Q}{U\Delta T} = \frac{113{,}800}{(383)(150)}(60) = 7{,}130 \text{ ft}^2$$

$$N = \frac{A_s}{a} = 1{,}376$$

Holdup of U-Bi:

a = heat flow area/ft of H.E. = 252

Volume = $(L)(A_{Bi})$ = 60.8 ft^3

Mass = 18.5 tons

5.2 Water heater, Boiler and First Primary Superheater

Data:

	Water Heater		Boiler		First Superheater	
	fused salt	water	fused salt	steam	fused salt	steam
T_{in}	727°F	508°F	874°F	592°F	917°F	592°F
T_{out}	700	592	727	592	874	759
Q BTU/sec		76,400		415,000		122,200
ΔT	27		147	0		43
ΔH		104.5		565.5		166.7
C_p	0.27	0.9	0.27	0.27		0.63
Lb/ft^3	103	49		103		
Ft/sec.	10	20	10		10	85.5
Lbs/sec	10,520	737	10,520	737	10,520	737
k	0.75	0.338	0.75		0.75	0.0348
Viscosity	3.87	0.278	3.87		3.87	0.0846

Flow areas:

	Water and steam	Fused Salt
Water heater	0.752 ft^2	10.22 ft^2
Boiler	3.68	"
Superheater	3.68	"

Heat transfer coefficients:

$h_{fused\ salt} = 2,410$

$h_{wh} = 5,900$

$h_{sh} = 580$

ΔT:

Water heater: $\Delta T_{lm} = \dfrac{\Delta T_1 - \Delta T_2}{\ln\left(\dfrac{\Delta T_1}{\Delta T_2}\right)}$

$\Delta T_1 = 192^oF \qquad \Delta T_2 = 135^oF$

$\Delta T_{lm} = 162^oF$

First Superheater:

$\Delta T_1 = 282^oF \qquad \Delta T_2 = 135^oF$

$\Delta T_{lm} = 212^oF$

Overall coefficients:

Water heater: U = 938

First superheater: U = 383

Areas:

Water heater = 1,810 ft^2

Superheater = 5,420 ft^2

Boiler area:

$$(U\Delta T_{lm}) = \frac{U_1\Delta T_2 - U_2\Delta T_1}{\ln \frac{U_1\Delta T_2}{U_2\Delta T_1}}$$

$U_1 = 938$ $U_2 = 382$

$T_2 = 282^oF$ $T_1 = 135$

$(U\Delta T_{lm}) = 114,200$

Area $= 13,100\ ft^2$

Number of tubes

Water heater	282
Superheater	1376
Boiler	1376

Fused salt holdups:

Water heater $= 357\ ft^3 = 18.4$ tons

First superheater $= 219\ ft^3 = 11.3$ tons

Boiler $= 531\ ft^3 = 27.3$ tons

6.0 PROPOSED REACTOR SYSTEMS

6.1 Proposed Sodium-Water Cooled System With Stationary Uranium Bismuth Liquid Fuel

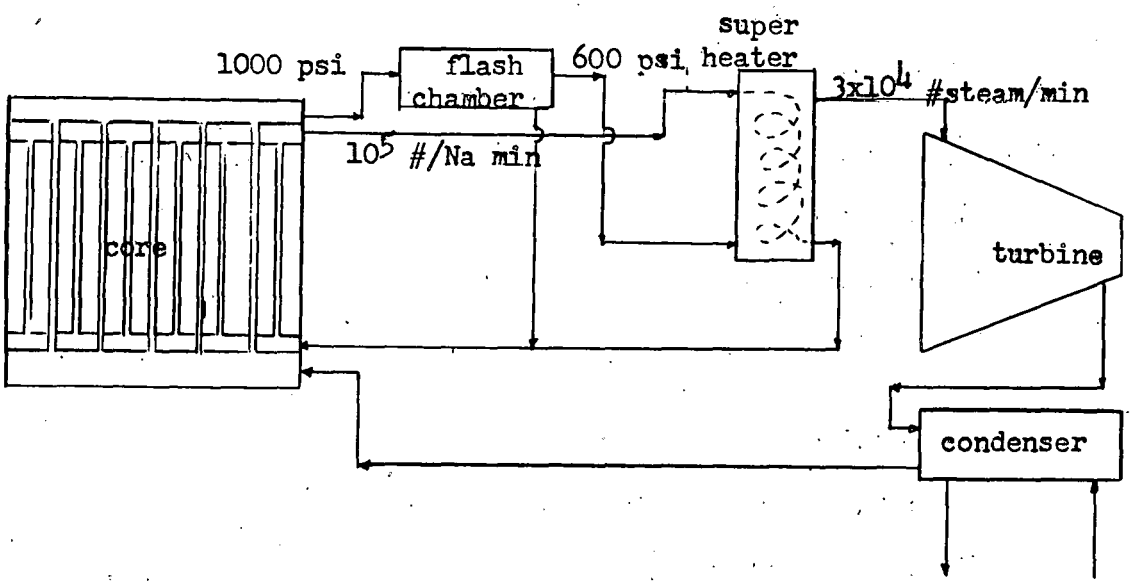

Fig. 27-System Lay Out For Proposed Na-H_2O Cooled Reactor

One of the systems that was considered for this study is indicated by Fig. 27. Liquid U-Bi fuel was to be contained in double walled tubes through which Na and H_2O were to be circulated. Water under 1000 psi, was to be circulated through part of the core where it was heated and allowed to flash down to 600 psi. Liquid Na, which was circulated through another section of the core was to be used for superheating;

A brief study was made to determine the feasibility of such a system as a design project. The power output was set at 300 MW electrical, from 600 psi steam at 800 °F.

As breeding was a necessary condition for the selection of the system, a simple model was used to obtain a value of the breeding gain that could be obtained from such a reactor. The parameters assumed for the reactor are given in the following table.

Moderator to Fuel Ratio	10
Sodium Tube Thickness	0.125 in
Water Tube Thickness	0.25 in
Fuel Channel Thickness	0.25 in
Water To Sodium Ratio	3.35

The model used was a bare cylinder, one velocity with the assumption that all neutrons leaking from the core were absorbed in Th^{232} to produce uranium. All poisons other than materials of construction were neglected.

$$g = \eta - 1 - \Sigma_a^o / \Sigma_a^U$$

$$\frac{V^F}{V^T} = \frac{D_c B^2 \Sigma_a^o}{\nu \Sigma_f^{U'} + \Sigma_a^{U'}}$$

$$B^2 = (2.405/R)^2 + (\pi/H)^2$$

$\eta - 1 = 1.33$

Σ_a^o = absorption in material other than U

Σ_a^U = absorption cross section of U in core

$\Sigma_a^{U'}$ = absorption cross section of pure U

From the above equation the breeding ratio for core diameters of 20, 10, and 5 feet were calculated. The results are given in the

following table.

Core Diameter	% U in Bi	g
20	0.500	0.19
10	0.516	0.23
5	0.566	0.33

As shown by the table breeding ratio was much too low for economical power and the U concentration required is above the solubility limit of U in Bi.

6.2 Powered Fluid Contacting Heat Exchanger

Another design considered for the summer project was a device similar to a centrifuge in which heat exchange takes place within a turning bowl. The powered heat exchanger is shown in Figure 28. It achieves four results.

1. Counter-current heat exchange through intimate mixing of the heatant and coolant. The fluids move in opposite directions under the combined effect of gravity and centrifugal force, taking advantage of the difference in density between the two fluids.

2. Separation of the fluids. The lighter fluid moves up through the hollow shaft to the coolant pump. The heavy heatant moves down, flows over a dam, and drops into the core outer annulus.

3. Pumping of the heatant by means of the axial impeller.

4. Pumping of the coolant by means of a separate centrifugal pump rotor.

ORNL-LR-Dwg.-10188
UNCLASSIFIED

Figure 28
POWERED FLUID CONTACTING HEAT EXCHANGER

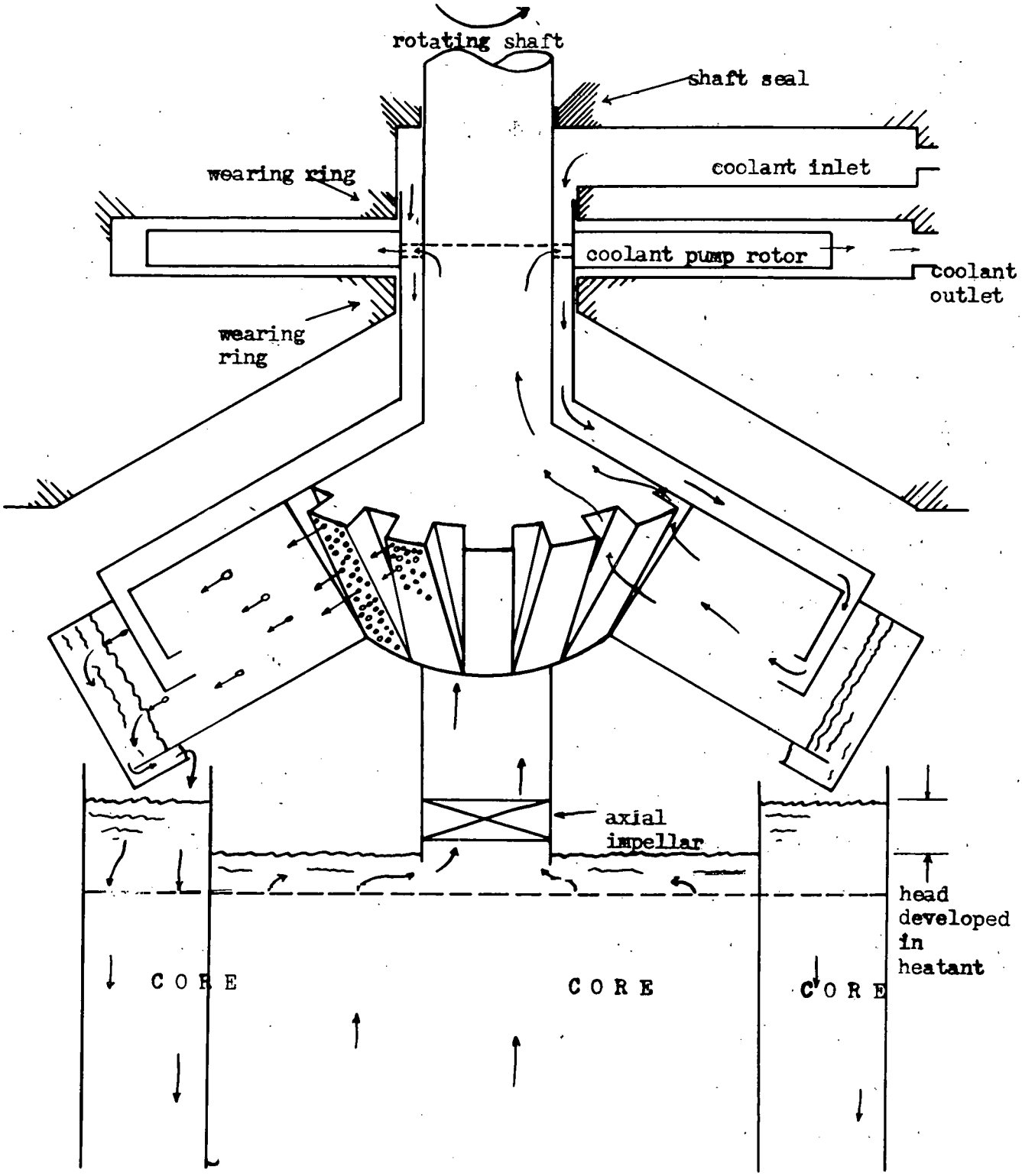

cross-hatches identify stationary members.
core is stationary.
heatant shown in dispersed phase.
heat exchange is counter-current.

The entire heat exchanger would be suspended from bearings outside the core casing. Note that there is only one shaft seal although there are two wearing rings, one on each side of the coolant pump rotor.

BIBLIOGRAPHY

1. Glasstone and Edlund, "The Elements of Nuclear Reactor Theory",D. Van Nostrand Co., Inc., 1952.

2. NAA-SR-280.

3. B and W - AED-501, March 1955; Babcock and Wilcox Company.*

4. BNL-178, June, 1952; Brookhaven National Laboratory.

5. R. G. Folson, "Jet Pumps with Liquid Drive", U. C. Berkely, Chemical Engineering Progress 44, p. 765, Oct., 1948.

6. "Fluid Dynamics of Jets", Shih - I PaI, Ph.D.; D. Van Nostrand Co., Inc., New York, 1954.

7. C. E. Lapple, "Fluid and Particle Dynamics", University of Delaware, March, 195.

8. J. M. Dallavalle, "Micromeritics", 2nd Edition, Pitman Publishing Corp., New York, 1948.

9. W. H. McAdams, "Heat Transmission", McGraw-Hill Book Co., Inc., 2nd Edition, New York, 1942.

10. Johnson, Bentley, Maurer, "Heat Transfer in Sphere Beds", MDDC-990, June, 1945.

11. "Heat Transfer from Drops", I.E.C. 42, 1481, 1950.

12. "Thermodynamics of Fluids in Gravitational and Centrifugal Fields", BNL-2116, 2117.

13. R.H. 2, Chapters 5.1, 5.2, and 5.3.

14. S. Peterson and R. W. Stoughton, CF-54-4-198.

* This preliminary report has been followed by the terminal report designated BAW-2.

THIS PAGE
WAS INTENTIONALLY
LEFT BLANK